UNIVERSITY OF SOUTHAMPTON

FACULTY OF NATURAL AND ENVIRONMENTAL SCIENCES

Department of Ocean and Earth Sciences

Fish and their Scales: On the Power Laws of Aggregation, Size Distribution and Trophic Interaction

by

Matthew Robert David Cobain

A thesis submitted in partial fulfilment for the

degree of Doctor of Philosophy

May 2018

A model in its elegance

Is better than reality

Its graphical simplicity

Denotes a rare intelligence

John M. Burns

In memory of Bob, my beloved Grandpa

He will never walk alone

Abstract

Power law relationships are ubiquitous in ecology, and complex systems in general, and can be used as metrics to describe many aspects of ecosystem structure and function. While ecological interactions and processes predominantly occur at the individual level of biological organisation, currently, most ecological studies aim to estimate "typical" ecosystem behaviour over large spatial and temporal scales. This disconnect results in the under- appreciation of ecosystem dynamics that are potentially important for developing ecological theory and ecosystem modelling. The research presented herein aims to estimate within-ecosystem dynamics, as quantified by power law relationships, to test whether expected ecological dynamics can be captured effectively at smaller scales.

I show that Taylor's power law, a metric of aggregation, varies systematically, both spatially and temporally within the North Sea fish community, with the abiotic environment when populations were considered as cohorts of individual body sizes. By combining estimates of the power law distribution of body size in fish with stable isotopes that can be used to infer trophic interactions, I show that seasonal trends in fish movement patterns and the incorporation of pulsed phytoplankton production can be quantified in a highly dynamic estuarine environment. Estimates of the *in situ* community predator-prey mass ratio, which describes trophic behaviour, and the apparent trophic transfer efficiency are then derived and shown to exhibit strong seasonal variation, indicative of an estuarine food web that is temporally variable. Finally, I quantify the degree of individual specialisation, a mechanism by which intraspecific competition is modulated, in the diet of a commercially important but over-exploited fish species to inform conservation efforts.

This work shows that ecological dynamics can be captured by a range of ecosystem metrics and that, therefore, small scale behaviours can be tested for empirically to direct

ecosystem models and theory.

Contents

List of Figures

List of Tables

Declaration of Authorship

I, Matthew Cobain, declare that this thesis, entitled 'Fish and their Scales: On the Power Laws of Aggregation, Size Distribution and Trophic Interaction' and the work presented in it are my own.

I confirm that:

- This work was done wholly or mainly while in candidature for a research degree at this university.

- Where I have consulted the published work of others, this is always clearly attributed.

- Where I have quoted the work of others, the source is always given. With the exception of such quotations, this thesis is entirely my own work.

- I have acknowledged all main sources of help.

- Where the thesis is based on work done by myself jointly with others, I have made clear exactly what was done by others and what I have contributed myself.

At the time of writing, none of the work presented herein is published, however I have collaborated on the following paper, the contents of which are not outlined in this thesis:

Cobain, S. L., Hodgson, D. M., Peakall, J., Wignall, P. B. and Cobain, M. R. D. (2018) A new macrofaunal limit in the deep biosphere revealed by extreme burrow depths in ancient sediments. *Scientific Reports*, 8(261)

Signed:

Date:

Acknowledgements

To begin with, I would like to extend my sincere gratitude to my main supervisor, Dr Clive Trueman, who after guiding me through my master's project, still willingly accepted another 4 years of me as his student. His direction has been invaluable to the work presented herein. Special thanks is also given to my badminton partner from times gone by, Dr Markus Brede, who took a genuine interest in my work, offered advice and input, and later took up the mantle of co-supervisor. I would like to thank my fellow members of office 566/03 for being generally awesome, particularly Katie, Elena, David and Clare, as we all journeyed (suffered) through our PhDs together from start to finish, but also Charlotte, Maartyn and Clarke the office shark for their moral support.

A special mention is needed for Dr Lawrence Hawkins, who was an attentive tutor during my undergraduate degree. As a colleague, he offered me much guidance and support through my PhD, and gave me the opportunity to pass on my knowledge to others as a demonstrator for 5 years, not to mention teaching me how to make sloe gin. I do hope he enjoys the retirement he most definitely deserves.

Many hours were spent in the labs and the field to conduct the research presented in this thesis, and of course this was not done in solitude. I offer my thanks to Cathryn Quick, Ed Wort, Naomi Allison, Kieran Murray, Chris Bird, Clare Prebble (again) and Will Steward who all volunteered their time to help me with my work. A special thanks is owed to both Julie Seager-Smith and Ruth Gardner, who both spent many hours with me to help process plankton samples. I also thank Charlie Thompson for kindly allowing me the use of her sedimentology lab, and Rona McGill for helping me process my stable isotope samples.

While all my friends have helped to keep me relatively sane during my PhD, there

are a few who deserve a special note. Firstly, Marc, who, without any form of coercion, kindly proof read most of the contents of this thesis. Who knew a theoretical physicist would dare to comprehend something as applied as fishes? Secondly, Greg, for our nights spent drunkenly discussing statistical philosophy. Once more, a special thanks goes to Ed who has been an awesome, sympathetic house mate during the period spent writing this thesis, having introduced me to the marvels of Marvel, keeping my spirits up through thick and thin. And to Andrew, Celia, Truby, another Ed, Mike, Julie, Oliver and Matthias among many others, for many nights of board games, pizza, gin and laughter. Oliver and Matthias I would also like to thank the various badminton clubs, notably Eagles and Westgate, and the sporting aficionados I have played at/with over the years, providing me with a great stress outlet throughout the past 8 years of university life.

Last but certainly not least, it goes without saying that I am deeply indebted to my family for the encouragement they have given me, providing me with an escape from the harsh realities of academic life when it was needed, and the stoic support that they have so lovingly provided me.

1 Introduction: Power Laws and Scaling Relationships in Ecology

1.1 A Simple Equation

Consider the following, rather humble, relationship:

$$y = \alpha x^{\beta}, \quad \alpha > 0 \tag{1.1}$$

Equation 1.1, which is defined by only 2 parameters: the normalisation coefficient α and the scaling exponent β, is known as a power law relationship, so named as y is proportional to x raised to some power. Examples of this function can be seen in Fig. 1.1. The power law relationship describes how one variable scales with another, or, in other words, how a relative change in one variable expresses as a proportional relative change in another, irrespective of the initial values, a property known as scale invariance:

$$\begin{aligned} f(x) &= \alpha x^{\beta} \\ f(cx) &= \alpha(cx)^{\beta} = \alpha c^{\beta} x^{\beta} = c^{\beta} f(x) \propto f(x) \end{aligned} \tag{1.2}$$

Another elegant property of power law relationships is that under a logarithmic transformation they become linearised (see Fig. 1.2):

$$\log(y) = \log(\alpha x^{\beta}) = \log(\alpha) + \beta \log(x) \tag{1.3}$$

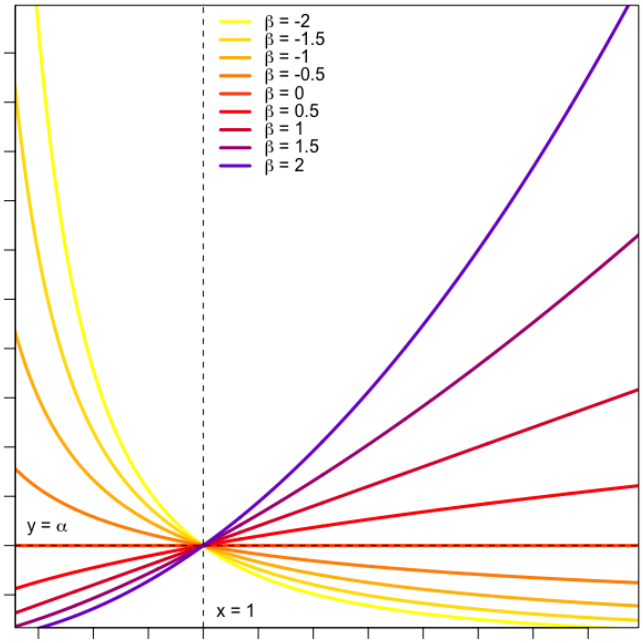

Figure 1.1: Schematic showing examples of power law relationships with changing scaling exponents, β, with the normalisation coefficient, α, held constant. Note that all the graphs cross at the point (1, α). At $\beta = 0$, y is invariant with x, and is equal to α. At $\beta = 1$, y varies linearly with x, and is equal to αx, with this special case termed isometric scaling. When $\beta \neq 0$ or 1, the scaling is termed allometric. Note the axes are on an arithmetic scale.

This provides a simple graphical method for checking for the presence of power law relationships in empirical data - a straight line between two variables when plotted on logarithmically scaled axes provides evidence for (but not conclusive proof of, see Clauset et al., 2009) a power law relationship.

The presence of power laws is prolific in both natural and artificial complex systems. For example, the Gutenberg-Richter law of earthquake magnitude (Gutenberg & Richter, 1950); Zipf's law on distribution of words in language (Zipf, 1949) or an average walker's speed in relation to settlement size - city dwellers are literally living life in the fast lane (Bettencourt et al., 2007). Even academics cannot escape this phenomenon whose scientific output follows Lotka's power law (Lotka, 1926).

Largely due to their apparent ubiquitous nature, power laws are not without their skeptics (Beggs & Timme, 2012; Stumpf & Porter, 2012). Much criticism stems from two issues: the statistical justification of a power law, particularly as distributions when many other heavy tailed distributions may explain data equally well; and the mechanistic

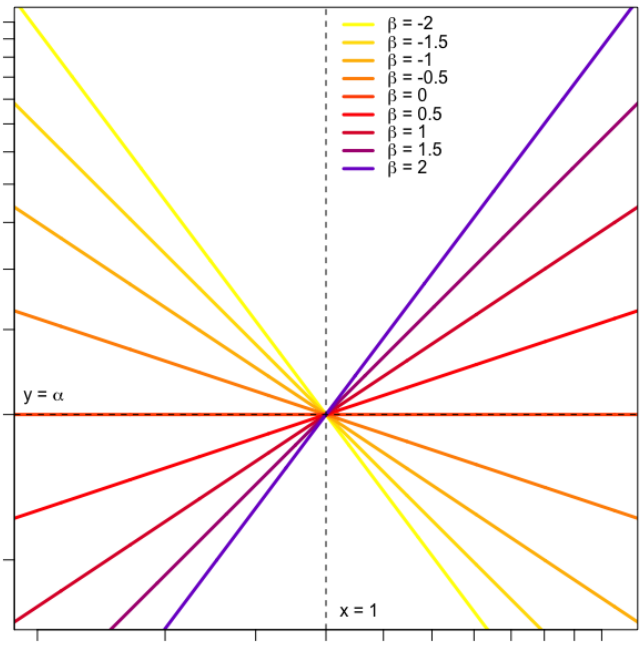

Figure 1.2: As Fig. 1.1, only plotted on a logarithmic, rather than arithmetic, scale, with all graphs now plotting as straight lines.

underpinning (or lack of it) that generates such a relationship (Stumpf & Porter, 2012). While considered, these issues are not specifically addressed here. Comparative analyses of the statistics of empirically quantifying the parameters of a power law and testing whether the relationship holds are relatively complex, both mathematically and philosophically (Newman, 2005; Clauset et al., 2009; Edwards et al., 2017). Such an undertaking would be beyond the scope of this thesis. However, care is taken to make sure all research presented herein is statistically robust in this regard, and acknowledged when evidence is not supportive of a power law relationship.

With regard to the second issue, the rest of this brief introduction is devoted to some of the more well-described power laws and their generative mechanisms found in the biological sciences, with examples covering multiple levels of organisation and including some of the power law relationships that are the subject of later chapters. While their origin is often empirical in approach due to the nature of research in this field, many biological power laws and the proposed models that generate them are grounded in geometric principles and derived from relatively simple assumptions.

1.2 Allometry - Scaling with Body Size

1.2.1 A Geometric Basis

In his seminal works, "On Growth and Form", Thompson (1942), among many other things, describes how many measures of shape, anatomy and physiology can be described as power laws based on simple linear dimensions of size, termed allometry. Take the simple case of a sphere, whose base linear dimension (l) is its radius, r. The volume, V, of a sphere is given by $\frac{4}{3}\pi r^3$ whereas its surface area, S, is $4\pi r^2$, and therefore:

$$V \propto l^3 \qquad \& \qquad S \propto l^2 \tag{1.4}$$

Assuming that changes in size maintain similarity in form, then:

$$S = \alpha V^{\frac{2}{3}} \tag{1.5}$$

were α is the normalisation constant, equal to $\frac{4\pi}{4/3\pi} = \frac{1}{3}$ in the case of the sphere. Equations 1.4 and 1.5 show how changes in the base linear dimension, l, cause proportionally greater changes in volume compared to the surface area. For example, a doubling of l would cause an 8-fold increase in volume but only a 4-fold increase in the surface area. This demonstrates that the surface area to volume ratio decreases with increasing size, which affects almost all physiological processes due to exchanges over semi-permeable membranes.

Such an approach can be used to derive other relationships of interest. Take for example a swimming fish of length l, which attains its velocity, v, by contracting its muscles to do work, W, acting against resistance, R, produced by friction with the water. The available energy required to do work depends on the mass of the muscle, which, since mass is equal to the product of material density and volume, is $\propto l^3$. Friction however scales with the surface area of the fish which is $\propto l^2$. Since $W \propto Rv^2$, then:

$$v^2 \propto \frac{W}{R} \propto \frac{l^3}{l^2} = l, \qquad \text{and therefore:} \qquad v \propto l^{\frac{1}{2}} \tag{1.6}$$

This is known as Froude's Law (Thompson, 1942) and shows how the speeds attained by fishes, or ships as it was originally described for, varies with size under constant form.

1.2.2 Empirical Allometry in Fishes

The relationships described in section 1.2.1 rely on the assumption that with changes in size, form, or the relative magnitudes and directions of shape, are maintained. As shown, the volume, and therefore mass of an object should scale with its linear dimension cubed, i.e. $\propto l^3$. Deviations from this cube scaling would therefore imply changes in form with growth. Focusing on fishes and taking l to be their length, then species for which the scaling exponent is > 3 would suggest that individuals become more rotund with increasing size and, conversely, exponents of < 3 would suggest individuals becoming more lean as they grow. Froese (2006) showed that across 1773 fish species, the median scaling exponent, β is close to, although significantly larger than 3, with a value of 3.03. This suggests that, on average, fish species increase in the relative bulkiness of their bodies with size, although exponents vary from approximately 2.5 to 3.5 around this median.

Under constant form, allometric, or more strictly isometric, scaling should exist between different linear dimensions with an exponent of 1, i.e. $l_a \propto l_b$. Recently, Dunic and Baum (2017) explored the allometric scaling of gape size (both mouth height and width) in coral reef fishes. Interestingly, they found that isometric scaling held for piscivorous and benthic invertivorous predators, whereas as positive allometry (scaling > 1) was observed in gape width for zooplanktivores and both gape width and height for herbivores/detritivores, suggesting that at least some variation in allometric exponents may be explained by functional traits.

1.2.3 Ecological Allometry

So far, the focus has been on allometric scaling at the level of the individual, with expected scalings grounded in geometry. However, allometric scaling has also been empirically observed in traits at the population level of biological organisation. Typically, these power law relationships take body mass (as a population average), rather than a

linear dimension of size, with which to scale other parameters. The reason behind this is based on energetics that intuitively relates to measures of biomass and is discussed in detail in section 1.4. For now, I merely outline three of the more well known ecological laws that exhibit scaling relationships (see Marquet et al. (2005) for a more substantive review).

Damuth's Rule

In 1981, Damuth empirically showed, by combing data taken from many ecological studies and surveys, that the population density (number per unit area), D, of mammals scales with the average body size of the population (mass), $\bar{M}_{\mathrm{P}}$, with such that:

$$D \propto \bar{M}_{\mathrm{P}}{}^{-\frac{3}{4}} \tag{1.7}$$

Variation around this relationship is large, unsurprisingly, as it incorporates data from around the globe from a wide variety of environments with very different levels of resource availability. This was corroborated by Brown et al. (2004), who showed that differences in population trophic level explained much of the variation, and that within trophic levels the exponents still approximated $\frac{-3}{4}$.

Fenchel's Law

Population growth dynamics are well described by the logistic equation:

$$\frac{dP}{dt} = r_m P(1 - \frac{P}{K}) \tag{1.8}$$

were the change in population size, P, depends on the carrying capacity of the environment, K, and the intrinsic growth rate, r_m. While it had long been known that larger organisms reproduced more slowly, by compiling data from various taxa, covering unicellular organisms, ectotherms and endotherms spanning approximately 20 orders of magnitude, Fenchel (1974) showed that r_m varies with body size as a power law:

$$r_m \propto \bar{M}_{\mathrm{P}}{}^{-\frac{1}{4}} \tag{1.9}$$

Calder's Law

Prior to the work of Calder (1983), long term oscillations had been observed separately in animal populations, for example, small rodents exhibited periodicities of approximately 3-4 years while hares had cycles every 8-10 years. Calder (1983) showed that, on average, the periodicity, T, of a population scaled with the average body size, $\bar{M}_{\mathrm{P}}$ as:

$$T \propto \bar{M}_{\mathrm{P}}{}^{\frac{1}{4}} \tag{1.10}$$

These three examples highlight how various ecological traits scale as power law relationships with body size. However it is important to note that the collective works of Peters (1983), Schmidt-Nielsen (1984) and Brown et al. (2004), among others, show that almost all characteristics of organisms scale predictably with body size.

1.3 The Size Spectrum

Given the breadth of described allometric relationships, it is obvious that body size is an important individual ecological indicator, particularly over large scales. Yet traditionally, biological studies use a classification system based on taxonomic identification. If ecosystem processes and responses, such as levels of production, are of interest, then using individual size as a classification may be more beneficial than one based on species (Kerr & Dickie, 2001).

A first approach to using a size based system would be to explore the distribution of individual body sizes within systems, regardless of taxonomy. Taking advantage of recently developed Coulter counter technology, Sheldon et al. (1972) derived the size-frequency distribution of phytoplankton in the Atlantic and Pacific. After they supplemented their data with estimates of fish and whales, to their surprise, plots of logarithmically transformed biomass against logarithmically scaled size classes were astonishingly "flat".

Following this observation, other authors sort to measure the size spectrum in other habitats, including the benthos (Schwinghamer, 1981) and the pelagic environment of lakes (Sprules et al., 1983; Sprules & Munawar, 1986; Sprules et al., 1991), and with

it, the introduction of normalising the biomass spectrum (Platt & Denman, 1977; Kerr & Dickie, 2001), for mathematical convenience (i.e. dividing the biomass per size class by the width of that size class). These normalised spectra typically exhibited straight lines on logarithmic plots, suggesting a power law relationship, with negative slopes of approximately -1 to -1.25. For a detailed review of the earlier work on the biomass spectrum see Kerr and Dickie (2001), and for a more recent but concise review see Sprules and Barth (2016).

Due to the various forms by which data are collected: size-frequency distributions; density/abundance or biomass estimates etc., various forms of the size spectrum have been estimated in different studies (White et al., 2007, 2008; Edwards et al., 2017), between which exponents are not equivalent to each other. Fundamentally, it is the distribution of individual body sizes that is of interest, and when expressed as probability distributions, makes data comparable. The individual size spectrum, which I use as the standard against which to compare other forms of size spectra throughout this thesis, is a power law distribution:

$$p(x) = \alpha x^{-\beta} \tag{1.11}$$

were x is the size of an individual and $p(x)$ is the probability of being size x. The exponent, β, is assigned a minus as the exponent is almost always negative in power law distributions. Increasing magnitude of the exponent results in an ever decreasing probability of ever larger sizes, often referred to as a steeping of the spectrum due to a larger slope when data are plotted on logarithmic scales. Estimation of the parameters of power law distributions has been well studied, including special cases such as discrete data, and comparing the goodness of fit with other heavy tailed distributions (Goldstein et al., 2004; Newman, 2005; White et al., 2008; Clauset et al., 2009; Virkar & Clauset, 2014; Edwards et al., 2017). Edwards et al. (2017) show how multiple methods of constructing spectra relate to the individual size spectrum, Eq. 1.11. Sheldon et al.'s (1972) method of logarithmically binned size classes regressed against logarithmic biomass produces a slope, b, that is equivalent to $-\beta + 2$, while the normalised biomass spectrum produces a slope of $-\beta + 1$.

The size spectrum is believed to be an emergent behaviour of individual trophic

interactions, the inefficiencies in biomass transfer and metabolic maintenance (Kerr & Dickie, 2001). For example, the exponent is steeper in food webs based on predation, where predators are gape limited in terms of the size of prey that can be consumed, compared to food webs dominated by detritivores (Blanchard et al., 2009). The mathematical simplicity of the size spectrum, coupled with allometric interactions and processes, see section 1.2, allow for complex ecosystem behaviours to be modelled in a relatively simplistic manner, for example, exploring the effect of different fishing regimes on ecosystem structure (Rochet & Benoît, 2011).

1.4 Metabolic Theory of Ecology

Biological material is far from thermodynamic equilibrium and therefore requires energy expenditure for it to be maintained - an organism's metabolism. Since ecological interactions, both biological and abiotic, involve exchanges of energy in various forms, understanding influences on metabolism is key to ecology (Sibly et al., 2012). Intuitively metabolic rates should scale with body size, because the amount of biological material fundamentally determines energy requirements for basal maintenance.

1.4.1 Kleiber's Law

By applying the principles of Euclidean geometry, heat loss across body surfaces was believed to constrain whole organism metabolism such that:

$$B = B_0 M^{\frac{2}{3}} \tag{1.12}$$

where B is whole organism metabolism, B_0 is the mass independent normalisation constant and M is the body mass (cf. eq. 1.5). However, in 1932, Kleiber showed empirically across a range of mammals and birds that basal metabolic rate actually scaled with a power exponent of $\frac{3}{4}$ with M. This work was later expanded to include most fauna and has since become known as Kleiber's Law:

$$B = B_0 M^{\frac{3}{4}} \tag{1.13}$$

with Kleiber recommending an average normalisation constant of $B_o = 3.4$ for basal metabolic rate (Kleiber, 1947, 1961). While Kleiber suggested potential causes in his original paper for this three quarter power scaling, a rigorous, generative process was still lacking.

It was not until 1973 when the first mechanistic model was proposed in order to explain this quarter-power scaling, although many suggestions were given by Kleiber (1932). T. McMahon (1973) applied Thompson's (1942) ideas of form to show, based on mechanical restrictions of animal limbs, that mass, M, is proportional to muscle diameter, d raised to the power $8/3$. Muscle cross-sectional area, $\propto d^2$, is the only variable that determines the maximum power and basal metabolic rate of a limb and therefore $B \propto d^2$, and substituting mass in for diameter gives $B \propto (M^{3/8})^2 = M^{\frac{3}{4}}$. Assuming that this is applicable to all muscles and not just limbs then Eq. 1.13 follows.

1.4.2 The WBE Model of Metabolic Scaling

West et al. (WBE) proposed, in 1997, that metabolism scales with body size due to geometric limitations in the distribution network for delivering oxygen and other metabolites, from the surfaces through which they diffuse to enter an organism's body to the end cell at which they are required. Their generative model is based on three underlying principles:

1. The distribution network of an organism if fractal, branching from larger to smaller similar units

2. The final branch of the network (e.g. capillaries in vertebrates and trachea in insects) is size invariant (i.e. $\propto M^0$)

3. The network is optimised so that energy dissipation is minimal

The WBE model derives, among many other allometric relationships, the three quarter power scaling observed in Kleiber's Law and spurred renewed interest in the field of metabolism and allometric scaling (Sibly et al., 2012). A second, less prominent model has also been proposed based on dynamic energy budget theory (DEB) that also generates the three quarter power scaling (Kooijman, 1986; Maino et al., 2014). The DEB model

is based on the premise that it is the mobilisation, and not distribution, of metabolites that limits metabolism, with the assumptions that:

1. Organism biomass is subdivided into two compartments: storage and structure
2. All assimilated material passes through storage before it is incorporated into biological structure
3. Storage is metabolically inert whereas structure is metabolically active and therefore has an intrinsic maintenance
4. Metabolites are mobilised at the surfaces of storage

Far from being in conflict with the WBE model, the DEB model can be considered complementary as it describes a different part of the metabolic system (Maino et al., 2014). If different parts of the system scaled differently with size then substantial re-organisation would be required during ontogenetic growth, something not typically seen in nature.

Both of these models have been subject to scrutiny and criticism, in terms of their generality and assumptions, as well as metabolic scaling in general (Savage et al., 2008; Isaac & Carbone, 2010; Kearney & White, 2012; Price et al., 2012). Regardless of the generative mechanism, the empirical evidence for metabolic scaling with body size with an exponent of $\frac{3}{4}$ is considerable (Kleiber, 1961; Sibly et al., 2012).

1.4.3 Metabolism and other Biological Processes

As metabolism is, at its core, biochemical pathways, temperature, which affects the kinetics of chemical reactions, accounts for much of the deviation from Eq. 1.13. To account for this temperature dependence, Gillooly et al. (2001), incorporated the Arrhenius function into metabolic scaling, giving:

$$B = B_0 M^{\frac{3}{4}} e^{-\frac{E_a}{kT}} \tag{1.14}$$

where E_a is the activation energy of the metabolic process ($E_a \approx 0.65$eV for processes governed by respiration and 0.32eV for photosynthesis), k is Boltzmann's constant ($8.62\times$

10^{-5}eVK^{-1}) and T is the body temperature in Kelvin (Gillooly et al., 2001; Brown et al., 2004; West & Brown, 2005).

Equation 1.14 is the central equation to the metabolic theory of ecology (Sibly et al., 2012) and, taking metabolism as the fundamental biological process, explains many other allometric scalings that have been observed. Consider the three examples of allometric scaling given section 1.2.3.

Damuth's Rule

Damuth's Rule, Eq. 1.7, stated that the scaling of density with body size was with an exponent of $-\frac{3}{4}$. The maximum number of individuals that can occupy an area will be in proportion to the resource production in an area (R), divided by the individual rate of resource use, which is determined by whole organism metabolism (B, see Marquet et al., 2005):

$$D \propto \frac{R}{B} \propto \frac{R}{M^{\frac{3}{4}}} \propto M^{-\frac{3}{4}} \tag{1.15}$$

Fenchel's Law

The scaling of population growth, r_m, with body size with an exponent of $-\frac{1}{4}$ is Fenchel's Law, Eq. 1.9. Population growth is determined by the rate of biomass accumulation, a biological rate. Since biological rates are mass specific (Brown et al., 2004) and limited by metabolic rate:

$$r_m \propto \frac{B}{M} \propto \frac{M^{\frac{3}{4}}}{M} \propto M^{-\frac{1}{4}} \tag{1.16}$$

Calder's Law

Calder's Law, which scaled with an exponent of $\frac{1}{4}$, is a biological time, which are inversely proportional to biological rates. Given Eq. 1.16, then it follows:

$$T \propto r^{-1} \propto \left\{ \frac{M^{\frac{3}{4}}}{M} \right\}^{-1} \propto \frac{M}{M^{\frac{3}{4}}} \propto M^{\frac{1}{4}} \tag{1.17}$$

As is shown by these three examples, metabolic theory predicts ecological patterns first described empirically. More recently, metabolic theory has been used to predict

ecosystem level processes such as carbon fluxes (Yvon-Durocher & Allen, 2012; Schramski et al., 2015) and community dynamics (Zaoli et al., 2017). Variations between theoretical predictions and empirical measures still remain however (Savage et al., 2008; Isaac & Carbone, 2010; Norin & Gamperl, 2018), yet it is these deviations from predictions based on metabolic theory and allometry that provides focus for future research (Sibly et al., 2012). It is worthy to note that, despite their imperfections, power law relationships capture and predict the majority of variation in complex behaviours found across the great diversity of life that we see (Peters, 1983; Sibly et al., 2012), even if all their underlying mechanisms are not yet wholly understood (Stumpf & Porter, 2012).

1.5 Thesis Aims, Objectives and Structure

Studies showing or utilising power laws in ecological studies are extensive, but typically work on very large temporal or spatial scales. For example, the ecological scaling laws cited in section 1.2.3 all compiled data globally, that were recorded disparately in time, from a very broad range of organisms. However, does the macroecological approach belie sensitivities in power law parameterisations that may be used to infer information about system behaviour at smaller scales? As mentioned previously, heterogeneity within scaling relationships is well accepted.

This thesis aims to explore the use of power law relationships in capturing community dynamics and ecosystem behaviours, at reduced spatial and temporal scales compared to previous work, and test for potential drivers of variation in observed power law exponents. To do this, I use coastal fish communities as model systems, utilising two datasets: a large fisheries survey dataset from the North Sea compiled over 40 years and my own data collection from a local estuarine community.

In Chapter 2, I test for the presence of systematic differences in the aggregation behaviour within the North Sea community, described by the exponent of the mean-variance scaling known as Taylor's Power Law (Taylor, 1961). I quantify this power law both across space and through time and, coupling this with modelled climatology of the North Sea, test for specific abiotic drivers in the temporal and spatial aggregation behaviour.

In Chapter 3, I assess the seasonal dynamics in the size spectrum of the fish and

plankton communities within a dynamic estuarine environment, calculated at a monthly resolution. Further, utilising *in situ* environmental data and stable isotope analyses, I assess the overall ecological interactions within the food web, which are known to influence the steepness of size spectra.

In Chapter 4, I use stable isotopes analyses to quantify community level predator-prey mass ratios throughout a seasonal cycle. I then couple these with the empirical size spectra to estimate *in situ* trophic transfer efficiencies in order to assess nutrient fluxes through the estuarine system at a bi-monthly temporal scale.

In Chapter 5, utilising both stable isotope analyses with gut content data, I quantify the degree of individual specialisation within the diet of juvenile sea bass, *Dicentrarchus labrax*, a commercially important species that is currently under threat from over-exploitation.

Finally, concluding remarks are presented in Chapter 6, where I provide a synopsis on the main findings of the research presented in this thesis. I outline the usefulness in applying power law relationships as ecosystem metrics, discuss potential caveats and summarise some future directions of research. Chapters 2 and 5 have been prepared for or are currently in review for publication at the time of writing and therefore are written as stand alone pieces of research. Styles may differ between chapters depending on the target journal.

2 | Taylor's Power Law in the North Sea Fish Community

This chapter is a reproduction of text currently in review with the *Journal of Animal Ecology*, and, as such, is written in the style of the journal.

Matthew R. D. Cobain, Markus Brede and Clive N. Trueman

MRDC processed data, conducted statistical analyses and wrote first manuscript draft, CNT conceptualised the study and all authors contributed equally to study development and manuscript review and editing.

2.1 Abstract

1. **Taylor's power law (TPL) describes the relationship between the mean and variance in abundance of populations, with the power law exponent considered a measure of aggregation of the data. However the usefulness of TPL exponents as an ecological metric has been questioned, largely due to its apparent ubiquity in various complex systems.**

2. **The aim of this study was to test whether TPL exponents vary systematically with potential drivers of animal aggregation in time and space, and therefore capture useful ecological information of the system of interest.**

3. **We derived TPL exponents from a long term, standardised and spatially dense data series of abundance and body size data for a strongly size-**

structured fish community in the North Sea. We then explored systematic aggregation responses as characterised by TPL exponents in time and space and tested for relationships with specific abiotic environmental drivers using modelled climatology.

4. **We find that, in general, TPL exponents vary more than expected under random conditions in the North Sea for size-based populations compared to communities considered by species. Further, size-based temporal TPL exponents are systematically higher (implying more temporally-aggregated distributions) along hydrographic boundaries characterised by temperature variability. We also show that size-based spatial TPL exponents differ between hydrographically distinct basins.**

5. **These findings support the notion that TPL exponents do contain ecological information, capturing community spatio-temporal dynamics as influenced by abiotic drivers.**

2.2 Introduction

In 1961, Taylor posited that the variance in the abundance of a population scales with the mean abundance of that population as a power law, such that:

$$\sigma^2 = \alpha\mu^{\beta}, \quad \alpha > 0 \tag{2.1}$$

where σ^2 is the variance in abundance of the population and μ is the mean abundance of the population, with the coefficient α and the scaling exponent β. His findings were based on empirical observations from a wide range of taxa, from worms and insects to molluscs and fishes, and became known as Taylor's power law (TPL). Conceptually, TPL describes the level of aggregation between individuals in populations, captured by the scaling exponent, β, while the coefficient α is taken to be an artefact of sampling methodology (Taylor, 1961). If individuals are distributed randomly, then the Poisson distribution is approached, giving $\sigma^2 = \mu$, and therefore $\beta = 1$. An increasing β describes

increasing heterogeneity beyond random (i.e. aggregation), whereas a decreasing β describes populations tending towards a uniform distribution.

Studies have since verified the presence of a power law relationship between the mean and variance in abundance in thousands of other datasets and taxa within differing communities (e.g. Xu et al., 2015; Döring et al., 2015; Ramsayer et al., 2012; Ma, 2015; J. E. Cohen, Xu, & Brunborg, 2013). In a wider context, equation 2.1 is also known as fluctuation scaling and is typical of complex systems including tornadoes and meteorology (Tippett & Cohen, 2016), the visual cortex (Medina & Díaz, 2016) and various physical systems such as traffic networks, stock markets and heavy-ion collisions (reviewed by Eisler et al., 2008).

Depending on how the parameters are estimated from data, TPL manifests itself in two variants. Mean-variance pairs calculated from abundances taken across space but at the same point in time describe the spatial aggregation or degree of patchiness in populations, referred to as spatial TPL. However if mean-variance pairs are estimated from abundances measured through time but at the same location then the temporal aggregation in the populations is described, referred to as temporal TPL. Spatial and temporal TPL exponents typically fall between 1 and 2, although estimates can vary outside of these limits (Taylor et al., 1980; Taylor & Woiwod, 1982) and, theoretically, any exponent value is feasible (J. E. Cohen, 2014).

Beyond a purely descriptive use, there have been many practical and theoretical applications of TPL in ecology. For instance, TPL has been used to improve sampling regimes for bioassessments (Monaghan, 2015; Xu et al., 2016). The residuals from TPL have been proposed as a measure of stability in crop yields (Döring et al., 2015) and heterogeneity in plant communities (Guan et al., 2016). Reed and Hobbs (2004) and Pertoldi et al. (2008) used modified forms of TPL to explore extinction risk in small-sized populations. Recently, TPL has been incorporated into a larger macro-ecological framework to explain commonness and rarity in reef communities (S. R. Connolly et al., 2017).

The mechanism by which TPL emerges is, however, still heavily debated in the literature. Taylor and Woiwod (1982) conceptually argued that TPL follows from explicit individual behaviours such as migration. Many theoretical models have been produced

that seek to explain the emergence of TPL in ecological systems including those based on: density dependent (Perry, 1994) or independent, stochastic population growth (R. M. Anderson & Gordon, 1982; J. E. Cohen, Xu, & Schuster, 2013); reproductive covariance (Ballentyne IV & Kerkhoff, 2007); dispersal distance (Shi et al., 2016); and direct and indirect competition (Kilpatrick & Ives, 2003). Others argue that the ubiquity of TPL suggests less system specific causes: data series length and sampling error (Kalyuzhny et al., 2014); the underlying phase space (Fronczak & Fronczak, 2010); generic long-range interaction (Arruda-Neto et al., 2014) or statistical artefacts of system configuration (Xiao et al., 2015). While all these bottom-up approaches seek to explain TPL emergence with a typical exponent of $1 \leq \beta \leq 2$, few offer widely applicable interpretation of variation in exponent values (but see J. E. Cohen, Xu, & Schuster, 2013 and Kilpatrick & Ives, 2003). Xiao et al. (2015) highlight the fact that, while TPL is statistically inevitable, the exact form cannot be predicted and so may still contain ecological information.

Given the wide applications and limited consensus on its mechanistic underpinning, relatively few studies have empirically explored potential drivers of variation in TPL exponents in an ecological setting, a top-down approach that could direct theoretical development of mechanism and better contextualise TPL exponents. Empirical data suggest that TPL exponents do contain ecologically relevant information. For instance, in fish communities, species with classically 'k-selected' life histories typically have lower spatial TPL exponents than those with more 'r-selected' traits (Kuo et al., 2016). A systematic reduction in temporal TPL exponents in fish populations was found along gradients of increasing connectivity and size of reefs, implying that temporal dynamics of populations on isolated, small reefs are more clustered in time (Mellin et al., 2010). Parasite loading influenced spatial TPL exponents in populations of free-living species in lakeshore communities (Lagrue et al., 2015). However, competition between populations does not appear to affect spatial TPL exponents in bacteria cultures compared to being grown in isolation (Ramsayer et al., 2012). The main challenge with empirical-based studies of TPL is acquiring standardised data that is broad enough to cover many different populations and encompasses a suitable range of the driver(s) of interest. For example, Ramsayer et al. (2012) only included two species of bacteria within their

cultures, severely limiting the general conclusions that can be drawn from their experiments, while Kuo et al. (2016) utilised larval data as a proxy for population abundance which limits interpretations to the spawning aggregation behaviours of reproductively active adults.

This current study extends the empirical, top-down approaches to identifying ecological or environmental drivers of TPL exponents by using one of the most spatially extensive, long-term fish survey datasets available, the North Sea International Bottom Trawl Survey (NS-IBTS, ICES, 2012). The IBTS data is derived from standardised trawl surveys and provides length and abundance data of more than 200 fish species sampled across 10 broad areas, subdivided into nearly two hundred standardised subareas, over several decades. In total, the dataset used here contains over one million observations. The North Sea is also intensively monitored and the subject of multiple climatological and biogeochemical simulation models, producing a rich suite of associated environmental data. Here, we couple spatial patterns in temporal TPL and temporal trends in spatial TPL at the community level of organisation with a 3-dimensional reconstruction of the North Sea climatology, to test whether variations in aggregation or patchiness implied by TPL exponents correlate with ecologically plausible, large scale environmental drivers. In other words, do TPL exponents contain information about the spatio-temporal dynamics of the North Sea benthic fish community?

We test the hypothesis that community temporal TPL exponents in the North Sea vary systematically in space with proximity to hydrographic boundaries, temporally averaged physiochemical environmental drivers and their variability. We also test for systematic differences in the spatial TPL exponents between the ecologically distinct shallow and deep-water regions of the North Sea, and whether the spatial TPL time-series of these two regions co-vary with differing environmental drivers. Due to the strong size structuring in aquatic systems, we further hypothesise that populations delineated by size will be more sensitive to environmental drivers compared to populations delineated by species in this system.

We found that, generally, TPL exponents varied systematically with presumed drivers of fish community dynamics when fish communities were defined as populations of

size cohorts. Size-based populations showed greater temporal aggregation closer to hydrographic boundaries with increased inter-annual environmental variability, particularly variance in the summer bottom water temperature. TPL exponents also suggested divergence in the spatial clustering of size-aggregated communities through time between the shallow, seasonally well-mixed southern region and the deep, permanently stratified northern region of the North Sea. This research empirically shows that abiotic environmental drivers systematically influence TPL, and therefore we infer that TPL exponents do capture information on spatio-temporal dynamics in ecosystems.

2.3 Materials and Methods

2.3.1 Data Sources and Processing

Fish community data from the ICES International Bottom Trawl Survey for the North Sea (NS-IBTS) were sourced from DATRAS (http://www.ices.dk/marine-data/data-portals/Pages/DATRAS.aspx) which provides abundance data as Catch Per Unit Effort (CPUE) for each species binned into length classes within subareas of 0.5° Latitude by 1.0° Longitude. Data included in this study were limited to the years 1977 through to 2015, after the commencement of gear standardisation and to quarter one to exclude seasonal affects on abundance (ICES, 2012). Fish less than 60mm in length were excluded due to inefficient sampling within the trawl gear following Daan et al. (2005). Length classes for all species were consolidated into 10mm bins, taxonomic identifications were corrected following Heessen et al. (2015) and subareas with fewer than 10 years of sampling were removed. The average depth of each subarea was taken as the mean depth using ETOPO1 1arc-minute global relief model with a resolution of 1800 data points per subarea (Amante & Eakins, 2009).

Climate data were sourced from the Adjusted Hydrography Optimal Interpolation (AHOI, v19.02), a reconstruction of the North Sea hydrography representing monthly temperature, salinity and mixed layer depth (MLD) maps at a resolution of 0.2° Latitude and Longitude, see Núñez-Riboni and Akimova (2015). Temperature and salinity data were limited to surface and bottom waters only, and, along with MLD, averages were

taken for each location for the months of January, February and March and separately for July, August and September giving measures for winter and summer. Data were then pooled into corresponding subareas and for each year and 10 parameter averages were calculated (minimum cut off of 5 spatial points per subarea): winter surface and bottom water temperature and salinity; summer surface and bottom water temperature and salinity; and summer and winter MLD.

2.3.2 Temporal TPL Analyses

From equation 2.1, it follows that the coefficient and exponent can be estimated from abundance data by regression analysis on the logarithms:

$$\log(s_i^2) = \log(\hat{\alpha}) + \hat{\beta}\log(\bar{x}_i) + \varepsilon_i \tag{2.2}$$

where $\bar{x}_i$ and s_i^2 are unbiased estimators of sample mean and variance in abundance of the i^{th} population respectively, either through time or across space, with ε_i residual error. Here, population refers to individuals grouped into either a single species (or lowest identifiable taxanomic unit) or length class. Mean-variance pairs were calculated for each population across all years sampled within each subarea and TPL parameters estimated for the whole community by ordinary least-squares linear regression (equation 2.2) for that subarea. Subareas were restricted to those that had at least 30 years of sampling to limit the influence of time-series length on the TPL parameters (Kalyuzhny et al., 2014) and those with at least 10 populations present. Populations were restricted to those that were present for at least 10 years within the subarea to exclude transient populations preventing zero inflation of variances. Years in which no individuals from a given population were observed were assigned zero abundance for that year. Equal weighting was given to all populations as they have the same degrees of freedom.

The spatial distribution in temporal TPL exponents was explored utilising the "feasible set" approach employed by Xiao et al. (2015), constructing a distribution of temporal TPL exponents for each subarea. Temporal mean-variance pairs were randomly resampled within each subarea across the whole dataset, giving a random configuration of the populations present. Temporal TPL exponents were then re-estimated for each subarea.

This process was permuted 10000 times to provide a random distribution of temporal TPL exponents for each subarea, given the data. Confidence intervals were then constructed by numerically integrating across the kernel density curves (n=1024) of each subarea.

Systematic spatial patterns in temporal TPL exponents were tested for by modelling the exponents as a linear function of distance from the nearest hydrographic boundary. Boundaries were taken as the subareas that contained: the 500m depth contour separating the North Sea from the Atlantic drift current; the 55°45′N line running between Denmark and Sweden separating the North Sea from the Baltic Sea; a straight line between Dover, UK, and Calais, France, separating the North Sea from the English Channel and the 50m depth contour from Oslofjord, Norway, to Scarborough, UK, which approximately demarcates the transition between the deep, permanently stratified waters and the shallow, seasonally well-mixed waters (Heessen et al., 2015; van Leeuwen et al., 2015).

For those subareas where modelled climate data was available, individual linear models were used to test for the influence of climatic drivers on temporal TPL exponents. For each climate variable, the mean and variance was calculated for each subarea over the whole time period. Parameters were tested for covariance and those showing collinearity were removed. Remaining parameters were then passed as linear descriptors of individual temporal TPL exponents.

2.3.3 Spatial TPL Analyses

Subareas were separated into deep and shallow regions based on mean depth (shallow $\leq 50m <$ deep, see Supplementary for map). For each year, mean-variance pairs were calculated for each population across subareas sampled within each region and TPL parameters estimated for the whole community by ordinary least-squares linear regression (equation 2.2). Typically, zero data in spatial TPL analyses are excluded *a priori*, however this causes selection bias in data where zero abundance can be valid, potentially influencing the estimates of α and β (B. Jørgensen et al., 2011). Here, this is accounted for by constructing a feasible area for each population by taking the overlap of the subareas sampled during any one year and all the subareas that the population has occurred in within that region over the whole time period. Populations were restricted

to those present within at least 5 subareas for any given year within a feasible area of at least 25 subareas to exclude vagrants and zero inflation of variances. Populations were given weights of $n_i - 1$, as ε_i is approximately inversely proportional to the degrees of freedom (Perry, 1981; B. Jørgensen et al., 2011).

Within each region, temporal trends in spatial TPL were explored using the "feasible set" approach as described above: spatial mean-variance pairs were resampled for each year across the two combined regions (i.e. the whole data set). For testing trends in spatial TPL with climatic drivers, the spatial mean and variance of all climate parameters were calculated across the subareas sampled for each region and time-series constructed. Parameters were then tested for covariance and those showing co-linearity were removed. Spatial TPL time-series and the remaining climatic time-series were then low-pass filtered with a 3 year running mean. Cross-correlation analysis was utilised to determine relationships, if any, between smoothed spatial TPL and environmental time-series. Lags were restricted to between 1 and 5 years relative to the TPL time-series (0 to 5 for the climate variables based solely on quarter 1 data, i.e. *in situ* at time of fish data collection for lag 0) to exclude erroneous correlations.

The significance of the correlations was tested by construction of confidence intervals following Akimova et al. (2016). Briefly, this was done by converting the correlation coefficients, $P(\tau)$, into normally distributed variables, $z(\tau)$, via the Fisher transformation:

$$z(\tau) = \frac{1}{2}(\ln(1 + P(\tau)) - \ln(1 - P(\tau))) \tag{2.3}$$

where τ denotes the lag. The standard error is given by:

$$\delta_z = \sqrt{\frac{1}{N^\star}} \tag{2.4}$$

$$\frac{1}{N^\star} = \frac{1}{N} + \frac{2}{N}\sum_{\tau=1}^{N}\frac{(N-\tau)}{N}\rho_x(\tau)\rho_y(\tau) \tag{2.5}$$

The effective degrees of freedom, $N^\star$, accounts for the autocorrelations, $\rho(\tau)$, across all lags, τ, of the two time-series, x and y, of length N. Desired limits can then be calculated on $z(\tau)$, e.g. $\pm 1.96\delta_z$ for the 95% confidence intervals as used in this study, and then

back transformed to $P(\tau)$ using the inverse Fisher function:

$$P(\tau) = \frac{e^{2z(\tau)} - 1}{e^{2z(\tau)} + 1} \tag{2.6}$$

Finally, to check the sensitivity of results to the method by which TPL exponents were calculated, all analyses were conducted on spatial and temporal TPL slopes estimated using the Siegel repeated medians regression (Siegel, 1982), which is highly robust to the influence of outliers (breakdown point of 50%). For each individual data point, this approach computes pairwise slopes with all other data points, from which the median is taken. The slope of the linear relationship is then taken to be the median of N median slopes. All analyses were conducted in R 3.3.2 (R-Core-Team, 2016), utilising the packages: "plyr" (Wickham et al., 2011); "data.table" (Dowle & Srinivasan, 2017); "mblm" (Komsta, 2013); "GGally" (Schlöke et al., 2017); "mctest" (Ullah & Aslam, 2014); and "caTools" (Tuszynski, 2014). Map production was done utilising the package "maps" (Brownrigg et al., 2017).

2.4 Results

The mean-variance data were well described by linear relationships in log-space across all TPL parameterisations, with consistently high r-squared values and low standard errors of coefficients. Tables of summary statistics and individual TPL plots can be found in the Supplementary.

2.4.1 Temporal TPL

The temporal TPL exponents, calculated for 169 subareas in total, are mapped in Fig. 2.1. For populations defined by species, TPL exponents ranged from 1.80 to 2.09 with a mean of 1.93. Only three of the subareas had exponents that fell outside the 95% confidence intervals, see Fig. 2.1a. Size-based temporal TPL exponents showed a greater range from 1.64 to 2.21, with a mean of 1.98. The size-based approach also had many more subareas with exponents beyond the confidence intervals - a total of 31, see Fig. 2.1b. Temporal TPL of size-based populations showed a systematic decrease with

increasing distance from hydrographic boundaries ($F_{1,167} = 40.0, P < 0.001$) whereas TPL exponents for populations defined by species showed no trend ($F_{1,167} = 0.975, P = 0.325$), see Fig. 2.2. Similar results were obtained when TPL exponents were calculated using Siegel repeated medians regression, see the Supplementary for figures.

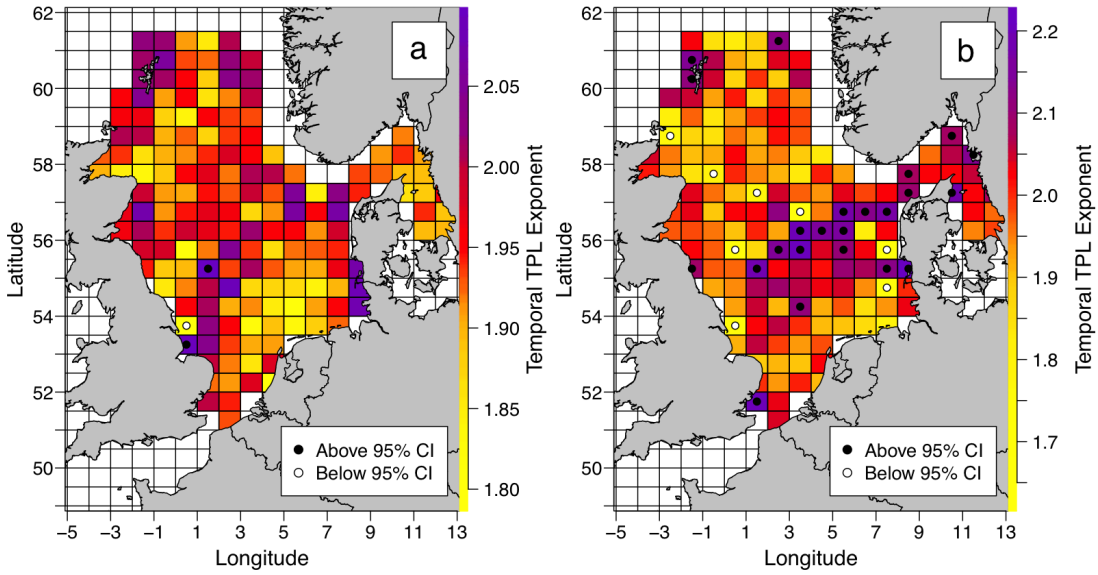

Figure 2.1: Maps of the temporal Taylor's power law (TPL) exponent estimates for the benthic fish community within 169 subareas across the North Sea, for populations by species (a) and size-class cohorts (b). Subareas with exponent estimates either above or below the 95% confidence interval (CI), calculated from 10000 random permutations of mean-variance pairs, are marked with black and white filled circles respectively. Note that the colour scaling for the temporal TPL exponents is based on distribution density and is therefore non-linear and differs between the two plots.

A total of 151 subareas with TPL estimates were also covered by data from the climatological model of the North Sea. Collinearity testing reduced the number of environmental parameters from 20 to 9 (listed in the Supplementary along with cross correlation plots). Species-based temporal TPL exponents, when estimated by either least squares linear regression or Siegel repeated medians regression, showed no significant linear relationships with any of the environmental parameters. However exponents estimated from populations defined by size-classes showed significant linear relationships with mean winter surface temperature ($F_{1,149} = 5.09, P = 0.0256$, slope = -0.020), mean summer surface temperature ($F_{1,149} = 5.33, P = 0.0224$, slope = 0.0042) and variance in summer bottom temperature ($F_{1,149} = 9.97, P = 0.00193$, slope = 0.089). Qualitatively

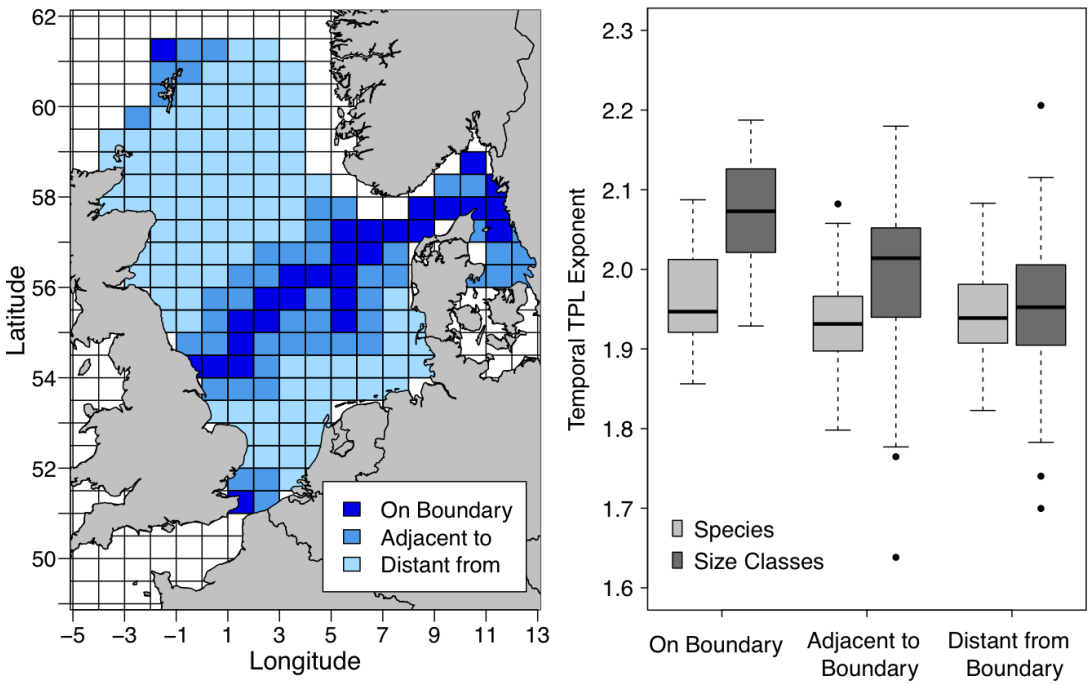

Figure 2.2: Map (left) showing the distribution of subareas in relation to hydrographic boundaries within the North Sea, as defined in the materials and methods. Box plot (right) showing the distribution of temporal Taylor's power law (TPL) exponents against hydrographic boundary assignment for 169 subareas of populations by species and size-class cohorts. Temporal TPL exponents decrease with distance from hydrographic boundary when populations were considered by size class ($F_{1,167} = 40.0, P < 0.001$), whereas no significant relationship was found when populations were considered by species ($F_{1,167} = 0.975, P = 0.325$).

similar results were found with the Siegel method; only these three parameters showed significant linear relationships with similar slopes, see Supplementary.

2.4.2 Spatial TPL

The spatial TPL exponent time-series calculated for 39 years are shown in Fig. 2.3. When populations were defined by species, only 3 years had TPL exponents outside the confidence interval for the shallow region and only 1 for the deep region. Generally, temporal trends in species-based TPL exponents were similar in deep and shallow regions over the whole period, with no difference in the mean of exponents ($t_{75.8} = -0.443, P = 0.659$). Populations by size-classes had many more spatial TPL exponents outside the confidence intervals compared to species: 13 for the shallow region and 19 for the deep. For the shallow region, 11 of these years had exponents above the confidence interval,

with a cluster from 2008 to 2012. For the deep region, 18 of the years had exponents below the confidence interval, with 4 clusters centred on 1984, 1991, 2001/2002 and 2008/2009. Both time series show considerable divergence over much of the period, with the deep region TPL exponents being significantly lower on average compared to the shallow region ($t_{73.0} = 5.61, P < 0.001$).

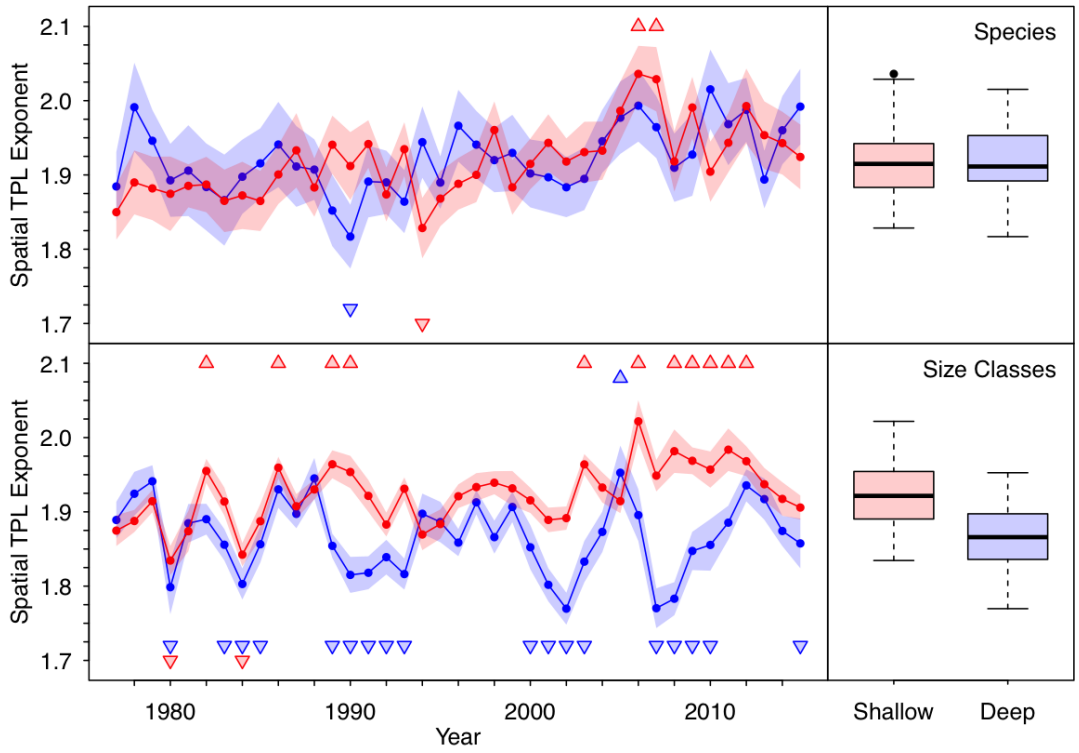

Figure 2.3: Time-series of the spatial Taylor's power law (TPL) exponents by species (top) and by size classes (bottom) calculated separately for deep (>50m, blue) and shallow (≤50m, red) regions of the North Sea, see Supplementary for map of the two regions. Standard errors of the regression estimates are plotted as opaque polygons to show periods of overlap and divergence. Years with TPL exponents either above or below the 95% confidence intervals, calculated from 10000 random permutations of mean-variance pairs of the whole dataset, are marked by triangles either above or below the time-series respectively. The distributions of spatial TPL estimates over the whole period are shown in adjacent box plots. Regional distributions did not differ for TPL exponents by species ($t_{75.8} = -0.443, P = 0.659$), but did for exponents by size classes ($t_{73.0} = 5.61, P < 0.001$).

Similar systematic trends are seen in the time-series when exponents are estimated by Siegel repeated medians regression. Where populations are defined by species, the two regions predominantly overlap each other with only one exponent in total outside the confidence intervals and now difference in means ($t_{76.0} = 1.36, P = 0.178$). Whereas

Table 2.1: Table of environmental parameter correlations and associated lag with time-series of spatial Taylor's power law (TPL) exponents, which have 95 percentile confidence intervals above or below zero. See materials and methods for details on confidence interval construction. Parameters are defined by: the season (summer or winter); the parameter (either bottom/surface water temperature/salinity or mixed layer depth); and the estimated statistic (mean or variance).

Environmental Variable			**Correlation**	**Upper Confidence**	**Lower Confidence**	**Lag**
Season	**Parameter**	**Statistic**	**Coefficient**	**Interval**	**Interval**	
Least squares linear regression						
Shallow Region - Populations by Species						
Winter	Mixed Layer Depth	Mean	-0.682	-0.070	-0.921	3
Deep Region - Populations by Species						
Winter	Bottom Temperature	Mean	0.677	0.924	0.031	5
Summer	Mixed Layer Depth	Mean	-0.736	-0.171	-0.937	3
Shallow Region - Populations by Size-classes						
Winter	Mixed Layer Depth	Mean	-0.711	-0.147	-0.926	3
Deep Region - Populations by Size-classes						
N/A						
Siegel repeated medians regression						
Shallow Region - Populations by Species						
N/A						
Deep Region - Populations by Species						
Winter	Bottom Temperature	Variance	0.672	0.905	0.132	0
Summer	Mixed Layer Depth	Mean	-0.685	-0.139	-0.912	3
Shallow Region - Populations by Size-classes						
Summer	Bottom Temperature	Variance	0.715	0.929	0.146	4
Deep Region - Populations by Size-classes						
Winter	Mixed Depth Layer	Mean	-0.636	-0.018	-0.902	3
Summer	Bottom Temperature	Variance	0.626	0.898	0.009	3

where populations are defined by size-classes, the time-series show large periods of divergence, with 27 exponents in total falling outside the confidence intervals, clustered similarly in time as the least-squared method and the deep region having lower exponents on average ($t_{75.4} = 4.27, P < 0.001$), see the Supplementary.

Collinearity testing reduced the number of environmental parameters from 20 to 7 in the shallow region and 10 in the deep region (see tables and cross-correlation plots in the supplementary). Only bottom temperatures and mixed layer depth showed significant correlations with TPL exponents across both species and size-class approaches, see Table 2.1. However the only pattern repeated by both regression methods was a negative correlation with average summer mixed layer depth with TPL exponents from populations by species in the deep region.

2.5 Discussion

Despite being one of the few widely verified patterns in macroecology, empirical investigations into the drivers of variation in the exponent of Taylor's Power Law are still limited.

While some studies have sought to address this knowledge gap more recently, these have typically focused on biotic factors that potentially affect TPL, e.g. life history traits (Kuo et al., 2016) and synchrony of populations (Reuman et al., 2017). By utilising a long-term and spatially dense community dataset, we have shown that there are systematic differences in both spatial and temporal TPL exponents within the North Sea associated with regional hydrography and therefore the *in situ* environment.

2.5.1 Individual Size vs. Taxonomic Identification

Systematic spatial and temporal trends in community TPL exponents were only apparent when populations were considered as cohorts of size classes. Given that fish communities are heavily structured by individual body size (Trebilco et al., 2013), this is unsurprising. When populations were defined by species, less variation in both spatial and temporal TPL exponents was expressed compared to size classes, suggesting reduced community sensitivity as hypothesised. For temporal TPL, species-based exponents were tightly constrained near a value of 2, the statistical null expectation for temporal TPL (Kilpatrick & Ives, 2003).

The only other two studies exploring drivers of TPL exponents in fishes, to the best of our knowledge, also support the importance of body size in explaining observed variation within this group. More 'k-selected' species, with larger maximum sizes, showed reduced spatial TPL exponents compared to 'r-selected' species (Kuo et al., 2016), with the authors suggesting this is due to enhanced buffering of environmental stress at larger body sizes leading to a more even dispersal of individuals. A species' maximum body size was an important descriptor in modelling temporal TPL exponents in reef fishes, explaining 35% of the deviance in exponents alone; with larger sizes showing reduced observed TPL (Mellin et al., 2010). Mellin et al. (2010) suggest that this is due to increased sensitivity to fluctuations in recruitment that coincide with smaller body sizes.

J. E. Cohen et al. (2012) predicted that allometric scaling exists between body size and variance in abundance by combining TPL with the biomass spectrum, the power law distribution of body sizes. Here, by grouping individuals into size the same information is captured in the TPL exponents, see Fig. 2.4. Tokeshi (1995) illustrates graphically

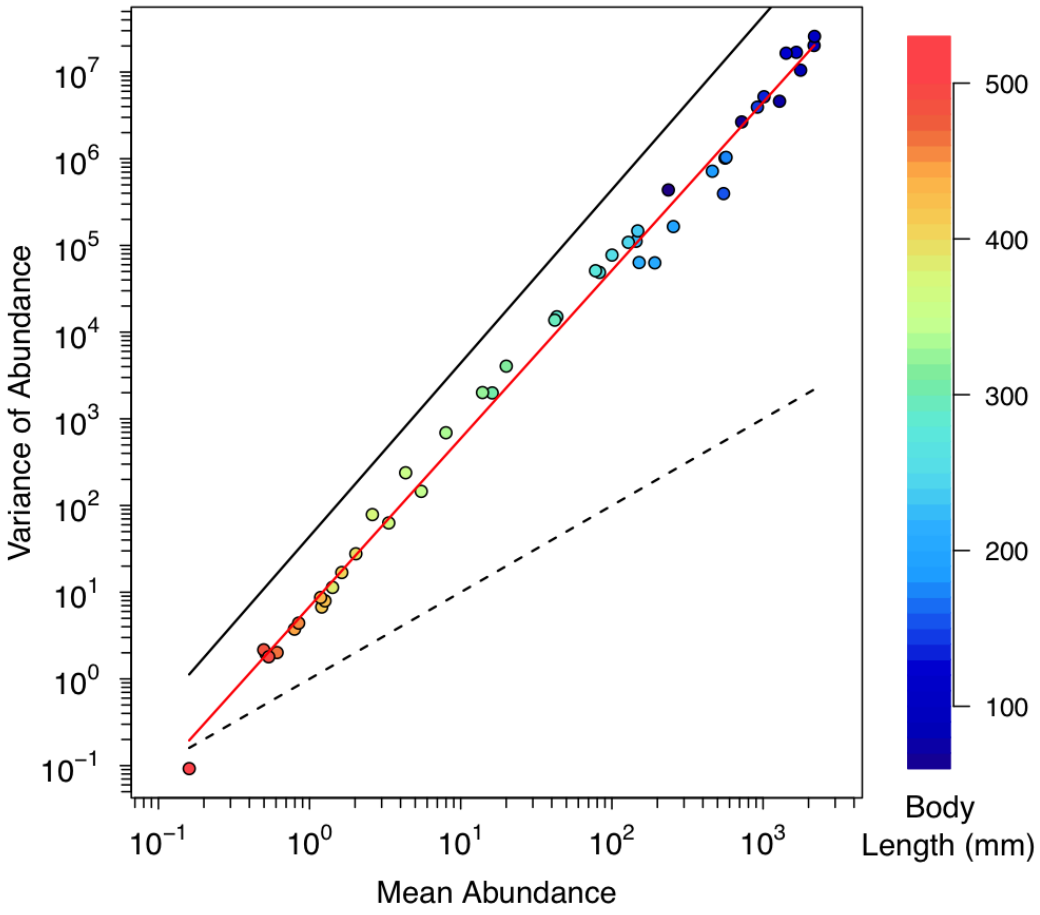

Figure 2.4: Example of a temporal Taylor's power law (TPL) exponent, visualised as the slope of the least-squares linear regression (solid red line), for populations considered by size class cohorts for the subarea "37F". Solid black line shows the hard upper bound of variance, which is the maximum variance for a given mean calculated from n data points and has a slope of 2. The dashed line indicates the soft lower bound of variance given the mean, the Poisson distribution with a slope of 1, following Tokeshi (1995). Data points are coloured based on size. The smaller and larger size classes occupy the extremes of mean abundance and so are more influential in TPL parameter estimation, however variance at low mean abundances (larger size classes) is heavily bounded which limits leverage. Note the base 10 logarithmic scale.

that estimates of TPL exponents are constrained due to a limited theoretical sampling area in logarithmic space, which is broad at high mean abundances and narrows towards lower mean abundances. Smaller sized individuals are typically orders of magnitude more abundant than larger individuals; therefore they occupy the area in log space that is less limited in possible variance to mean ratios. This means that they occupy the area in log space that is broad and so have more leverage in regressions for estimating

TPL exponents, Fig. 2.4. Recruits and juveniles are also the most vulnerable life stages of fish and so will be more variable in their distributions in response to environmental stochasticity. Further, this conceptually explains the expectation that it is the TPL exponents, and not the intercepts, in a size-structured fish community that will vary in response to drivers.

Empirically estimating TPL parameters requires individual abundance data along two dimensions of variability, one to measure mean and variance of abundance in (e.g. space for spatial TPL and time for temporal TPL) and a second to scale mean-variance pairs for parameter estimation. In most studies, this is the opposing temporal or spatial component. To explore potential drivers of variability in TPL exponents, a third dimension is needed to track changes in TPL over which the drivers also vary. For most studies, the third dimension is the method by which individuals are assigned into populations, i.e. species. It is argued that this produces TPL estimates for populations that have experienced the same, although not quantified, spatio-temporally dynamic physical environment (Kuo et al., 2016), assuming census data is consistent between species. This explains why, to date, empirical studies into the drivers of variation within TPL exponents have focused on biotic factors, because it is biotic factors that vary between species, e.g. competition and life history traits. In the current study, by scaling mean-variance pairs over the delineation of populations (species or size class), we have been able to explore the effects of the physical environment as it varies through time or space on TPL exponents as a community response.

2.5.2 Temporal TPL

Since temporal TPL exponents track fluctuations in time, temporal TPL values can be considered as a measure of temporal stability. Our results showed that temporal TPL exponents systematically increased with proximity to hydrographic boundaries (Fig. 2.1b & 2.2), where inter-annual environmental variability is typically high due the lack of a dominant regime (van Leeuwen et al., 2015). This leads to increased environmental stochasticity through time, a fundamental component in theoretical models that seek to explain temporal TPL (e.g. R. M. Anderson & Gordon, 1982). Modelling individual

temporal TPL exponents as a linear function of environmental parameters corroborated the importance of stochasticity in influencing TPL: increasing variance in the summer bottom water temperature was strongly associated with increasing TPL exponents.

Other studies exploring *in situ* abiotic environmental factors on temporal TPL are rare; the only other study the authors are aware of is by Grman et al. (2010), were the addition of fertiliser had no effect on the temporal TPL slopes of annual and perennial plant communities. However the addition of fertiliser to field plots does not necessarily cause changes in environmental stochasticity *per se*, only the average chemical environment. Increasing habitat size and decreasing isolation, which are theorised to increase temporal population stability, have also been shown to decrease temporal TPL exponents in reef fishes (Mellin et al., 2010).

2.5.3 Spatial TPL

While temporal TPL describes the temporal stability of populations, spatial TPL exponents describe their patchiness in space. Within the North Sea, the shallow southern basin showed elevated spatial TPL exponents compared to the deeper northern basin. The 50m depth contour defining the two basins roughly delimits the depth beyond which surface-tidal mixing no longer influences the benthos (Heessen et al., 2015; Huthnance et al., 2016). Therefore the environment in the deep region is expected to be more spatially homogenous than the shallow region that is exposed to heterogenous surface climate effects. However tests for influences of specific environmental drivers on spatial TPL exponents were inconclusive, as significant correlations differed between the two estimation methods of the TPL exponents. It is possible that whole-basin measures of environmental means and variances poorly reflect the *in situ* drivers at this regional scale. Nevertheless, the periodicity seen in the deep region is potentially suggestive of the influence of decadal-scale climatic drivers, such as the North Atlantic Oscillation.

Environmental drivers for variation in spatial TPL exponents have been explored within tree communities by J. E. Cohen et al. (2016), who found that elevation and soil chemistry had no influence. One might expect the spatial TPL exponents of immobile organisms to be less sensitive to environmental drivers as they cannot exhibit migratory

responses when conditions become less favourable but not detrimental. Xu et al. (2015) found that species composition influenced community spatial TPL exponents for trees. In this study, shallow water communities in the North Sea are typically comprised of warm-water, more southern species whereas cool-water northern species occupy the deeper waters, broadly creating two differing species compositions (Heessen et al., 2015). Our results therefore differ from the findings of (Xu, 2015), as the spatial TPL time-series for populations by species of the two regions matched each other closely. However caution should be used when comparing these systems that have very different ecological and environmental contexts.

2.5.4 Concluding Remarks

In this study we have empirically shown that exponents of the power law relationship between mean and variance in abundance pairs (Taylor's Power Law) vary systematically within the North Sea, following broad patterns in the stability of the abiotic environment as expected from theory. We therefore argue that TPL exponents may be informative ecosystem metrics describing aspects of community stability and patchiness in response to environmental change. The NS-IBTS dataset lends itself to such analyses because it is numerically dense; is in a highly studied area with abundant environmental data; and the spatial and temporal scales at which the data are collected are ecologically relevant to the functional group of interest – fishes. The temporal and spatial scales of study organisms and survey data are important to consider in TPL studies, and their influences still remain poorly resolved (Certain et al., 2007; Xu, 2015). Data used here were collected annually, on the same order as the lifespans of most of the included fish species, thus capturing single cohorts within multiple surveys and multiple generations over the duration of the data collection. Spatially, although mapped onto large subareas, abundance data refers to areas swept by a standard 30-minute trawl, which captures movements such as shoaling behaviours. If the spatial scale is too small, differences may just reflect the small random variations imposed on larger behavioural patterns and not capture responses to environmental drivers. Likewise if the spatial scale is too big then only the general distribution of the cohort may be captured. With ever larger ecological

datasets become more readily available, it is likely that empirical studies addressing the uncertainties that still surround the mechanisms underpinning Taylor's Power Law are likely catch-up with the wealth of theoretical studies.

2.6 Acknowledgements

This work was funded by a NERC SPITFIRE PhD studentship (award number 1498909). We would like to thank the contribution of all scientists and colleagues working on the collection and processing of data within ICES. The authors declare no conflict of interest with regard to the work presented here.

2.7 Data Accessibility

All data used in this study are publicly available online. Fish trawl data was accessed via the DATRAS data portal (http://www.ices.dk/marine-data/data-portals/Pages/DATRAS.aspx). The AHOI climatology data (v19.02) was accessed directly from the Thünen Institute website (https://www.thuenen.de/en/sf/projects/ahoi-a-physical-statistical-model-of-hydrography-for-fishery-and-ecology-studies/) and an earlier version (v18.11) is also available via the figshare data portal (https://figshare.com/articles/AHOI_v18_11/3458837/1). The ETOPO1 1arc-minute global relief model was accessed via the NOAA metadata bank (Doi:10.7289/V5C8276M).

3 | Temporal Dynamics of the Size Spectra and Isotopic Ecology of Southampton Water

3.1 Abstract

Current ecological tools are commonly applied at large spatial and temporal scales to infer typical ecosystem behaviour. However the interactions and processes that give rise to ecosystem behaviour are often highly dynamic, occurring over smaller scales than those normally measured. To test the applicability of standard ecological tools at determining dynamic ecosystem behaviour, I estimated the size spectrum and measured stable isotope values, which quantify size structure and trophic interactions respectively, of a seasonally varying estuarine community. I show that the size spectrum of the fish community exhibits strong seasonal periodicity, matching well with known movement patterns. Further, stable isotopes revealed that the food web is predominately based on seasonally pulsed *in situ* phytoplankton production that is rapidly incorporated into fish biomass, faster than expected compared to published isotopic turnover rates. These results indicate that both size spectra and stable isotopes can capture dynamic system behaviour at smaller temporal scales than which they are currently used.

3.2 Introduction

Although the size spectrum was introduced as a concept in section 1.3, in this introduction I briefly expand on its empirical and theoretical applications in ecology. I then introduce stable isotope analyses and their applications for exploring trophic interactions within food webs. Finally, I outline the aims of the research presented within this chapter.

3.2.1 Size Spectra

Condensing information on the community size composition was first introduced as an ecological concept by Elton (1927), who summarised bins of size classes as pyramids of numbers, which later became modified to the classic pyramids of biomass (Bodenheimer, 1938). While the concept of the size spectrum originated from an independent avenue of research (Sheldon et al., 1972, see section 1.3), Trebilco et al. (2013) showed that ecological pyramids and size spectra are merely different representations of the same information, see Fig. 3.1, with a steepening of the size spectrum exponent being equivalent to an increasingly bottom-heavy pyramid.

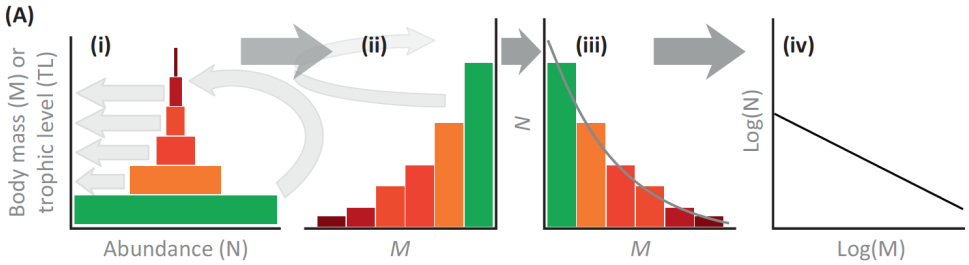

Figure 3.1: When beginning with a trophic-level (TL) pyramid, first convert TL to body mass (M) to give an M pyramid. From the M pyramid, left-align M class layers and rotate 90° counter-clockwise (i to ii); flip the plot onto its vertical axis (ii to iii); express both axes on the log scale, to linearize (iii to iv). Taken from Trebilco et al. (2013).

The distribution of individual body sizes, and therefore biomass, is determined by various ecological and physiological rates, such as growth (both somatic and reproductive), predation, ingestion and egestion, mortality, and metabolism, which act to regulate the flow of energy through the food web (Sprules & Barth, 2016). Since physiological rates and ecological interactions occur at the individual level and are related to body size as

power laws (Peters, 1983; Brown et al., 2004), the emergence of size spectra as power-law distributions is theoretically well-grounded (Kerr & Dickie, 2001).

Changes to underlying ecological processes, or system perturbations, will cause shifts in energy flow and therefore result in changes in the size spectrum, either as shifts in its parameterisation or its functional form (e.g. curvature indicative of departure from steady state). This makes the size spectrum a potentially powerful ecological metric (Gómez-Canchong et al., 2013). For example, Duplisea and Kerr (1995) showed that within a 22-year time series of size spectra of a demersal fish community, the year with exceptionally strong curvature of the spectra (in logarithmic space) coincided with a natural perturbation: an anomalously large biomass of squid. Changes in basal productivity, which affects growth rates throughout the food web, have also been shown to influence size spectra. Increasing oligotrophic conditions, determined by water phosphate concentration, caused a steepening in the plankton size spectra exponents across North American lakes (Sprules & Munawar, 1986). Similarly, Finlay et al. (2007) found increased curvature when measuring the zooplankton size spectra in more productive lake systems.

Fishing applies a notably size-selective pressure as direct mortality and biomass removal of larger bodied individuals in aquatic systems. The use of size spectra as an indicator has been well studied in this regard, showing a steepening with prolonged fishing pressure (e.g. Blanchard et al., 2005; Daan et al., 2005; Yemane et al., 2008). This is apparent even in areas where the magnitude of fishing pressure is relatively low (Dulvy et al., 2004). Robinson et al. (2017) showed changes in size spectra exponents occur in reef fish communities that are highly remote from fish markets and, as an ecosystem metric, were more sensitive than measuring bulk community biomass. However coral reef habitat degradation, which increases predation risk for small fish, results in a shallowing of the spectra, opposite to the effect of fishing (Wilson et al., 2010). This demonstrates that not all anthropogenic impacts will impart the same resultant change on size structure, and makes teasing apart the effects of multiple perturbations challenging. Other anthropogenic driven changes in size spectra have also been demonstrated empirically. Yvon-Durocher et al. (2011) used mesocosm experiments to show the potential effects of

global warming, with a 4°c temperature increase resulting in a steepening of plankton size spectra and an overall reduction in biomass.

Predicting the form of the size spectra under varying conditions allows empirical estimates to be placed into the context of the underlying conditions of the system, a powerful tool in terms of management. For example, Jennings and Blanchard (2004) reconstructed the baseline size spectra of the North Sea based on metabolic theory and compared it to the observed spectra, which had a fish community biomass reduced by 38% compared to the calculated baseline, attributed to fishing. The mathematical simplicity of size-based approaches and their well-defined relationships with biological processes has culminated in a wealth of theoretical modelling that has rapidly increased in complexity and scale over the past decade, with the size spectrum as the primary emergent property (Guiet et al., 2016; Blanchard et al., 2017). This includes incorporation of complex dynamics, such as seasonality (Datta & Blanchard, 2016), predicting the effects of various system perturbations and system resilience (e.g. Rochet & Benoît, 2011; Blanchard et al., 2011), and forecasting the large-scale ecosystem effects of climate change (Blanchard et al., 2012; Woodworth-Jefcoats et al., 2013). For a review on theoretically modelling size spectra see Blanchard et al. (2017).

3.2.2 Stable Isotopes in Food Webs

Following the conjecture of "you are what you eat (plus a few per mil)" (DeNiro & Epstein, 1976), stable isotope analysis (SIA), particularly of carbon, nitrogen and sulfur (δ^{13}C, δ^{15}N and δ^{34}S respectively), has become a fundamental tool in trophic ecology for elucidating diets (Parnell et al., 2010, 2013; Phillips et al., 2014), assigning trophic positions and estimating food chain length (Vander Zanden, Shuter, et al., 1999; Vander Zanden, Casselman, & Rasmussen, 1999a; D. M. Post, 2002), describing individual and population level behaviours (Matthews & Mazumder, 2004; Araújo et al., 2007; Layman et al., 2012), determining resource acquisition (Cherel et al., 2005) and quantifying energy fluxes (Peterson & Fry, 1987; Hecky & Hesslein, 1995; Trueman et al., 2014; Grey, 2016), for reviews see Martínez del Rio et al. (2009) and Boecklen et al. (2011). The premise is that as dietary material is assimilated into organismal tissues, those tissues

incorporate and therefore equilibrate to the isotopic composition of the diet (you are what you eat), offset by the tendency of preferential excretion of lighter elements during physiological processes causing an enrichment of the heavier isotope (plus a few per mil), termed the trophic discrimination factor (TDF). Therefore if the TDF is known and different dietary (basal production) sources are isotopically distinct, then one can infer information on the trophic ecology of the system in question.

Sources of variability in TDFs are numerous, yet often poorly resolved, and include composition and quality of diet (protein content etc.); metabolic/physiological state; species and tissue type effects on physiological routing; and abiotic environment (Caut et al., 2009; K. W. McMahon et al., 2010; Bastos et al., 2017; Blanke et al., 2017; Britton & Busst, 2018). While more sophisticated approaches are being developed to help predict this variability in a modelling approach (Boecklen et al., 2011; Healy, Guillerme, et al., 2017; Healy, Kelly, et al., 2017), point estimates or normally distributed TDFs are more commonly utilised (D. M. Post, 2002; Phillips et al., 2014, but see Bastos et al., 2017).

Carbon is typically assumed to have a negligible TDF (Boecklen et al., 2011), with empirical estimates typically on the order of 0.4-1‰ (DeNiro & Epstein, 1978; D. M. Post, 2002; McCutchan et al., 2003), although values of up to 4‰ have been recorded (Elsdon et al., 2010; K. W. McMahon et al., 2010; Britton & Busst, 2018), making it useful in discriminating between basal production sources fuelling food webs (D. M. Post, 2002; R. Ramos & González-Solís, 2012). This is facilitated by physiological differences in photosynthetic (and chemosynthetic) pathways, e.g. C3/C4 plants, creating disparate δ^{13}C values between different production sources (B. N. Smith & Epstein, 1971). Environmental effects also cause large variation in basal δ^{13}C values (along with other elements), which can impart further separation between sources (R. Ramos & González-Solís, 2012).

In contrast to carbon, empirically estimated TDFs for nitrogen are high, typically on the order of 3-3.4‰, although the variation around this can be large, with estimates ranging from approximately 1 to 8‰ (DeNiro & Epstein, 1981; D. M. Post, 2002; McCutchan et al., 2003; Elsdon et al., 2010; Florin et al., 2011; Heady & Moore, 2013; Blanke et al., 2017; Britton & Busst, 2018). Due to this high rate of fractionation across trophic interactions, nitrogen is useful in determining food web structure and

estimating trophic position (D. M. Post, 2002; Boecklen et al., 2011; Nielsen et al., 2018). Similarly to carbon, sulfur is assumed to have a negligible TDF, although estimates of approximately -3 to 4‰ have been recorded (McCutchan et al., 2003; Florin et al., 2011), and it is particularly useful at separating pelagic and benthic, and marine and freshwater production due to varying nutrient sources (R. M. Connolly et al., 2004).

Another key, but often neglected, source of variability in isotopic composition is the rate at which isotopes are incorporated into body tissues. The isotopic signature of assimilated material fluctuates in natural systems due to changes in diet composition (e.g. seasonal prey availability) and spatiotemporal changes in the isotopic composition of basal production sources (e.g. periods or locations of nutrient upwelling) that determines the isotopic signatures of the diet. Therefore the often implicit assumption that individuals are in equilibrium with their diet (Parnell et al., 2010; Phillips et al., 2014) is likely egregious and can lead to gross misinterpretations of data (O'Reilly et al., 2002).

Isotopes are incorporated into tissue through two process: catabolic turnover of tissues and growth of new tissue mass (Fry & Arnold, 1982). The rate of incorporation depends upon the tissue type in question, typically related to its metabolic activity / protein turnover: blood plasma and liver > muscle and red blood cells > bone collagen (Hobson & Clark, 1992; Martínez del Rio et al., 2009; Crowley et al., 2010; Boecklen et al., 2011). Some tissues, such as bird feathers and fish otoliths, are metabolically inert, therefore incorporate no new material post deposition and do not change in isotopic composition over time (R. Ramos & González-Solís, 2012). Modelling isotopic incorporation into tissues to determine turnover rates typically involves diet switch experiments and the use of mass balanced box models (Martínez del Rio & Carleton, 2012). Typically, one compartment models are used, such that isotopes are incorporated into the tissue of interest from a single source pool (e.g. Fry & Arnold, 1982; Carleton & Martínez del Rio, 2005; Podlesak et al., 2005). However it is possible that this assumption does not hold, with potentially multiple internal source pools might being utilised during turnover, each with separate kinetics. Therefore use of multi-compartment box models has been advocated (Cerling et al., 2007). However empirical support for the use of one or multiple compartment models appears to depend upon the tissue being studied

(Carleton et al., 2008; Heady & Moore, 2013). Importantly, Cerling et al. (2007) showed that tissue growth, if unaccounted for, causes over-estimation of turnover rates.

Recent meta-analyses have found that isotopic turnover rates broadly scale with body size with an exponent of -0.19 and -0.22 (Thomas & Crowther, 2015 and Vander Zanden et al., 2015 respectively), close to that predicted from metabolic theory (-0.25, Brown et al., 2004), however variation around these allometric relationships is large. Further, almost all estimates of isotopic turnover rates are determined experimentally, under varying diet shift scenarios and environmental conditions. Due to limited testing it is unclear whether such estimates reflect 'realised' turnover rates in the field, taking into account factors such as *in situ* growth rate.

3.2.3 Aims

Size spectra and stable isotope analyses offer complementary approaches in exploring energy flows through food webs: size spectra represent the emergent behaviour of size based interactions and processes whereas stable isotopes can be used to infer the movement of biomass through the food web. Currently, empirical studies typically measure across and average over large scales, providing estimates of ecosystem steady-state conditions, i.e. equilibrium solutions (e.g. Jennings, Warr, & Mackinson, 2002; Daan et al., 2005), implying that the structuring within food webs is relatively fixed. However, ecological dynamics do occur over smaller spatial and temporal scales compared to those of such studies. For example, in temperate and polar climes, seasonality causes large periodicity in planktonic production, such that inputs are pulsed rather than continuous (Trebilco et al., 2013). Theory predicts that such behaviour should cause dynamic oscillations within community size spectra (Datta & Blanchard, 2016), corroborated by limited empirical results (Gaedke, 1992). As well as there being seasonal changes in plankton isotope composition (Goering et al., 1990), pulsed plankton production causes temporal variability in the proportion of basal sources fuelling *in situ* food webs and isotopic fractionation processes (Savoye et al., 2003). This variability is expected to propagate up the food chain in a lagged manner due to the rates at which stable isotopes are incorporated into tissues (Thomas & Crowther, 2015; Vander Zanden et al., 2015; Datta

& Blanchard, 2016).

Large scale determinations can fail to capture such dynamical behaviour, as these are either averaged out as noise or missed completely, leading to differing inferences when processes are measured at different scales (Davis & Pineda-Munoz, 2016). Recently, the mismatch between ecological processes of interest and the spatial and temporal scales over which data are collected has been highlighted as a limitation in modern ecology (Chave, 2013; Estes et al., 2018). Smaller scale dynamics are potentially important for accurately modelling whole ecosystem processes such as fisheries production, especially in coastal areas that are poorly resolved (Woodworth-Jefcoats et al., 2013; Jennings & Collingridge, 2015). A first step is to determine whether expected dynamics are suitably captured at the community level by these commonly utilised ecological tools: size spectra and SIA.

In this chapter, I utilise a highly dynamic estuarine environment to test whether the strong seasonal behaviours exhibited within the fish community are captured by size spectra and stable isotope analyses at a monthly temporal resolution - finer than that which is typical of current ecological studies. Fish community size composition was monitored over a seven year period, over which I show that the fish size spectra exhibit consistent seasonal periodicity, matching well with the known influx of small juveniles and emigration of larger individuals during the summer period. Physical samples for SIA, representative of the fish community, were collected over 15 months spanning a complete seasonal cycle, coupled with environmental data measured *in situ* to verify expected seasonal trends. I demonstrate that production from the spring phytoplankton bloom is rapidly incorporated into the fish community at a rate faster than otherwise expected compared to predicted incorporation rates.

3.3 Materials and Methods

3.3.1 Study Site & Data Acquisition

Study Site

Southampton Water is a partially mixed estuary located in southern England (50°52′N, 01°22′W, Fig. 3.2) that is 1.96km wide at its mouth and approximately 10km in length. It has an artificially deepened channel for much of its length that is maintained by periodic dredging. It is fed by three rivers, the Test, Itchen and Hamble, which have a catchment area of around 1500km^2. The estuary itself is hypernutrified with relatively low turbidity: suspended particulates average 40mgl^{-1} at the mouth falling to 5-10mgl^{-1} at the head, making it a highly productive environment (Townend, 2008).

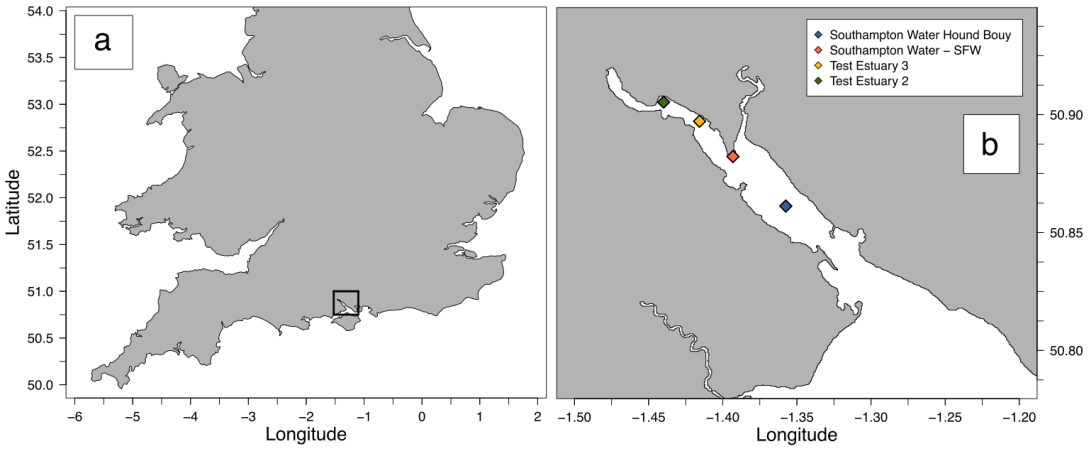

Figure 3.2: Map showing the location of Southampton Water, bounded by the black box, within southern England (a), with an enlarged view of the estuary (b). Coloured diamonds denote sampling locations of environmental data.

Fish Community Data

Due to the industrial and port activities within the estuary, the fish community of Southampton Water are subject to continual ecological monitoring. Species abundance, biomass and size-frequency data were collected monthly from a cooling water intake system (work here using data spanning the period from July 2009 through to November 2016). As the data are commercially sensitive, the exact location is not given, however,

briefly, the sampling methods are as follows. Water from the estuary is drawn in through a large intake, where it passes through a series of filtrations. Very large items, typically branches and large clusters of floating macroalgae, are removed via a coarse grid which is periodically cleaned by a grab system. Rotating drum screens are then employed to separate out weed, plastic and other debris, including fish and invertebrates, which are directly returned to sea via a fish return system. Each month, the return system is netted for a 24-hour period (one 18-hour overnight sample plus 6 hourly samples) for environmental monitoring. Catches are sorted, identified to species level, counted and length-frequency measurements recorded. Representative subsamples are taken for highly abundant species. The results, coupled with the known abstraction rates, can be used to estimate total catches of fish, crustaceans and other invertebrates

Physical samples were collected monthly from the same site from October 2015 through to January 2017 inclusive, providing a representative distribution of the total catch. These were bagged, individual lengths and weights recorded and then frozen for future analyses. Due to the scarcity of large individuals, these samples were supplemented with samples from quarterly trawl surveys within Southampton Water. Each quarter consisted of 6 hauls of approximately 10 minute duration using a 10m bottom otter trawl with a cod end mesh size of 10mm. All trawls occurred within approximately 3km of each other within Southampton Water, centred around the sampling site.

Plankton Community Data

Plankton samples were collected each month from October 2015 through to December 2016 inclusive. Pre-filtered water that excluded macroscopic organisms and debris from the return system was passed through a plankton net with 100μm mesh size for approximately 30 minutes. The net was submerged in a tank to reduce flow through pressure and filtrate volume recorded from outlet flow rates. Samples were condensed to 1 litre volumes, preserved using Lugol's iodine and stored in standard plankton bottles until further analysis.

Plankton community composition was estimated from counts of broad taxonomic identification of 5ml subsamples determined using a standard light microscope. *In*

situ plankton clade concentrations were then estimated using total filtrate volume. Subsamples were diluted when required with dilutions accounted for in concentration estimates. The size distribution of the plankton was determined using a Beckman Coulter LS130 particle analyser, with 6 replicates run per sample, which provides estimates as equivalent spherical diameters of particle volumes. Samples were then filtered onto GF/F filters (Whatman1825 - 047, 0.7μm effective mesh size) using a vacuum pump and then frozen until stable isotope analyses were conducted.

Environmental Data

Nitrate concentration data over the period were sourced from the Environment Agency via the water quality data archive (public sector information licensed under the Open Government Licence v3.0), with sampling locations shown in Fig. 3.2b. Temperature, chlorophyll-a and turbidity time series data were obtained from the Xylem data buoy, located approximately at the Southampton Water Hound Buoy location (Fig. 3.2b). The buoy was fitted with a YSI EX02 multi-parameter mounted with antifouling guards and cleaning rotary wiper brushes on the sensors, providing almost continuous environmental monitoring - data are measured every 15 minutes. Here, data was limited to the 11^{th} of December to the 31^{st} of January inclusive. Prior to this period, the buoy was out of operation for maintenance. The buoy sensors are maintained at a water depth of between 1m and 2m. Data reported here are daily means (95 data points spanning from 00:00 through to 23:45) to average over tidal and diurnal induced fluctuations.

3.3.2 Stable Isotope Analyses

The bulk carbon, nitrogen and sulfur isotopic compositions were determined for monthly samples representative of the fish community and the total plankton filtrate samples. Additionally, various macroalgae, one common bryozoan species (*Tricellaria* sp.), and leaf litter that were sampled during July 2016, upon which they were frozen, were also analysed.

For the fish community, representative samples were determined using the total species and size-frequency data. For each month, individuals were binned into 5mm

length classes (size-frequency data multiplied up for those estimated from subsamples) and then summed over the 7 year period. A random sample (n = 25) of the size distribution was then drawn from these bins for each month with weighting as the square root of the total in each bin, giving a representative, inter-annually averaged, size distribution for each month. Separately, the frequency of occurrence of each species and the total biomass of each species was calculated for each month summed over the 7 year period. A random sample (n = 25) was then drawn with each species given weighting as the fourth root of the product of total frequency and the total biomass, so as to avoid biasing towards either small, abundant species, or large but infrequent species. The monthly random draws were then combined and individuals selected to best match the size and species distributions for each month.

For stable isotope analyses (SIA), small plugs of muscle (*circa* 0.5cm^3) were taken from individual fish below the second dorsal fin, with skin removed, and stored in Eppendorf tubes and refrozen. For small individuals, whole fillets were taken with skin, spines and bones removed were possible to avoid isotopic disparity between tissue types. All samples for SIA were freeze-dried at -55°c for 24 hours (Heto Power dry LL3000, whole samples in tin for macroalgae, bryozoan and leaf litter, whole filters for plankton filtrate) then stored at room temperature in sealed containers. Dehydrated tissue samples were homogenised using a pestle and mortar and 1.9mg +/- 0.1mg samples were measured into tin boats using a Sartorius microbalance with a precision of 0.001mg. For plankton filtrate, 3 small semicircular plugs of 12mm diameter were taken from the filters for each month and wrapped into tin boats (area taken determined by a small pilot study of varying plug sizes to determine optimal area). Samples were analysed at NERC Life Sciences Mass Spectrometry Facility, SUERC, using an Elementar vario Pyrocube (Hanau, Germany) coupled to an IsoPrime (now Elementar) VisION Mass Spectrometer (Cheadle, UK). We assume that Lugol's iodine does not influence the isotopic signatures of plankton as the preservative does not include carbon, nitrogen or sulfur containing compounds.

All isotopic values are reported relative to their respective international standards: Pee Dee Belemnite (PBD) for carbon, atmospheric air for nitrogen and Cañon Diablo

Troilite (CDT) for sulfur. Isotopic compositions are expressed as delta (δ) per mille (‰) notation, given by:

$$\delta X = \left[\frac{R_{sample}}{R_{standard}} - 1 \right] \times 1000 \tag{3.1}$$

where X is either ^{13}C, ^{15}N or ^{34}S and R is the ratio of ^{13}C:^{12}C, ^{15}N:^{14}N or ^{34}S:^{32}S. Equipment calibration and compensation for drift over time was corrected for by internal standards run between every 10 samples, with analytical measurement errors of 0.1‰, 0.2‰ and 0.6‰ for δ^{13}C, δ^{15}N and δ^{34}S respectively.

3.3.3 Estimation of Size Spectra

For each month, fish size-frequency data were pooled across species (multiplied up for those estimated from subsampling). Data were limited to fish above 30mm in length due to reduced catch efficiencies at smaller sizes. Individual measures of length were binned into 5mm classes to match size-frequency data. Size spectra were then estimated for each month following the maximum likelihood methods for binned data following Edwards et al. (2017), with the x_{min} for each month limited to the most abundant size-class. Months with fewer than 100 individuals in total were excluded. Since length data were used, this produces individual length spectra. Typically, size spectra are reported using individual biomass or volumes (Kerr & Dickie, 2001). Given that:

$$S_L \approx L^{\beta_L} \tag{3.2}$$

where S_L is the length spectra with exponent β_L, and that the mass-length relationship of fish is also a power law (Froese, 2006):

$$M = aL^b \tag{3.3}$$

it follows that the exponent for the individual biomass spectra, S_M, can be approximated by:

$$S_M \approx M^{\beta} \propto L^{\frac{\beta_L}{b}} \tag{3.4}$$

where exponents β_L and b are from Eqs. 3.2 and 3.3 respectively. Previous studies have estimated eq. 3.3 separately for individual species and applied corrections to length data prior to estimating the size spectra. Here, we simply use the median value of $b = 3.025$, which is an average taken from 1773 species (Froese, 2006), to approximate the individual biomass spectra from length data following Eq. 3.4.

The size distribution for the plankton samples, estimated from the Beckman Coulter LS130 particle analyser, is provided as proportions within predefined, logarithmically-scaled size classes. Since information is not provided on individual particle size, maximum likelihood methods cannot be directly applied. Instead, mean proportions for each size class were calculated across replicates and normalised to the width of the respective size-class. Data were limited to those size-classes with equivalent spherical diameter intervals spanned $\geq 100\mu$m, the plankton net mesh size. The size spectrum exponent, β, was then estimated as the slope of the linear regression of logarithmically transformed normalised mean proportion (equatable to normalised abundance) and the size-class interval mid-point (Sprules & Barth, 2016; Edwards et al., 2017), with the x_{min} limited to the size-interval with the highest abundance.

3.3.4 Statistical Analyses of Stable Isotope Data

Fish species were assigned to a functional group, either benthic, bentho-pelagic or pelagic, based on prey consumed as described in Heessen et al. (2015). Further, statistical analyses of the fish community were limited to those species with a minimum number of 7 individuals over the sampling period. Flounder, *Platichthys flesus*, were excluded as the majority of individuals were young of the year (standard length $<$ 80mm, n = 7 of 10) occurring in March and April 2016, with juveniles being known to inhabitat the far upper reaches of estuaries (salinities $<$ 3, Kerstan, 1991) and therefore are exposed to very different isotopic baselines. Thornback rays, *Raja clavata* (n = 9), were also excluded as urea-based osmotic physiology results in differing muscle isotope fractionation pathways (N. Hussey et al., 2012; Kim & Koch, 2012). The δ^{13}C of all fish samples were lipid corrected following Kiljunen et al. (2006) prior to statistical analyses.

Temporal trends and effects of individual traits on stable isotope composition were

tested for using mixed effects models conducted separately for each element. Models included size (as base 10 logarithmically transformed wet weight), functional group (FG) and month as fixed effects with random intercept and individual slope with mass effects by species. Model selection was conducted sequentially by analysis of variance between models in a hierarchical manner (i.e. only nested model structures were compared). All analyses were conducted in *R* 3.3.2 (R-Core-Team, 2016), utilising the package "lme4" for mixed effects models (Bates et al., 2015).

3.4 Results

3.4.1 Fish Community Size Spectra

The time series of the monthly size spectra calculated for the fish community are shown in Fig. 3.3. The time series shows strong seasonality, with a steepening of the spectra in late spring to early summer, peaking typically in May, and minima during winter. A second, smaller peak often occurred during the autumn. The variation exhibited by the slope of the size spectra is large, ranging from 0.551 in December 2015 to 4.82 in May 2012. Size spectra exponents were not dependent on the value of x_{min} ($F_{1,78} = 0.236$, $p = 0.628$).

3.4.2 Plankton Community Composition and Size Spectra

The phytoplankton community (size $\geq 100\mu m$) was dominated throughout the year by diatoms including *Odontella, Coscinodiscus, Rhizosolenia* and *Thalissosira* spp.. Calanoid copepods (and to a lesser extent, their nauplii larvae) numerically dominated the zooplankton except for June 2016 were various meroplanktonic invertebrate larvae showed increased abundance, particularly bivalves and cirripedia. Broad relative proportions are shown in Fig. 3.4. Abundance estimates of sampled phytoplankton, zooplankton and detritus are shown in Fig. 3.5. Phytoplankton abundances were low throughout the winter months, but peaked in June 2016 before slowly decreasing to winter levels. Zooplankton abundances showed a similar pattern to phytoplankton, with a large increase concurrent with the peak in phytoplankton, but peaking in August before decreasing to

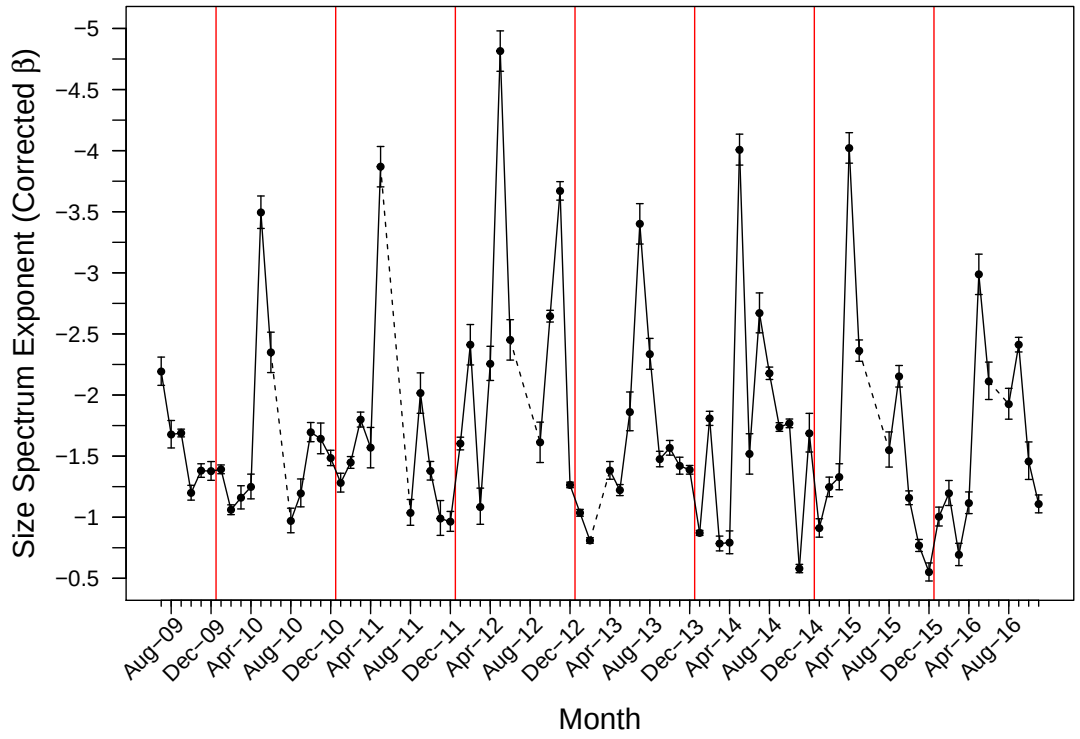

Figure 3.3: Time series of the estimated monthly exponents of the individual size spectra, corrected following Eq. 3.4 with 95% confidence intervals plotted as error bars. Period spans from July 2009 to November 2016. Dashed black lines indicate months have been excluded due to having less than 100 individuals (no data were available for March 2013). Solid red lines mark the commencement of new years. Note that the y-axis is reversed so that steeper size spectra are plotted higher.

winter levels. Levels of detritus were variable throughout the period, but proportionally dominated samples in January and November 2016. Detritus included suspended sediment grains, zooplankton moults, plant matter and fibres.

Individual plots of plankton size spectra are shown in Fig. 3.6. The results show a strong steepening of the spectra during May 2016, coincident with the dominance of phytoplankton within the sample. However most spectra show systematic curvature, suggesting deviation from a power law distribution and therefore are not considered any further during analyses.

3.4.3 Environmental Data

The nitrate concentration data are plotted in Fig. 3.7, and show high variability between stations, particularly during the winter months. Nitrate concentrations in the winter

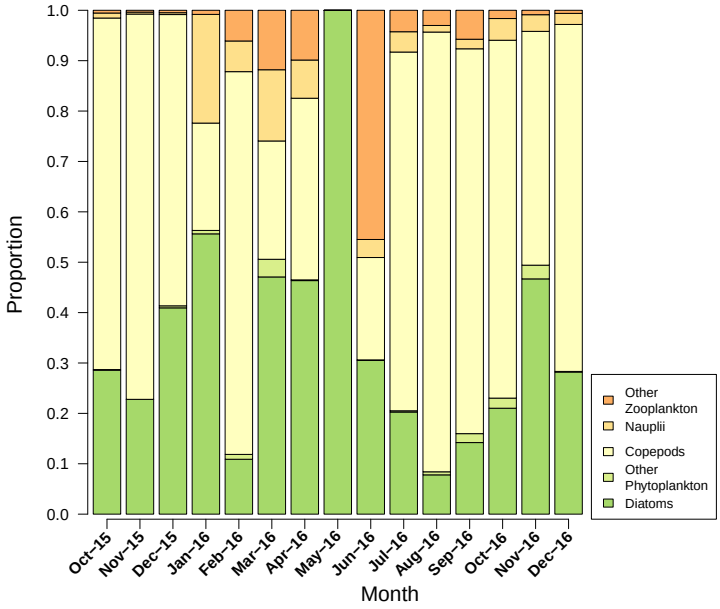

Figure 3.4: Overview of the relative plankton community composition, excluding detritus, from October 2015 through to December 2016.

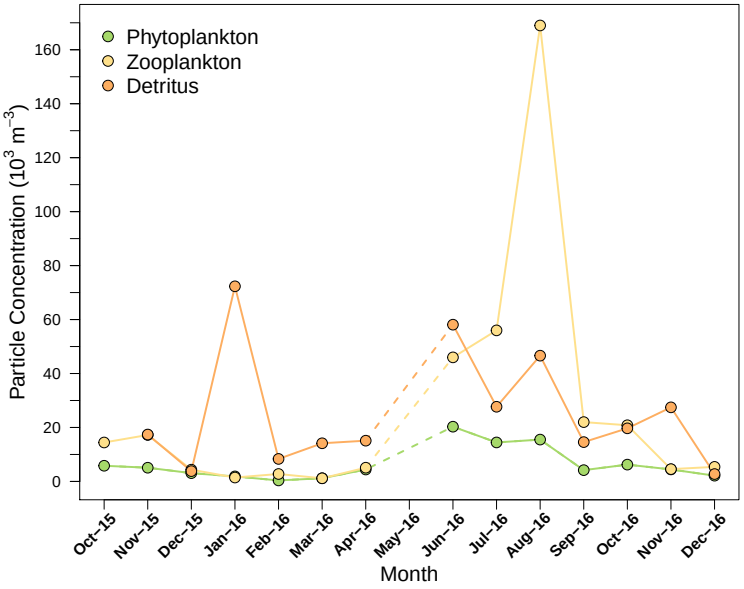

Figure 3.5: Time series of phytoplankton, zooplankton and detritus abundance estimates from October 2015 through to December 2016. No estimates are available for May 2016 due to high densities of diatoms and their associated phyto-detritus causing obscuration even under large subsample dilutions. No detritus estimate is available for October 2015.

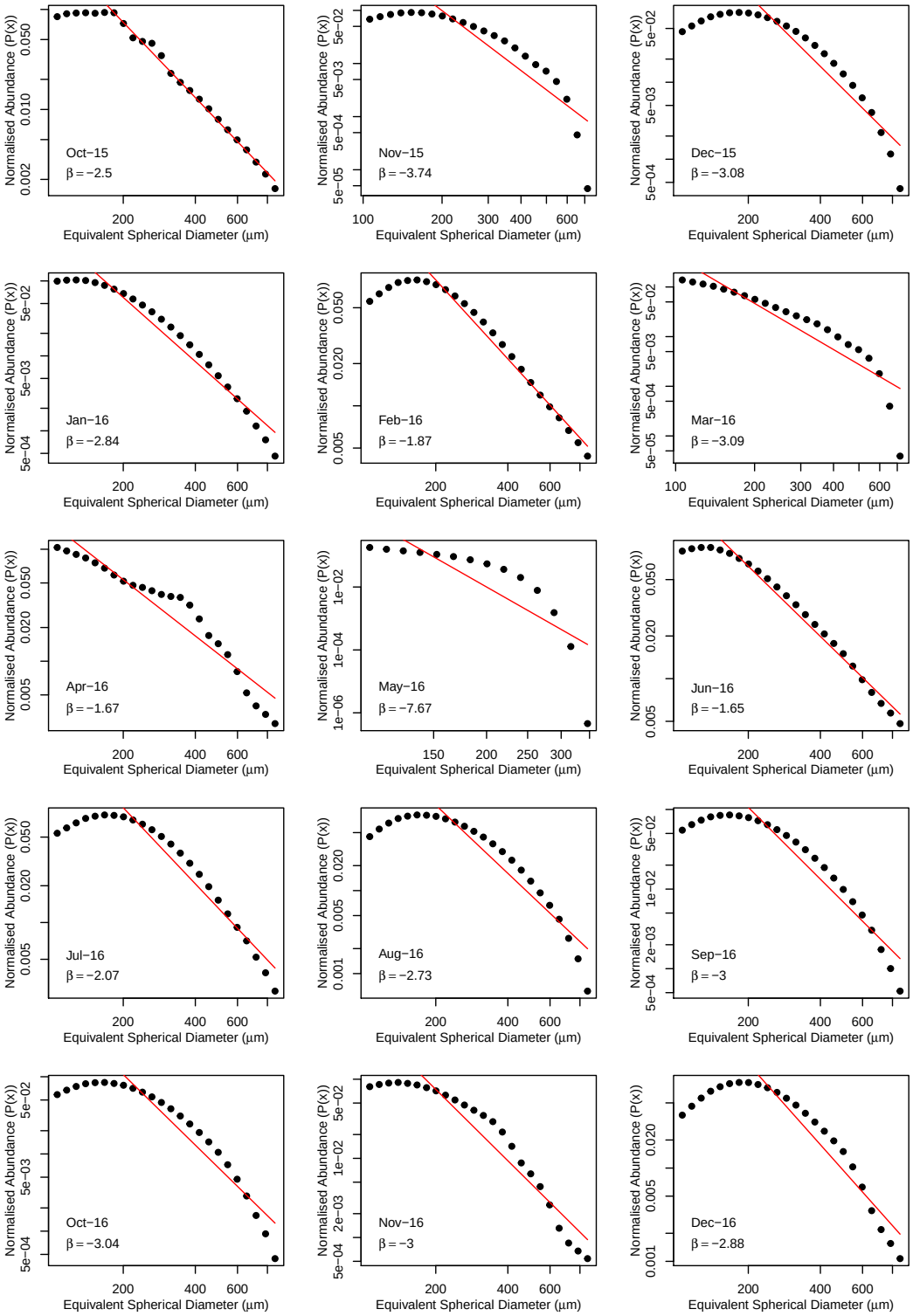

Figure 3.6: Individual plots of sampled plankton filtrate normalised mean proportion, $P(x)$, where x is the mid-point of the size class, against the equivalent spherical diameter (μm). Note the axes are on logarithmic scales. Solid red line indicates linear regression on logarithmically transformed data, with a minimum cut-off from the highest abundance size-class, used to estimate the size spectra exponent β ($b = \beta$). However strong, systematic curvature across multiple months indicates deviation from a power law distribution.

are relatively high, with a sharp decrease from May to June (change in mean from approximately 145 to 26 μMl^{-1}), after which there is a gradual increase through to winter.

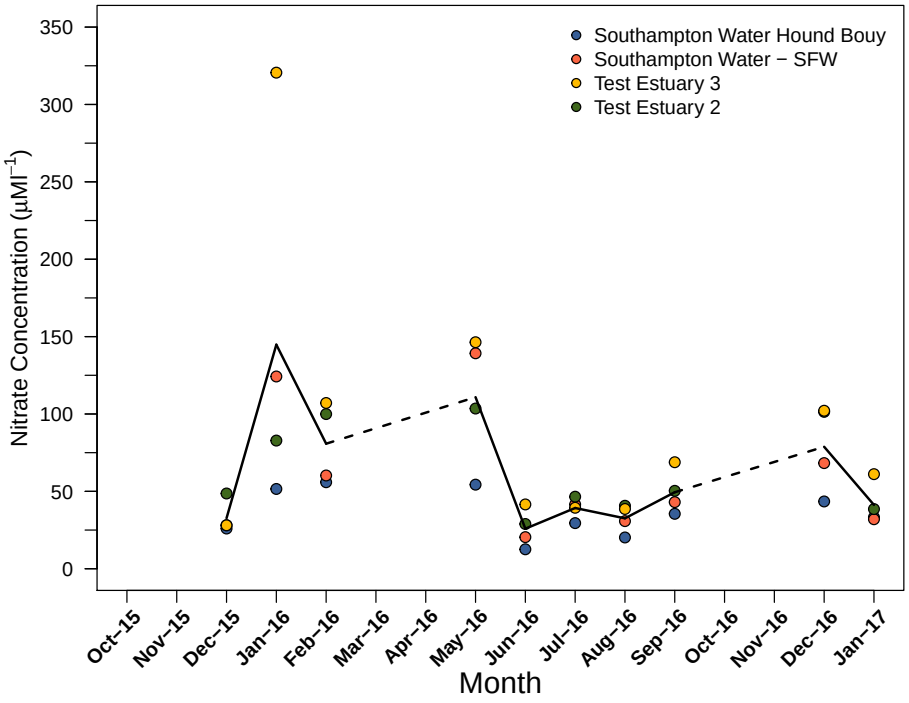

Figure 3.7: Time series of water N-nitrate concentrations recorded at four sampling stations (see Fig. 3.2b for station locations) acquired from the Environment Agency. Only winter and summer months are monitored. Line shows mean concentration of the four stations, and is dashed when spanning non-sampled months.

Temperature, chlorophyll-a and turbidity time series are shown in Figs. 3.8, 3.9 and 3.10 respectively. The temperature data show the typical seasonal cycle exhibited by temperate estuaries, Fig. 3.8. For 2015-2016, the winter minimum occurred in February and March, with temperatures as low as 8°C. From April 2016, water temperature rapidly increased, reaching approximately 20°C by the end of July 2016, a peak which is maintained until early September, after which temperatures rapidly decrease through autumn to winter, reaching as low as 6°C by January 2017. The data here indicate that the winter of 2015-2016 was milder compared to that of 2016-2017.

The daily chlorophyll-a concentrations, a proxy for phytoplankton abundance, show the seasonally variability in phytoplankton, Fig. 3.9. Winter concentrations are low,

typically $0.5\mu gl^{-1}$, with the bloom commencing in April and peaking in May after increasing by 3 orders of magnitude to approximately $500\mu gl^{-1}$. Chlorophyll-a concentrations then decrease through June and July, however a smaller second bloom occurs in August, peaking at approximately $10\mu gl^{-1}$, after which concentrations decrease again through autumn, reaching a minimum by December 2016. Superimposed upon this overall trend is an approximate two week periodicity which is particularly apparent in the autumn.

The turbidity within Southampton Water was highly variable, and appears to show periodicity throughout the year with peaks occurring approximately every two weeks, Fig. 3.10. Although variability is high, a seasonal trend is apparent: the summer period from May through to early August shows mean turbidity at approximately 0FNU with the periodicity highly dampened. The spring, winter and autumn periods all show an elevated mean turbidity compared to the summer of approximately 4FNU , with periods of strong fluctuations in late March to early April and October through to the end of November 2016.

3.4.4 Stable Isotope Analyses

Plankton

Time series of the isotopic composition of plankton filtrate, i.e. the combined phytoplankton, zooplankton and detritus, are shown in Fig. 3.11. Across all three elements, January 2016 showed strong depletion in the heavier isotopes, particularly in sulfur. A similar, but less pronounced, pattern can also been seen in November 2016. This coincides with high proportional dominance of detritus within the samples, see Fig. 3.5. Excluding these two months, variability in $\delta^{13}C$ was relatively low with values typically of -24‰, except for a peak in April of -22.7‰ followed by strong depletion in May to -26.8‰ when the sample solely consisted of diatoms and their phytodetritus. More pronounced seasonal trends can be seen in the $\delta^{15}N$ values. Late winter to early spring (December 2015 through to April 2016) showed elevated levels of between 9‰ and 10.5‰. Following the large phytoplankton bloom, see Figs. 3.4 and 3.9, a minimum is observed of 7.1‰ after which values slowly increase until August when zooplankton dominated the sample. Values then decrease again in September, coinciding with the commencement of the smaller

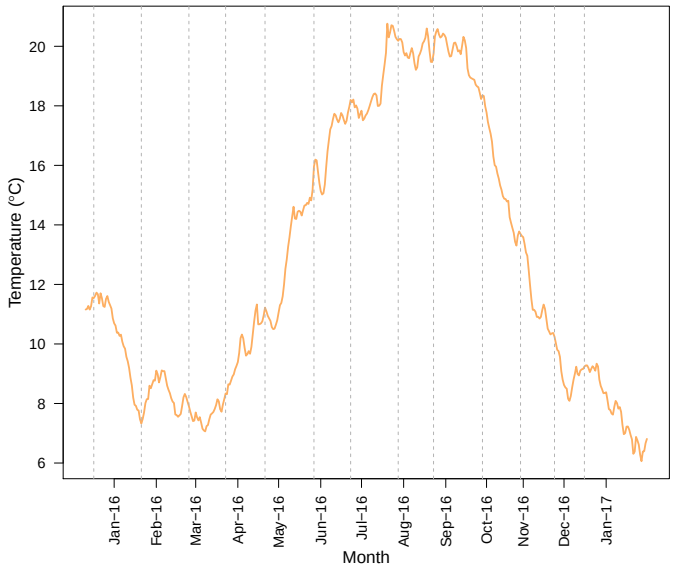

Figure 3.8: Time series of average daily water temperature recorded by the Xylem data buoy from the 11^{th} of December to the 31^{st} of January inclusive. Ticks on the x-axis show the commencement of individual months. Dashed grey lines indicate dates when physical plankton samples were collected.

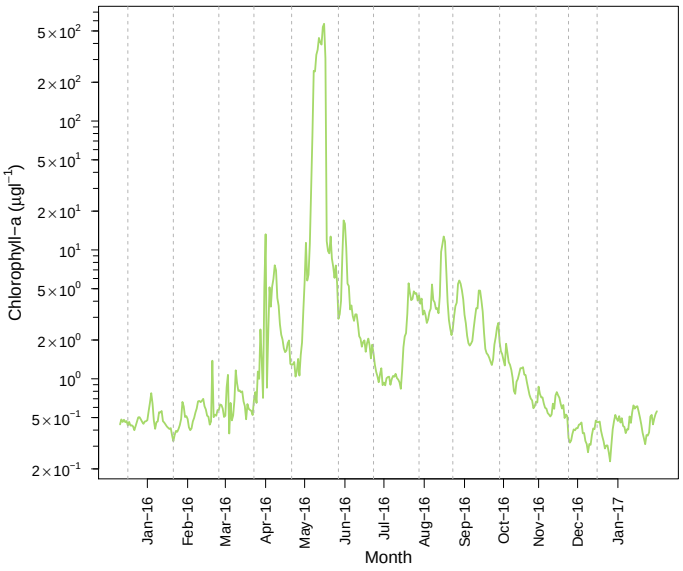

Figure 3.9: Time series of average daily chlorophyll-a concentration estimated from water fluorescence recorded by the Xylem data buoy from the 11^{th} of December to the 31^{st} of January inclusive. Ticks on the x-axis show the commencement of individual months. Dashed grey lines indicate dates when physical plankton samples were collected. Note the y-axis is on a logarithmic scale.

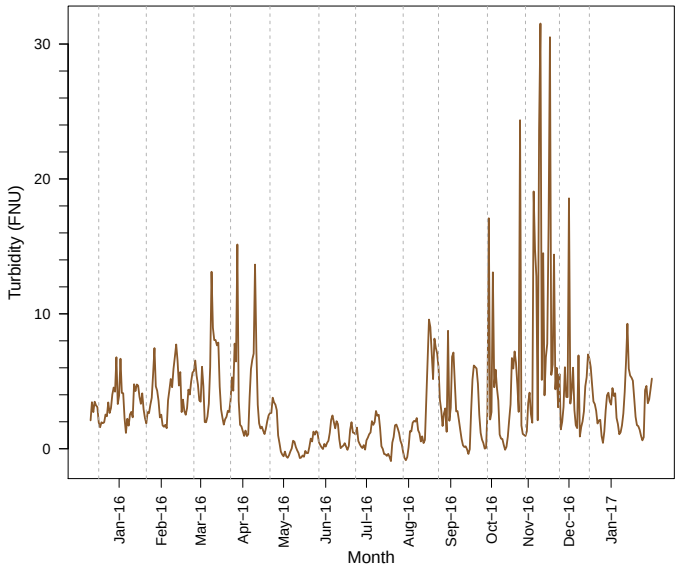

Figure 3.10: Time series of average daily water turbidity, given in Formazin Nephelometric Units (FNU), estimated from the degree of scattering of emitted infrared light, recorded by the Xylem data buoy from the 11^{th} of December to the 31^{st} of January inclusive. Ticks on the x-axis show the commencement of individual months. Dashed grey lines indicate dates when physical plankton samples were collected. For clarity, three exceptionally high data points have been removed: 14^{th}, 15^{th} and 18^{th} of August 2016 with values of 73.5, 66.9 and 88.7FNU respectively.

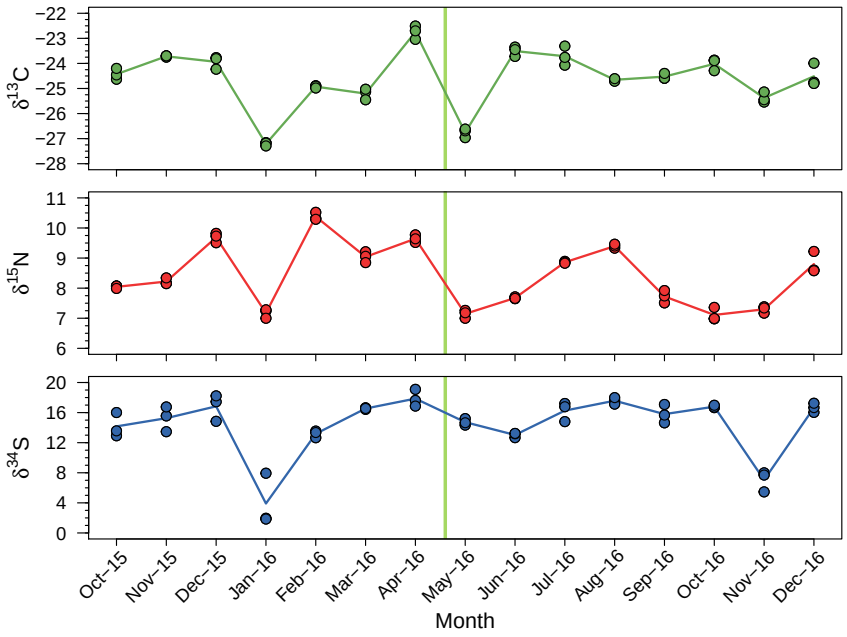

Figure 3.11: Time series of the δ^{13}C, δ^{15}N and δ^{34}S isotopic composition of plankton filtrate sampled from Southampton Water. Solid lines connect monthly means of 3 samples. Green vertical line demarcates the approximate position of the peak phytoplankton bloom.

second phytoplankton bloom, Fig. 3.9, to a second minimum of 7.1‰ in October, after which values increase going into winter. Sulfur isotopic composition appears to remain quite stable throughout the year within the plankton community at approximately 16‰, except for during the early summer where a minimum of 13.0‰ occurs in June 2016, shortly after the major phytoplankton bloom. Such trends should be interpreted with caution however, as the filtrate composition was highly variable across sampled months.

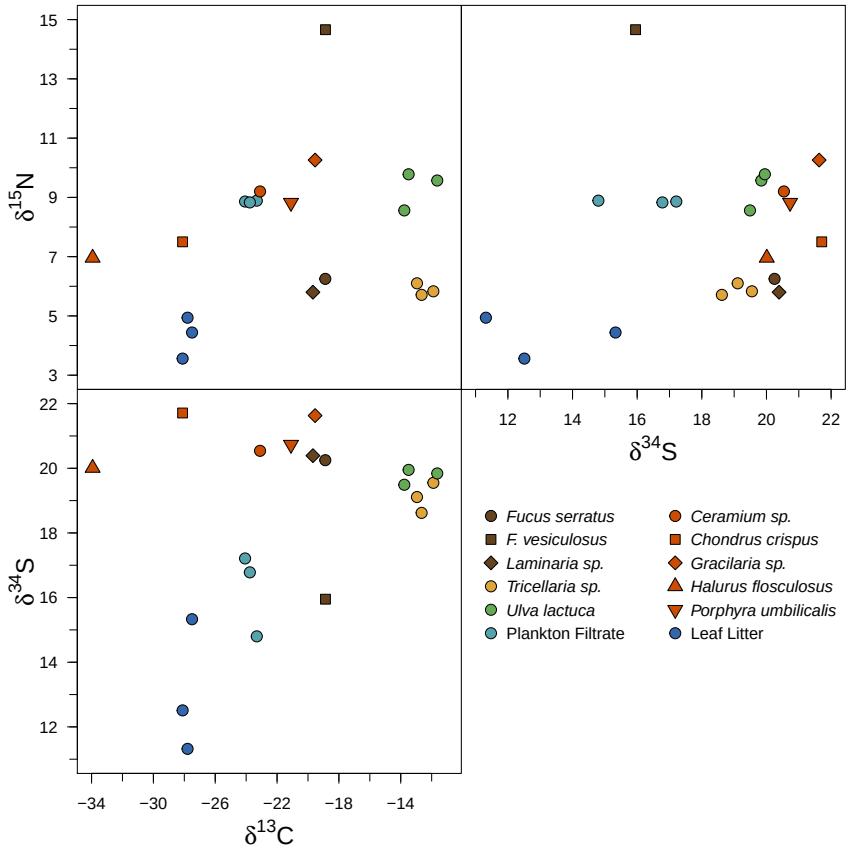

Figure 3.12: Bi-plots of the δ^{13}C, δ^{15}N and δ^{34}S stable isotope composition of various macroalgae, leaf litter, a bryozoan species and plankton filtrate sampled in July 2016. Colours indicative of broad taxonomic clade (red = red algae, green = green algae, brown = brown algae, yellow = bryozoa, dark blue = leaf litter and light blue = plankton filtrate). Unique symbols within brown and red algae denote separate species. Samples of *Ulva lactuca* and *Tricellaria sp.* were taken from the same macroalgae cluster and colony respectively.

Bi-plots of the various macroalgal species, leaf litter and bryozoa sampled in July 2016 are shown in Fig. 3.12, along with the concurrently sampled plankton filtrate. Variability across all three elements is high, with ranges from -33.6 to -11.4, 3.6 to 14.7 and 11.3 to

Table 3.1: Major fish species (n > 7) by functional group included in the statistical analyses of stable isotope composition of the Southampton Water fish community, excluding flounder, *Platichthys flesus*, and thornback rays, *Raja clavata*. Complete list of fish species can be found in the Appendices.

Benthic		**Bentho-Pelagic**		**Pelagic**	
Common Name	**Species**	**Common Name**	**Species**	**Common Name**	**Species**
Sand Goby	*Pomatoschistus minutus*	Pout	*Trisopterus luscus*	Sprat	*Sprattus sprattus*
Rock Goby	*Gobius paganellus*	Whiting	*Merlangius merlangus*	Herring	*Clupea haregus*
Black Goby	*Gobius niger*	Sea Bass	*Dicentrarchus labrax*	Transparent Goby	*Aphia minuta*
Sole	*Solea solea*	Sand Smelt	*Atherina spp.*		
Tub Gurnard	*Chelidonichthys lucerna*				

21.7‰ for δ^{13}C, δ^{15}N and δ^{34}S respectively. Macroalgae span the range of δ^{13}C values, with *U. lactuca* being notably high (*circa* -12‰), brown macralgae clustered around -19‰ and red algal species spanning from -33.6 to -19.5‰. For δ^{15}N, the majority of samples had values around 8‰, although leaf litter was slightly lower at approximately 4‰ and *F. serratus* appears anonymously high at 14.7‰. Leaf litter have notably low δ^{34}S values, and to a lesser extent, the plankton filtrate, compared to the macroalgae, which, apart from *F. serratus*, are clustered around values of $\sim$ 21‰.

Fish Community Isotopic Ecology

The exclusion of transient species (those with fewer than 7 individuals over the whole period), as well as flounder and thornback rays, reduced the total sample size from 450 to 379 and the number of species from 32 to 12. The species included in statistical analyses are listed in table 3.1, whose individual carbon to nitrogen ratios ranged from 3.05 to 4.52, with a mean of 3.32 ($\pm$ 0.18 standard deviation). Overall, the fish community showed large variation in stable isotope composition (although less than that exhibited by the productions sources) across all three elements, see Fig. 3.13, with ranges from -21.3‰ to -13.9‰, 10.4‰ to 18.7‰ and 9.8‰ to 19.5‰ for δ^{13}C, δ^{15}N and δ^{34}S respectively.

Model selection determined that several factors beyond random species effects explained variation in individual stable isotope composition. Interactive effects and correlations between random intercept and slope effects were excluded due to the high number a parameters causing models to become degenerate. The optimal mixed effects models for

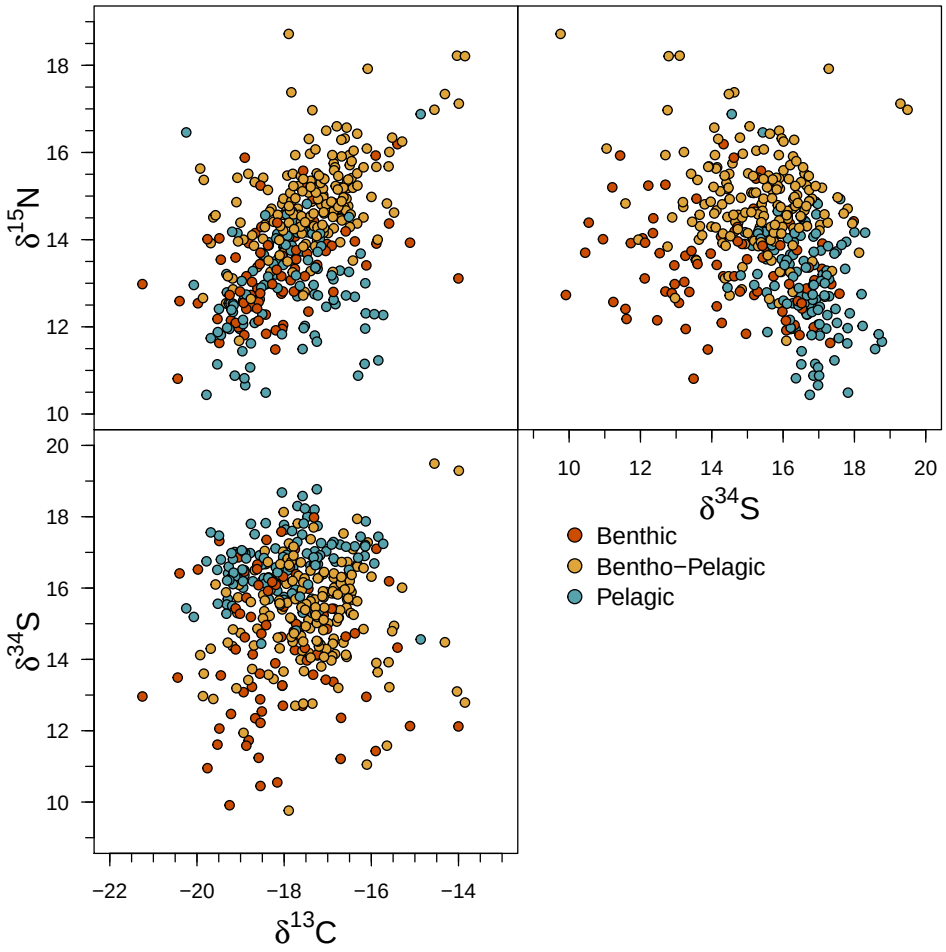

Figure 3.13: Bi-plots of the δ^{13}C, δ^{15}N and δ^{34}S stable isotope composition of individual fish included in mixed effects models (n = 379), coloured by functional group.

each stable isotope element within the fish community were:

$$\begin{aligned}
\delta^{13}\text{C} &\sim \log_{10}(\text{Mass}) + \text{Month} + (1 \mid \text{Species}) + (0 + \log_{10}(\text{Mass}) \mid \text{Species}) \\
\delta^{15}\text{N} &\sim \log_{10}(\text{Mass}) + \text{Month} + (1 \mid \text{Species}) + (0 + \log_{10}(\text{Mass}) \mid \text{Species}) \\
\delta^{34}\text{S} &\sim \log_{10}(\text{Mass}) + \text{FG} + (1 \mid \text{Species}) + (0 + \log_{10}(\text{Mass}) \mid \text{Species})
\end{aligned} \tag{3.5}$$

For all three elements, there was a global change in delta values with increasing mass: for δ^{13}C and δ^{15}N, an order of magnitude increase in mass resulted in an average increase of 0.44‰ and 0.45‰ respectively, however for δ^{34}S an order of magnitude increase in mass caused a change of -0.48‰, see Fig. 3.14. Around these global averages were random species effects with standard deviations of 0.37, 0.46 and 0.23 for δ^{13}C, δ^{15}N

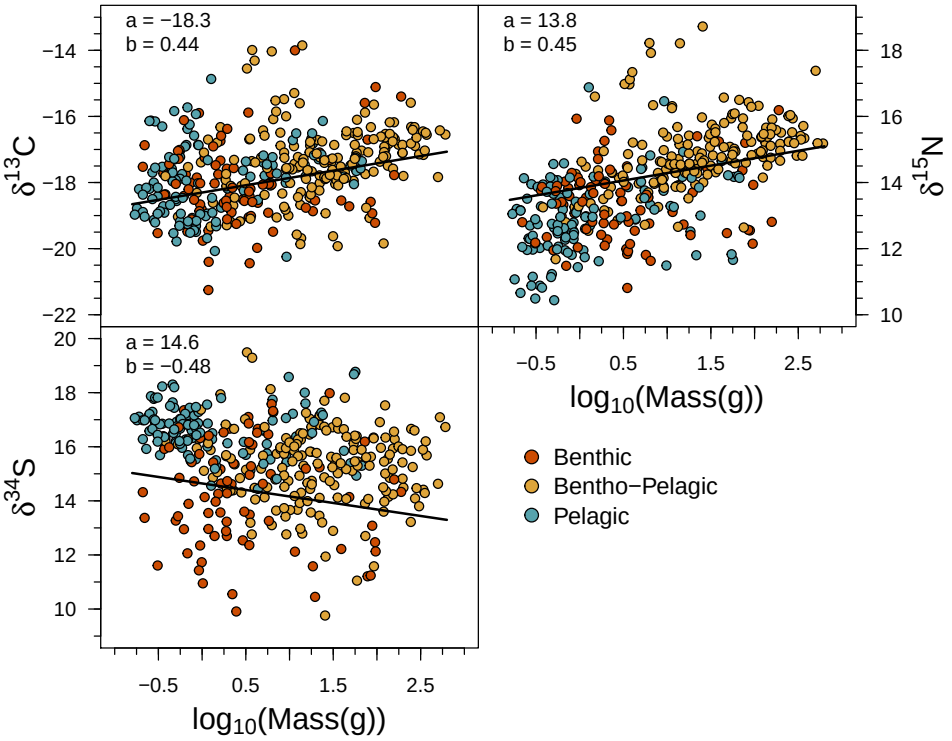

Figure 3.14: Plots of δ^{13}C, δ^{15}N and δ^{34}S against the logarithmic (base 10) size of individual fish included in mixed effects models (n = 379), coloured by functional group. Solid black lines show global effect of size on respective element from optimal mixed effects models described in Eqs. 3.5 with coefficients inset. Note that, for δ^{34}S, the global effect is referenced to the benthic functional group.

and δ^{34}S respectively.

Significant temporal trends were observed in the δ^{13}C and δ^{15}N values of the fish community, eqs. 3.5, which are shown in Fig. 3.15. For carbon, May was significantly higher than the reference month of January (mean difference of 2.58‰), with June and August also being significantly higher, although less pronounced (mean differences of 0.59‰ and 0.62‰ respectively). For nitrogen, δ^{15}N values showed a smoother temporal trend, with higher levels in winter and significantly lower values through the summer (May through to October inclusive, with a minimum in June of -1.30‰ mean difference). While there were no significant temporal trends in δ^{34}S, it was the only element which showed significant mean differences between functional groups: globally, benthic individuals had an average δ^{34}S of 14.6‰ increasing significantly by 1.33‰ and 2.00‰ for the bentho-pelagic and pelagic group respectively ($p = 0.022$ and $p <$

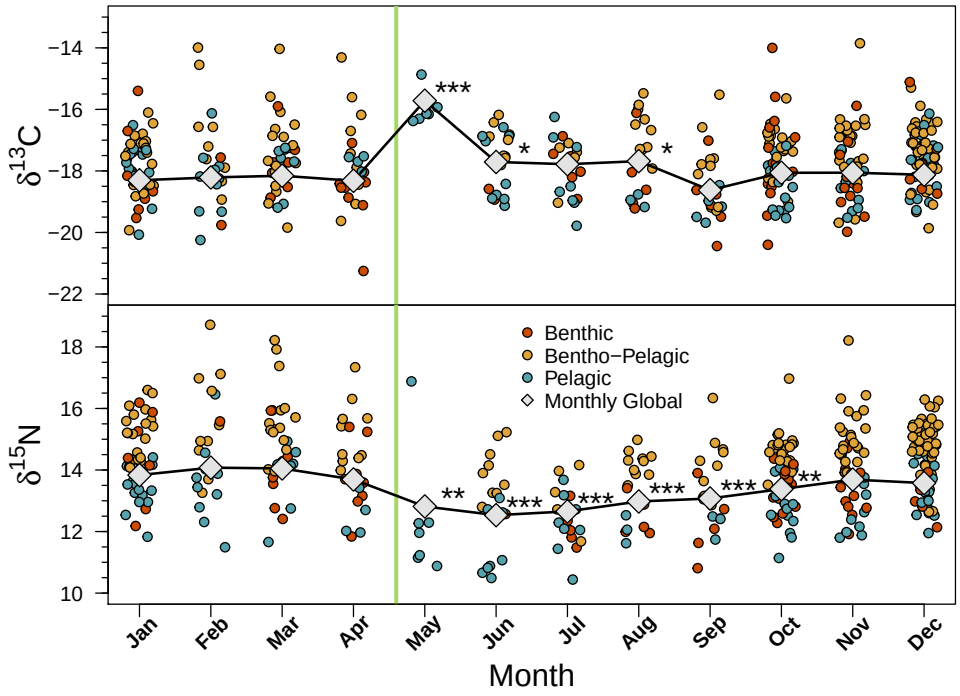

Figure 3.15: Time series of δ^{13}C and δ^{15}N values of individual fish included in mixed effects models (n = 379), coloured by functional group. Solid black lines and grey diamonds show global effect of month on respective element from optimal mixed effects models described in eqs. 3.5. Asterisks denote months that are significantly different from the reference month, January (* = $p < 0.05$, ** = $p < 0.01$ and *** = $p < 0.001$). Green vertical line demarcates the approximate position of the peak phytoplankton bloom. Data are jittered along the x-axis for visual clarity.

0.001, see Fig. 3.13). The random species effects are shown in table 3.2, with remaining residual standard deviation of 0.93, 0.76 and 1.25 for δ^{13}C, δ^{15}N and δ^{34}S respectively.

3.5 Discussion

3.5.1 Seasonality in Size Spectra

The data presented here, which span over 7 seasonal cycles, exhibit consistent cyclical patterns, of a rapid steepening of the fish size spectra from winter lows of $\beta \approx -1$ to late spring / early summer highs of $\beta \approx -4$. In all years except for 2013 (and, to a lesser extent, 2010), a second smaller peak in the autumn is also apparent. This pattern is almost certainly driven by the inshore migrations and spawning behaviours of the dominant smaller-sized species within Southampton Water: sprat (Munk, 1991),

Table 3.2: Table of the random effects of individual species (common name given, latin names can be found in table 3.1) on the intercept, (1 | Species), and the slope with size, $(0 + \log_{10}(\text{Mass}) \mid \text{Species})$ determined by the optimal mixed effects models in Eq. 3.5.

Fish Species	δ^{13}**C**		δ^{15}**N**		δ^{34}**S**	
	Intercept (‰)	Slope	Intercept (‰)	Slope	Intercept (‰)	Slope
Black Goby	-18.6	0.45	13.0	0.59	14.0	-0.50
Rock Goby	-18.8	0.21	13.0	-0.11	16.1	-0.39
Sand Goby	-18.1	0.26	14.1	0.65	14.0	-0.59
Sole	-18.6	0.20	12.6	0.44	14.3	-0.50
Tub Gurnard	-18.3	0.76	13.8	0.66	14.8	-0.52
Pout	-18.1	0.36	14.7	0.29	14.9	-0.60
Sand Smelt	-18.4	0.39	13.8	0.79	14.0	-0.63
Sea Bass	-17.2	0.042	15.9	-0.017	14.3	-0.61
Whiting	-18.6	0.64	14.0	0.70	15.3	-0.34
Herring	-18.2	0.36	14.2	-0.096	14.6	-0.30
Sprat	-18.9	1.09	12.8	0.30	14.6	-0.31
Transparent Goby	-17.9	0.52	14.1	1.21	14.7	-0.48
Standard Deviation	**0.52**	**0.37**	**0.92**	**0.46**	**0.66**	**0.23**

sandsmelt (Henderson et al., 1984), transparent gobies (Heessen et al., 2015) and sand / common gobies (Miller, 1975; Arruda et al., 1993); coupled with the movement of larger fish out of the estuary during the warmer summer months (Claridge et al., 1986; Potter et al., 1986). Previous studies exploring the seasonality of size spectra have mostly focused on the small end of the particle size distribution, notably the phytoplankton and zooplankton compartments (Bailey-Watts, 1986; Villate, 1991; Gaedke, 1992; Lam-Hoai et al., 2006; Zhou et al., 2009), with the typical pattern being of dominance of smaller body sizes in the spring and summer bloom leading to a steepening of the spectra compared to winter distributions. However, comparatively, the changes exhibited in the fish spectra here are much more stark, for example, Gaedke (1992) noted a decrease in the plankton size spectra of only approximately 0.3 from spring to autumn in large temperate lake system.

To the best of my knowledge, the only other study exploring the seasonal trend in size spectra for a fish community was by McGarvey and Kirk (2018), although their study included macroinvertebrates and was limited to only four temporal samples. Comparatively, they also noted much smaller changes in the size spectra compared to here, with β ranging from -1.81 in May to -1.65 in October. Other temporal studies of fish size spectra study more long term, inter-annual trends (Rice & Gislason, 1996; Jennings, Greenstreet, et al., 2002; Nicholson & Jennings, 2004). It is even suggested that size spectra are relatively insensitive at detecting more short term responses in fish

communities to perturbations (Nicholson & Jennings, 2004). While it is expected that seasonal oscillations in size spectra are dampened towards the larger body sizes (Guiet et al., 2016), estuaries are highly productive environments that are key nursery grounds for many fish and invertebrate species (Beck et al., 2001), and therefore some of the most dynamic habitats in terms of community structure and composition. It is not surprising therefore that the seasonality is so strongly expressed in the size spectra here.

3.5.2 SIA and Incorporation of Production

In general, sulfur SIA showed results as expected. Sulfur present in the water column that is incorporated into phytoplankton production is typically in the form of sulfates and is isotopically enriched in heavy sulfur (approximately 20-21‰) whereas benthic production utilises bacterially produced sulfides that have lower δ^{34}S values (approximately -24‰) due to high fractionation during reduction processes (Rees et al., 1978; Fry, 2002; R. M. Connolly et al., 2004). This was apparent in the plankton filtrate isotope composition, were months with high amounts of detrital inputs, and assumably associated sedimentary bacteria, caused a large reduction in δ^{34}S, see Fig. 3.11. Despite limited to negligible fractionation of sulfur occurring during photosynthetic fixation (Fogel & Cifuentes, 1993), δ^{34}S values for plankton filtrate were lower than 20‰ throughout the year even when proportional detritus was low: in May 2016, when the filtrate consisted only of diatoms, the δ^{34}S value was still only $\sim$ 15‰. This suggests bacterially processed benthic sulfides partially contribute to pelagic production within the estuary, likely as nutrient inputs through resuspension of sediments into the water column which occurs throughout the year as inferred by water turbidity (Fig. 3.10). Interestingly, this sulfur source does not appear to be incorporated into the macroalgae, which also obtain their nutrients directly from the water column. Macroalgae δ^{34}S values clustered around 21‰ (Fig. 3.12), matching closely to the expected marine sulfate value that dominates estuarine water (Rees et al., 1978; Fry, 2002).

Overall, the fish community δ^{34}S values reflected a similar pattern to the plankton, with almost all values below 18‰ suggesting that bacterially derived sulphides and their production contribute to the entirety of the Southampton Water food web. Assuming

that macroalgae δ^{34}S values have limited temporal variation, their relatively high levels compared to the overall fish community excludes them as a major contributor of production to higher trophic levels. Similarly, low δ^{34}S values of leaf litter suggest propagation of terrestrial detritus through the food web is minimal, although sampling of these production sources was limited. Fish functional groups were separated by their average δ^{34}S values, with pelagic individuals having the highest values and benthic individuals the lowest, although individual variation was high. This is expected, as the benthic food chain incorporates invertebrate deposit feeders that directly process sediments. However, the comparatively low disparity between functional groups ($\sim 2‰$) suggests only a small difference in the overall importance of bacterial production. The absence of any temporal trend in global δ^{34}S values indicates that the importance of bacterially sourced production does not change seasonally. It is also further evidence for the limited contribution of macroalgal and terrestrial production inputs that, like phytoplankton, are seasonally pulsed: the autumnal macroalgal die-off and degradation after which it can be utilised in the benthic pathway and high rates of riverine and therefore terrestrial detrital inputs during the winter. This has been noted elsewhere, for example, Garcia et al. (2017) found an apparent lack of assimilation of macroalgal production into an omnivorous fish despite the macroalgae dominating in terms of biomass within the studied lagoonal system. With regard to increasing body size, δ^{34}S showed a decreasing trend, implying an overall increasing importance of pelagic predation at larger body sizes.

Neither carbon nor nitrogen isotopes differentiated between functional groups, however both showed significant temporal trends. In May, linear mixed effects models indicated a significant increase in δ^{13}C, although this had reduced by June. Concurrently in May, a significant and prolonged decrease in δ^{15}N was seen that lasted until October. The commencement of these trends coincided with the late spring phytoplankton bloom, which peaked in May, see Fig. 3.9. It has been shown that the δ^{13}C of phytoplankton depends upon the *in situ* dissolved inorganic carbon (DIC) utilised for fixation, with fractionation rates reducing and therefore phytoplankton δ^{13}C increasing under low, limiting concentrations of DIC (Laws et al., 1995; Riebesell et al., 2000). These conditions are known to occur during peak spring phytoplankton blooms with increases in δ^{13}C

values recorded in natural systems (C. Ramos et al., 2003; Savoye et al., 2003), and would explain the trend in the fish community δ^{13}C seen here, with the peak δ^{13}C restricted to May 2016 when the spring bloom occurred.

Changes in phytoplankton δ^{15}N are also known to occur under bloom conditions, with increases associated with depleting nitrate availability due to reduced fractionation (Goering et al., 1990; Nakatsuka et al., 1992; York et al., 2007). However this only occurs at very low nitrate concentrations ($<25\mu\text{Ml}^{-1}$, Goering et al., 1990; Nakatsuka et al., 1992), whereas Southampton Water is hypernutrified (Townend, 2008). Here, the minimum nitrate concentration was recorded a month after the spring bloom in June 2016, with concentrations only falling to $26\mu\text{Ml}^{-1}$, Fig. 3.7. Since the nitrate minimum occurred post bloom, during which concentrations remained relatively high, phytoplankton appear not to be nitrogen limited within Southampton Water. Changes in δ^{15}N values therefore are unlikely to be associated with changes in fractionation rates as they were with δ^{13}C. The spring bloom would have provided a large flux of new production into Southampton Water, which eventually becomes remineralised. The remineralisation process causes an increase in δ^{15}N values in particulate organic nitrogen (York et al., 2007). It is likely that the trends in δ^{15}N in the fish community seen here is a reflection of the new phytoplankton production fuelling the food web from late spring through to autumn, causing the protracted period of reduced δ^{15}N values. Once this new production is depleted, there is reliance on remineralised production over the winter and the associated increase in δ^{15}N values.

The tight coupling exhibited between the phytoplankton bloom and changes in fish community isotopic composition suggests that the phytoplankton production was rapidly incorporated into fish biomass, on the order of 4 weeks or fewer (the May 2016 sample was taken approximately 2 weeks after the spring bloom). This conflicts with previous research that suggests seasonal trends in production sources are essentially unobservable within fish communities (Jennings et al., 2008). By inserting the average body mass of sampled fish and the typical water temperature for May (0.61g and 11°c, see Fig. 3.8, respectively) into the tissue turnover rate equations estimated by Thomas and Crowther (2015), the expected half life is on the order of 29 and 30 days for δ^{13}C

and δ^{15}N respectively (16 days using the estimates from Vander Zanden et al., 2015). The validity of these estimates were tested by inserting them into a toy model of carbon isotope incorporation across two trophic levels: phytoplankton to zooplankton to fish, under the assumption that Southampton Water is DIC limited and therefore the δ^{13}C of phytoplankton is a function of their density. The model output is shown in Fig. 3.16, see Appendices for model summary and parameterisation.

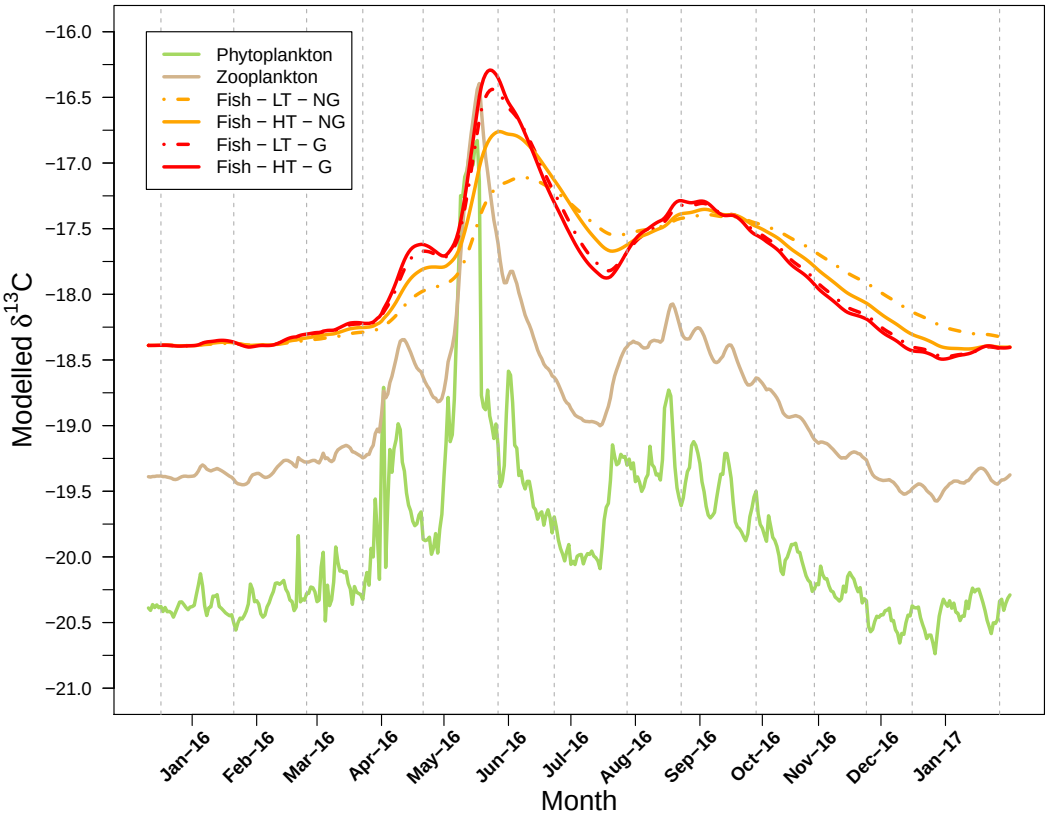

Figure 3.16: Time series of modelled δ^{13}C of phytoplankton, zooplankton and zooplanktivorous fish. For fish, the four combinations of 29 (LT - dashed lines, estimated from (Thomas & Crowther, 2015)) and 16 isotopic half lives (HT - solid lines, estimated from (Vander Zanden et al., 2015)) coupled with no growth (NG) and high growth rate (G, $\lambda_g = 0.05\text{d}^{-1}$). Dashed grey lines indicate sampling.

Isotope incorporation depends upon both catabolic turnover of tissues, as well as the formation of new biomass - somatic growth, which acts to dilute the current tissue mass with assimilated material (Fry & Arnold, 1982). Qualitatively, the trend seen in Fig. 3.15 is best described when fish growth rates are high, at which point the difference

between the two turnover rates is limited. When the model fish are not growing, then the magnitude of the increase in δ^{13}C is reduced and the peak is more drawn out, contrasting with the sharp, sudden peak seen in the data. This emphasises the importance in recognising growth in isotope dynamics, especially when this coincides with rapid changes in basal isotopic composition (Jardine et al., 2014). Asymmetric seasonal growth patterns are well described in temperate fish, particularly juveniles (Pannella, 1971; Mann, 1971; Bacon et al., 2005), with dynamics having been incorporated into the von Bertalanffy growth equation to account for such variation (Pitcher & MacDonald, 1973; Cloern & Nichols, 1978). Peak growth rates typically occur during the late spring and summer period when production is high, with reduced or even cessation of growth during the winter (Bacon et al., 2005). It is important to note however that somatic growth can be reduced during spawning periods as assimilated material is preferentially shuttled to gamete production (Miller, 1975; Heessen et al., 2015), even when food intake is high. Nevertheless, high somatic growth rates explain the apparent rapid incorporation of the phytoplankton bloom production within the fish community via the zooplankton.

3.5.3 Implications

The results presented here suggest that size spectra and stable isotopes are sensitive to within-system ecological dynamics and therefore can be utilised at finer temporal scales in future research. Size spectra within the fish community exhibited large fluctuations between months with consistent seasonal patterns over 7 years of data, in keeping with the movements of fish into and out of the estuary. The dynamics within the size spectra may therefore provide a useful indicator of environmental conditions or shifts in community composition, especially when adult movements and juvenile influxes act in tandem to steepen the spectra. For example, shifts in the timing juvenile influxes, which are sensitive to water temperatures, would be reflected in timing of the early summer peak of the size spectra. Additionally, recent developments in maximum likelihood methods, which do not require averaging into size classes, are likely to facilitate higher resolution temporal sampling regimes through their ability to parameterise power law distributions at reduced sample sizes compared to other methods (Edwards et al., 2017).

Compared to Southampton Water, which functions as an important nursery ground, other fish communities may be less seasonally variable and therefore exhibit relatively dampened size spectra dynamics. Nevertheless, the strong seasonal differences observed advocate exploring these dynamics in other systems. Long term studies on fish size spectra have estimated a slow continual increase in the steady state size spectrum exponent of fish communities at the inter-annual scale (Rice & Gislason, 1996; Jennings, Greenstreet, et al., 2002; Blanchard et al., 2005). How this change is manifested remains an open question, for example, it may be an average increase in the size spectrum across the whole year or a larger but seasonally periodic increase. Knowledge of the dynamics in the size spectra at the seasonal rather than annual scale will help improve understanding of the functioning of these ecosystems and therefore fisheries management.

Although various basal production sources are available to the food web within Southampton Water, SIA, particularly δ^{34}S, revealed that pelagic phytoplankton was the dominant source, although some benthic bacterial production is also incorporated steadily throughout the year. Interestingly, macrophytes and terrestrial inputs, which show strong seasonality, did not appear to be incorporated into the food web in any appreciable amount. Monthly sampling of SIA also revealed the dynamics of phytoplankton production through the food web, with new production being utilised for approximately 6 months after the commencement of the spring bloom. Knowledge of such trophic behaviour is important when modelling ecosystem processes such as nutrient cycling and carbon sequestration, which are poorly resolved in coastal systems (Jennings & Collingridge, 2015).

For studies utilising SIA, either equilibrium with the *in situ* diet or slow tissue turnover is assumed in order to, for example, elucidate information on diet (Parnell et al., 2010), categorise niches or traits (e.g. Wood et al., 2017; Rader et al., 2017) and retrospectively geolocate animals (R. Ramos & González-Solís, 2012). However results here indicate that this assumption is invalid in a dynamic food web, where pulsed production sources appear to be rapidly incorporated at higher trophic levels, contrary to previous research (Jennings et al., 2008). Such assumptions have come under increasing scrutiny recently, as the number of studies utilising SIA grows rapidly.

For example, Gorokhova (2018) showed experimentally that when individuals are in equilibrium with a fixed diet, physiological state influences TDF values and therefore can influence interpretation of data. On the other hand, the rapid incorporation suggests SIA are suitable for quantifying dynamic energy flows through food webs and, under suitable sampling regimes, can help elucidate ecosystem properties at reduced temporal scales.

4 | Quantifying Energy Fluxes within Southampton Water

4.1 Abstract

Knowledge on the trophic structure and biomass transfer in ecosystems is important for the estimation of ecosystem services such as fish production. However current ecosystem models assume steady-state conditions and are often parameterised from studies utilising only single time point sampling. It is currently unknown whether or not such approaches are suitable, as the temporal dynamics of *in situ* trophic structure and biomass transfer are currently poorly resolved. To address this, I quantified the seasonal variability in the realised predator-prey mass ratios (PPMR) and apparent trophic transfer efficiency (TE) utilising stable isotope methods in a highly dynamic estuarine fish community. I show that both the PPMR and TE vary over several orders of magnitude between summer and winter, which is associated with changes in size structure due to known size-segregated movements of individuals and likely predator foraging mode. Since ecosystems may rarely be considered as energetically closed, this research suggests that empirical measures of TE do not conceptually reflect the theoretical TE as used in models, but encompasses size-dependent rates of system biomass exchange. The seasonal trends observed in PPMR and TE imply that when such metrics are only single point estimates, they may poorly reflect average system behaviour, and therefore should be used with caution in ecosystem

models.

4.2 Introduction

The structure of trophic food webs are shaped by the flow of biomass through biological communities, and therefore ultimately depend upon the interactions between predators and their prey. Determining general patterns of interactions and energy flows has been a key goal of ecology since its emergence as a scientific field (Elton, 1927; Lindeman, 1942). Individual body size, which determines many biological traits (Brown et al., 2004; Sibly et al., 2012), limits the range of predator-prey interactions that can occur. Increasingly small prey leads to a decreasing rate of capture success for ever more nutrient limited gains. Likewise, predators become physically constrained in utilising increasingly larger prey, leading to a limited range of viable predator to prey mass ratios (PPMR) (Brose, 2010; Nakazawa, 2017). The energy flow between these size constrained predator-prey interactions can be quantified by the assimilated biomass that becomes available to the rest of the food web relative to the biomass acquired by the predator from its prey, the trophic transfer efficiency (TE) (Andersen et al., 2009). These processes determine the size spectra of the community (Kerr & Dickie, 2001) and therefore measuring PPMRs and TEs is key for modelling and understanding other ecosystem processes. For example, ecosystem rates of nutrient uptake are hypothesised to be determined by the vertical diversity of food webs, which is a function of the community PPMR (Wang & Brose, 2018), whereas both are required in models for predicting fisheries production (Jennings & Collingridge, 2015).

4.2.1 Predator-Prey Mass Ratios

As predator-prey interactions occur at the individual level, empirical estimates of PPMR are frequently measured from direct observation of these interactions, typically via stomach content analyses (Brose et al., 2005; Barnes et al., 2010; Nakazawa, 2017). However, due to varying data quality and study designs, various forms of PPMR have been quantified, such as species-based averages (e.g. Brose et al., 2006; Gaeta et al., 2018) versus individual-based averages (Nakazawa et al., 2011; Nakazawa, 2017), which

can complicate interpretations. For example, species-based PPMRs are typically one order of magnitude lower compared to individual PPMRs, although the bias is data dependent (Woodward & Warren, 2007; Nakazawa et al., 2011), and these two forms appear to co-vary with different factors. Meta-analyses of stomach content data show individual PPMRs are dependent upon size but invariant with environment (Barnes et al., 2010) whereas species based PPMRs tend to vary with ecosystem and prey type (Brose et al., 2006). Current consensus is that, particularly in size-structured systems, species-based PPMRs should be used with caution as they average over size effects that are key at the individual level and therefore may not reflect the actual *in situ* feeding relationships (Guiet et al., 2016; Nakazawa, 2017).

Empirical estimates of PPMRs capture the actual predator-prey interactions, the realised PPMR, however the original conception of the PPMR was to represent the prey preference of predators for numerical modelling of food webs, the preferred PPMR (Nakazawa, 2017). These conceptual differences are important as realised PPMRs reflect the preferred PPMR compounded by the probability distribution of *in situ* prey sizes, the size spectrum. Tsai et al. (2016) showed that the apparent size dependency in realised individual PPMRs (Barnes et al., 2010) is a result of the prey distribution, with preferred PPMRs being size invariant once feeding mode (pelagic or benthic) was accounted for, a key finding for modelling approaches that typically assume size invariance in preferred PPMR (e.g. Blanchard et al., 2009).

Rather than utilising stomach contents, individual realised PPMRs can be estimated as a community average using SIA (Jennings, Warr, & Mackinson, 2002; Jennings et al., 2008). Nitrogen exhibits a relatively high trophic discrimination factor, typically of 3-3.4‰ (D. M. Post, 2002; McCutchan et al., 2003; Nielsen et al., 2018). Therefore the PPMR can be estimated from the slope of the relationship between δ^{15}N and logarithmically transformed body size and the known (or assumed) fractionation of δ^{15}N (Jennings, Warr, & Mackinson, 2002):

$$\text{PPMR} = L_B^{\frac{\text{TDF}_N}{b}} \tag{4.1}$$

where b is the linear slope between δ^{15}N and logarithmically transformed mass with base

L_B and TDF_N is the trophic discrimination factor of $\delta^{15}\text{N}$.

Empirical estimates of PPMR using stomach contents vary widely in aquatic systems from approximately 1 to 1,000,000 (Barnes et al., 2010; Naisbit et al., 2011). Community estimates of PPMR using stable isotopes are less common but also appear to vary widely, from 109 in the North Sea fish community (Jennings, Warr, & Mackinson, 2002) to 244000 for nekton within the pelagic sub-tropical Pacific (Hunt et al., 2015). While many sources of variation in PPMRs have been identified, including locality, phylogeny and feeding mode (Barnes et al., 2010; Naisbit et al., 2011; Tsai et al., 2016), the degree to which PPMR varies temporally within systems has, as of yet, not been thoroughly explored (Reum & Hunsicker, 2012).

4.2.2 Trophic Transfer Efficiencies

Estimating the efficiency at which production or biomass is transferred through a food web has historically relied upon a mass-balance modelling approach (Pauly & Christensen, 1995; Rousseau et al., 2000; Tanaka & Mano, 2012), with the typical expectation that the TE per trophic level should be approximately 0.1 (or 10%). Because size spectra are determined by the community PPMR and TE (Kerr & Dickie, 2001), one can use this relationship as another method to directly estimate the TE of a size-structured system:

$$\text{TE} = \text{PPMR}^{\beta+\frac{3}{4}} \tag{4.2}$$

where β is the size spectrum exponent, with $\frac{3}{4}$ being the assumed scaling of consumption driven by metabolic rate (Andersen et al., 2009; Barnes et al., 2010; Trebilco et al., 2013). Whilst applying eq. 4.2, many authors have assumed a size spectra exponent β (Barnes et al., 2010; Hunt et al., 2015), which may not accurately represent the system of interest. More recently, other authors have suggested that the ratio of biomass between predators and prey can be used as a proxy for TE (García-Comas et al., 2016; Ersoy et al., 2017). However, since the predator-prey biomass ratio is an expression of the biomass spectrum, which has an exponent of $\beta + 1$, there is an implicit assumption of a fixed PPMR (unless dynamics in PPMR are measured and accounted for). Overall, few studies have measured both PPMR and the size spectrum *in situ* in order to estimate

TEs (but see Jennings, Warr, & Mackinson, 2002), and therefore the *in situ* variability in TE, like PPMR, remains poorly resolved.

4.2.3 Model System

Southampton Water provides an excellent model system in order to test for the temporal variability in realised PPMRs and apparent TEs. As shown in Chapter 3, the size spectrum of the estuarine fish community exhibits strong seasonal dynamics, with stark steepening in the summer associated with an influx of juveniles and the emigration of larger individuals out of the estuary. These movements correspond with the commencement of the phytoplankton bloom, which provides a large pulse of new production which is rapidly incorporated into the community. This production is then remineralised during the winter to fuel both the benthic and pelagic pathways within the estuary. Given eq. 4.2, it follows that seasonal variation must occur within the realised PPMR and / or apparent TE within Southampton Water in order to account for the observed seasonal changes in the size spectrum (assuming a closed system).

4.2.4 Aims

Determining and quantifying ecosystem energy fluxes is crucial for modelling fisheries production and other ecosystem functions (e.g. Blanchard et al., 2012; Jennings & Collingridge, 2015). However such models often assume static behaviour in trophic interactions and transfer efficiencies. Further, these models are often parameterised using data from studies that utilise single temporal point samples but covering a large spatial area. The implicit assumption therefore is that spatial variability is very much larger than temporal variability, however, to date, this assumption has not been thoroughly tested. The purpose of this study is thus to quantify the effects of known, size-segregated movement patterns on the realised PPMR and the apparent TE within Southampton Water. If these two ecosystem metrics exhibit seasonal dynamics then this has implications not only for studies utilising only a single time point sample, but also other systems were movement patterns are poorly constrained.

I show that the community PPMR does exhibit strong seasonality, covering the range

of values estimated across different marine systems. Coupling the PPMR with the known size structure, I demonstrate that the apparent trophic transfer efficiency also exhibits strong seasonality, implying temporally variable energy fluxes within Southampton Water. The work presented in this chapter highlights empirically the importance of temporal variability in these two metrics, rather than just spatial variability. Temporal dynamics, particularly of fish movements, should therefore be considered when estimating energy fluxes and determining ecosystem structure and function (Barneche & Allen, 2018).

4.3 Materials and Methods

For details on sample collection and processing see section 3.3. All individuals sampled for stable isotope analyses are included except for flounder, *Platichthys flesus*, and European eel, *Anguilla anguilla*, due to their inhabiting of fresh water (Kerstan, 1991; Henderson, 2014; Heessen et al., 2015), giving a total of n = 438.

PPMRs were estimated, following eq. 4.1, separately for the benthic functional group and combined pelagic and bentho-pelagic feeding individuals. The parameter b was determined from the slope of ordinary least squares linear regression of individual δ^{15}N against logarithmically transformed body mass ($L_b = 10$). The mean TDF_N was assumed to be 3.2‰. Error was incorporated into the PPMR estimates by assuming b and TDF_N are normally distributed variables, were the standard deviation of b was taken as the standard error from the linear regression. For TDF_N, a standard deviation of 0.2‰ was assumed, giving 95% limits of approximately 2.8-3.6‰, which broadly encompasses most empirical estimates of TDF_N (DeNiro & Epstein, 1981; D. M. Post, 2002, see section 3.2.2). Since L_b is fixed (in this study at 10), PPMR is a function of the ratio of TDF_N/b. Analytically solving for the probability distribution of ratios of normal variables is non-trivial (Marsaglia, 1965; Hinkley, 1969), therefore a *quasi* Monte Carlo approach was utilised. Samples were drawn (n = 10000) for TDF_N and b giving estimates of their ratio. When b approaches zero, a singularity is reached causing the magnitude of the ratio to rapidly approach ∞. Therefore, the ratio distribution was taken as the 99% confidence intervals of the samples to exclude such erroneous estimates, providing a sample of estimated PPMRs. Desired confidence intervals were then calculated by

numerically integrating along kernel density (n=4096) of logarithmically transformed, estimated PPMRs and then back calculated. As the ratio distribution was unimodal and asymmetric, the median PPMR was taken as the estimate of central tendency.

In situ measures of PPMR (and therefore TE) using δ^{15}N are dependent upon the assumed TDF_N, as biomass moves from one trophic level to the next. Here, I assume a normally distributed TDF_N that is additive, i.e. is independent of the trophic level of the predator and the isotopic composition of its prey. Recently, N. E. Hussey et al. (2014) suggested that this simple additive approach inadequately describes the enrichment process and that using a TDF_N that scales with trophic level should be used instead. This scaled approach reduces estimated community PPMR values, increases the assumed trophic level at size and increases estimated food chain length (Reum et al., 2015; Ohshimo et al., 2016). Reum et al. (2015) also noted that the scaled approach reduces apparent spatial variability observed in estimated PPMRs.

N. E. Hussey et al. (2014) drew their inference from relatively limited experiments whereby dietary δ^{15}N was varied beyond that reflecting natural diet compositions (and therefore naturally observed physiological routing processes). Additionally, the scaled approach implies that the TDF is directly affected by prey δ^{15}N values (as this is used to estimate trophic level). While variations in TDFs have been noted between trophic levels, this is typically due to the quality of diet, and not the dietary δ^{15}N value *per se* (McCutchan et al., 2003; K. W. McMahon et al., 2015). The implication of the scaled approach is that changes in dietary δ^{15}N values not due to changes in composition, e.g. the seasonal recycling of pelagic production as shown in Chapter 3, would also impart changes to the TDF. The scaling approach is thereby mechanistically flawed, making the applicability of TDF_N scaling to ecological data questionable. Further, in testing this approach, Ohshimo et al. (2016) found little difference in estimated PPMRs between the additive and scaled approaches, given the confidence intervals around the estimates. Therefore I have confidence that a simple, normally distributed TDF is suitable for PPMR estimation.

PPMRs were estimated for the fish community over the whole sampling period as well as for each bi-monthly period. To test for significant temporal differences in seasonal

PPMR (bi-monthly periods), pairwise comparisons were conducted on the regression slopes of δ^{15}N and logarithmically transformed mass, since theTDF$_N$ distribution was assumed to be fixed. The Z-statistic was calculated as:

$$Z = \frac{b_1 - b_2}{\sqrt{{SE_{b_1}}^2 + {SE_{b_2}}^2}} \tag{4.3}$$

where b_1 and b_2 are the two regression slopes with respective SE_{b_1} and SE_{b_2} standard errors (J. Cohen et al., 2013).

If the PPMR and the size spectra exponents are known then the TE can be estimated following eq. 4.2. For each bi-monthly period and across the whole period, the size spectra exponents were estimated for the fish community following the methods described in section 3.3 separately for bentho-pelagic and pelagic feeding individuals and the benthic functional group. As fish community data was not available for December 2016 and January 2017, a size spectrum, and therefore a TE, could not be estimated for this period. Limits for TE were estimated by directly inserting the 75% confidence intervals for PPMRs and the 95% confidence intervals for the size spectra into eq. 4.2. All analyses were conducted in *R* 3.3.2 (R-Core-Team, 2016).

4.4 Results

Over the whole sampling period, the grouped community of pelagic and bentho-pelagic feeding individuals showed a significant linear increase in δ^{15}N with log body size (b = 0.926, $F_{1,322}$ = 178.3, p < 0.001) whereas the benthic functional group showed no significant trend ($F_{1,102}$ = 0.187, p = 0.667), see Fig. 4.1. Following eq. 4.1, the pelagic and bentho-pelagic community have an estimated PPMR of 2890 (95% confidence interval of 534 to 15500). The lack of a significant trend in the benthic group suggests that there is no apparent change in trophic level with body size within these fishes.

The size spectrum exponent for the pelagic and bentho-pelagic individuals over the total period was $\beta = -1.31$ (-1.29 to -1.33 confidence intervals at 95%) calculated from 7459 individuals. Combining the estimated PPMR and size spectrum as in eq. 4.2 yields a TE of 0.012 (ranging from 0.0056 to 0.023), or 1.2%. For the benthic community, the

spectrum was steeper at $\beta = -1.68$ (-1.62 to -1.74 confidence intervals at 95%) calculated from 2257 individuals. Since there is no estimate of PPMR, a TE cannot be estimated for this group.

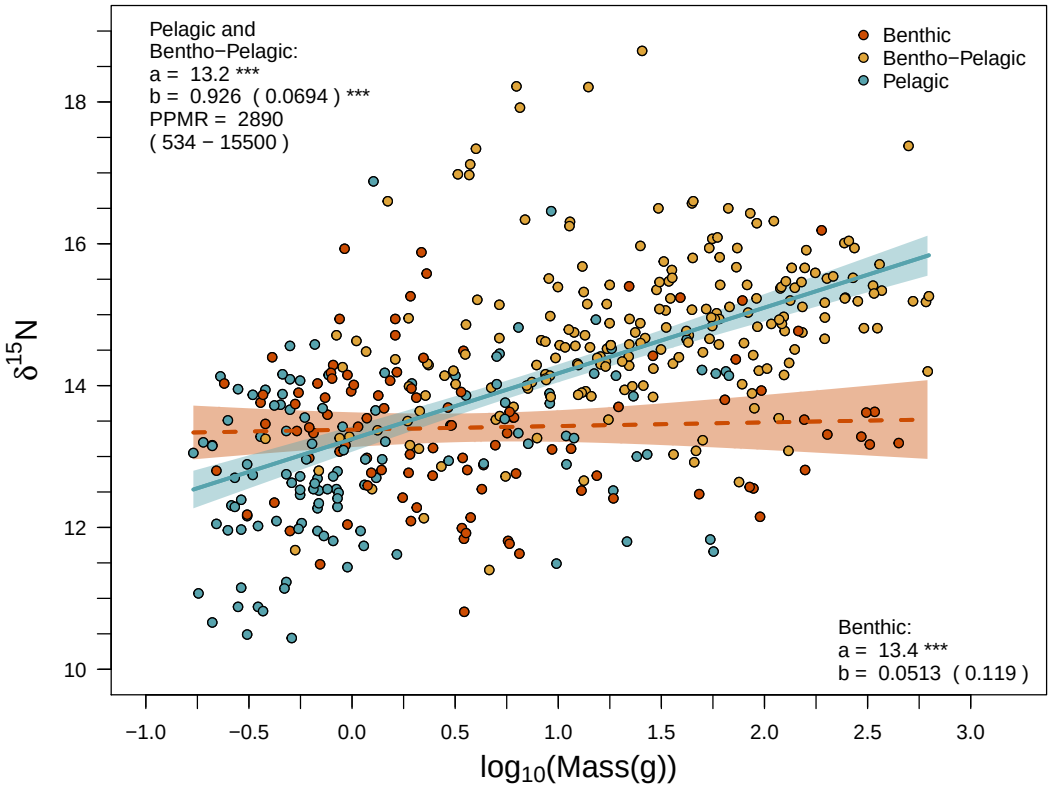

Figure 4.1: Plot of δ^{15}N against logarithmically transformed (base 10) individual mass. There was no significant linear trend within the benthic functional group (broken red line), whereas for bentho-pelagic and pelagic individuals combined δ^{15}N significantly increased linearly with logarithmic mass (solid blue line) - model parameters inset with asterisks denoting significance (* = $p < 0.05$, ** = $p < 0.01$ and *** = $p < 0.001$) and standard error in parentheses for slope. Median PPMR calculated following eq. 4.1, with 95% confidence intervals given in parentheses.

The bi-monthly plots of δ^{15}N with body size for pelagic and bentho-pelagic feeding individuals and the benthic functional group are shown in Figs. 4.2 and 4.3 respectively. For pelagic and bentho-pelagic feeders, all periods showed a significant positive regression slope, implying median PPMRs ranging from 304 in April-May 2016 to 200000 in February-March 2016. For the benthic functional group, no period showed a significant trend in δ^{15}N with body size. Pairwise comparisons of the regression slopes for individual periods are given in table 4.1. Only the periods June-July 2016 and and October-November

Table 4.1: Pairwise matrix of probabilities of mean slopes from regressions of δ^{15}N against logarithmically transformed (base 10) individual mass of bentho-pelagic and pelagic individuals of bi-monthly periods being the same, determined by Z-tests, eq. 4.3. Significantly different periods ($p < 0.05$) highlighted in grey. Letters correspond to periods as those inset in Figs. 4.2 and 4.3.

	a	b	c	d	e	f	g
b	0.882						
c	0.735	0.600					
d	0.088	0.078	0.058				
e	0.042	0.018	0.027	0.707			
f	0.851	0.729	0.891	0.077	0.043		
g	0.077	0.044	0.048	0.613	0.827	0.072	
h	0.776	0.670	0.994	0.085	0.063	0.909	0.094

2016 showed significantly higher regression slopes and therefore lower PPMRs compared to other periods.

The PPMRs and size sprectra exponents for the bentho-pelagic and pelagic group are plotted as a time series in Fig. 4.4, which shows that the decrease in PPMR commencing in April-May 2016 coincides with a steepening in the size spectrum exponent from $\beta = -1.06$ to $\beta = -2.02$. The error in PPMR estimation is highly variable but particularly large in February-March 2016 and August-September 2016, resulting in uncertainties spanning approximately 4 to 5 orders of magnitude.

The estimated TEs are plotted in Fig. 4.5. Over the winter, values of TE are high with a maximum of 0.27 in October-November 2015. A gradual decrease occurs until a low of 3.6×10^{-7} in August-September 2016 is reached, after which the TE increases to 0.039 in October-November 2016. Uncertainties for TEs varied in magnitude, but roughly corresponded to the uncertainties in PPMRs. Despite this, the non-overlapping errors suggest that late spring to early autumn TEs are notably reduced compared to winter values.

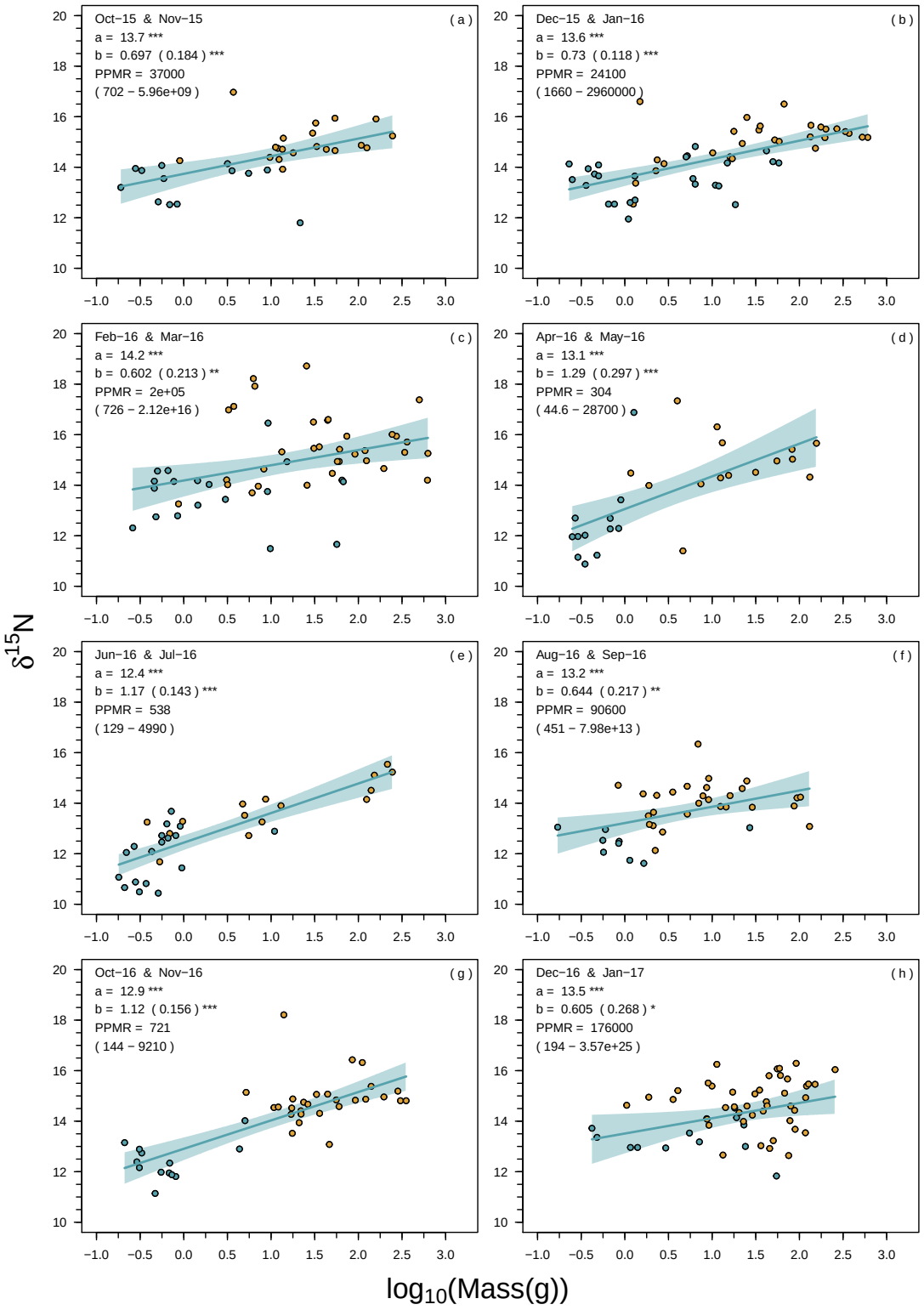

Figure 4.2: Bi-monthly plots of δ^{15}N against logarithmically transformed (base 10) individual mass for pelagic and bentho-pelagic individuals. Significant linear regressions plotted as solid blue lines. Sampling months and linear regression parameters inset (with standard error of slope given in parentheses) with asterisks denoting level of significance (* = $p < 0.05$, ** = $p < 0.01$ and *** = $p < 0.001$). PPMRs were estimated following Eq. 4.1 for significant regressions only (with 95% confidence intervals).

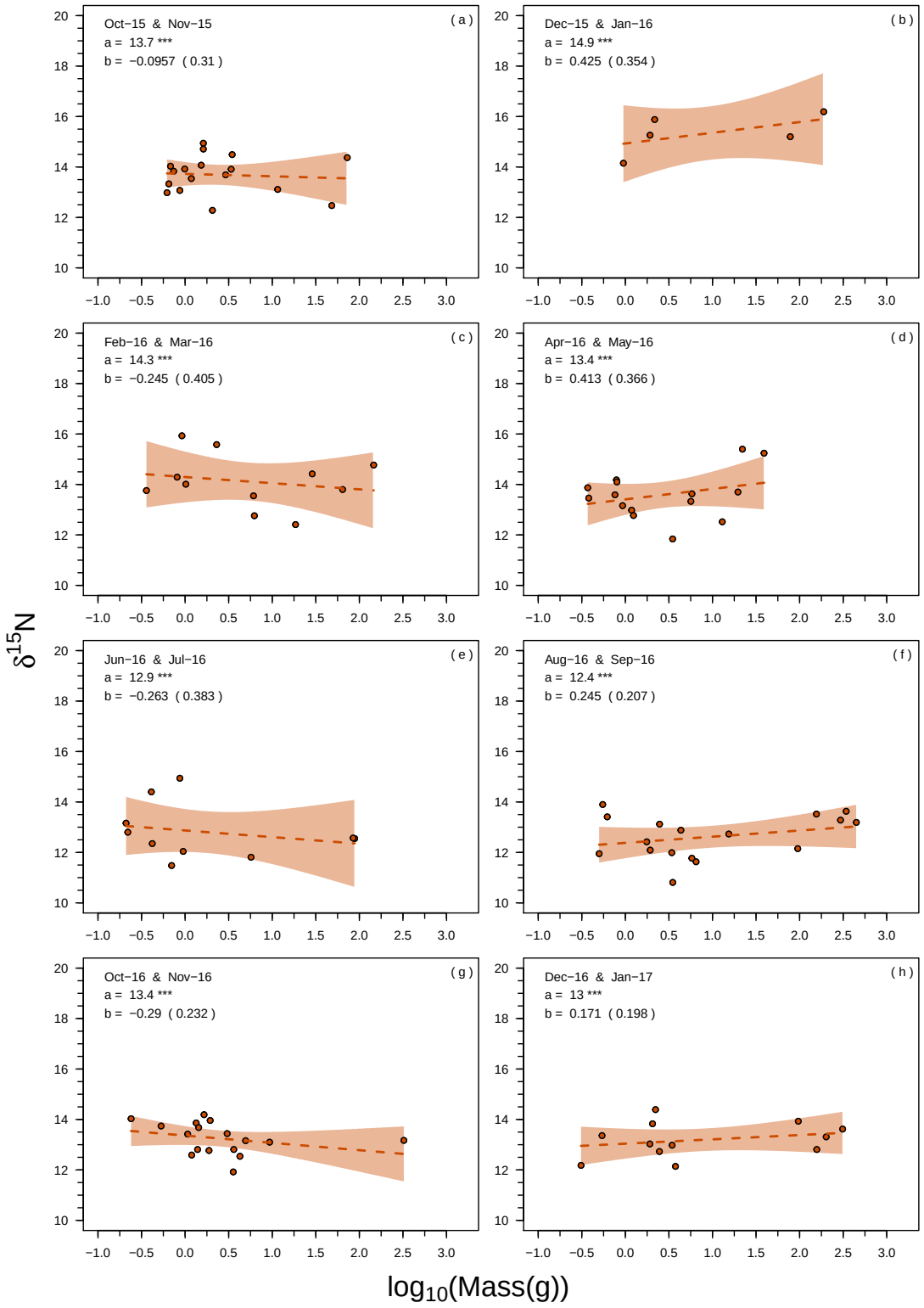

Figure 4.3: Bi-monthly plots of δ^{15}N against logarithmically transformed (base 10) individual mass for benthic individuals. Non-significant regressions as dashed lines. Sampling months and linear regression parameters inset (with standard error of slope given in parentheses) with asterisks denoting level of significance (* = $p < 0.05$, ** = $p < 0.01$ and *** = $p < 0.001$). No PPMRs were estimated as no period showed significant regressions.

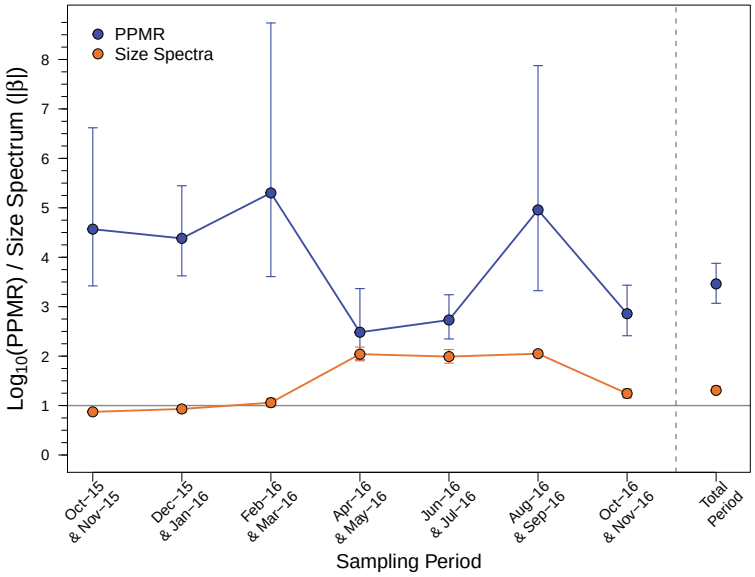

Figure 4.4: Time series of PPMR (logarithmically transformed with base 10) and the magnitude of the size spectrum exponent (β), for pelagic and bentho-pelagic individuals. Error bars as 75% and 95% confidence intervals for PPMRs and biomass spectra respectively (some months the errors are contained within the size of the plotting symbols). Grey horizontal line marks the β value below which pyramids of biomass become top-heavy (i.e. inverted). Estimates for the total period are plotted for reference.

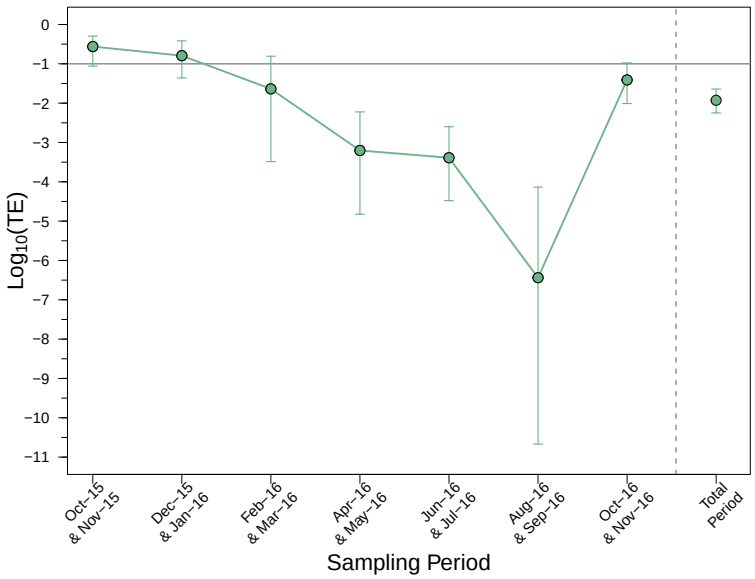

Figure 4.5: Time series of the trophic transfer efficiency, TE, (logarithmically transformed with base 10) for pelagic and bentho-pelagic individuals, estimated from eq. 4.2. Error bars are calculated by incorporating errors of PPMR and size spectra exponents, see Fig. 4.4. Grey horizontal line marks 10% trophic transfer efficiency. Estimate for the total period is plotted for reference.

4.5 Discussion

4.5.1 Predator-Prey Mass Ratios

Measures of community PPMRs, estimated from δ^{15}N, are known to vary spatially and between functional groups. Hunt et al. (2015) found a shift from a PPMR of 3683 for macrozooplankton to 244000 for nekton within the pelagic sub-tropical Pacific. A value of 5032 has been estimated for the pelagic food web in the Western Pacific (Ohshimo et al., 2016), whereas in the North Sea fish community, Jennings, Warr, and Mackinson (2002) estimated a mean PPMR as low as 109. This large variation emcompasses the range of seasonal PPMRs within the pelagic food web estimated here, which varied between 304 to 200000. The temporal average PPMR of 2890 estimated here matches well with that from inshore kelp forest fish communities (PPMR of 1650, Trebilco et al., 2016). The lack of any significant trends between δ^{15}N and logarithmically transformed body mass for the benthic functional group suggests that for this part of the food web, trophic level is not a function of body size (and hence why a PPMR cannot be calculated for this group using the stable isotope approach).

Temporal dynamics in PPMR are poorly resolved: the only study exploring the seasonal variability of PPMR within a system that I am aware of is that by Reum and Hunsicker (2012). The authors used gut content analyses to estimate individual PPMRs in the Puget Sound fish community (Seattle, US) and found that, on average, realised PPMR was higher in summer compared to autumn and winter. They argue that this is due to predators feeding down prey sizes when invertebrate production and larval / juvenile fish abundances are high. This extends from food web theory whereby a steeper size spectrum combined with a size invariant preferred PPMR produces a larger realised PPMR (Tsai et al., 2016).

Here, the opposite trend was observed within Southampton Water, apparently in contradiction to what is expected from theory, given that here the size spectrum is also steep during the summer period. Results show that fish community PPMR during the winter months is high, on the order of 50,000-200,000, but that PPMR sharply reduces by 2-3 orders of magnitude with the commencement of the phytoplankton bloom

until the end of summer. These realised PPMRs, are estimated using stable isotopes, specifically δ^{15}N, for the pelagic and bentho-pelagic feeding fish. It is important to note that, given the tight coupling between the pelagic and benthic pathways, δ^{15}N cannot differentiate between different feeding modes (see Fig. 3.15). During the winter, pelagic prey abundances are relatively reduced, as can be seen by the shallowing of size spectrum in Figs. 3.3 and 4.4. It is likely therefore that during this period, bentho-pelagic predators switch to being more "benthic" in their feeding mode. Such behaviour would cause a reduction in the slope of δ^{15}N against logarithmic mass (cf. Figs. 4.2 and 4.3) and therefore increase the realised PPMR, explaining the seasonal pattern seen here. Bentho-pelagic coupling through predation is theorised to increase the resilience of size structured food webs to perturbation (Blanchard et al., 2011), such as pulsed pelagic production, and is important to consider when quantifying ecosystem processes (Griffiths et al., 2017). Interestingly, Reum and Hunsicker (2012) also found feeding mode effects on PPMR, with invertebrate prey resulting in an order of magnitude increase compared to fish prey, a pattern that has been suggested in other studies (J. E. Cohen et al., 1993; Juanes et al., 2001).

4.5.2 Trophic Transfer Efficiences

Direct, *in situ* measures of TE are difficult to obtain, however some studies have estimated TE under varying assumptions. Irigoien et al. (2014) quantified the biomass differences between primary produces and mesopelagic fishes globally. By assuming a trophic level difference of 2 between these two groups, they estimated a TE within the mesopelagos of 14% per trophic level from primary produces to fishes, higher than they had expected. By assuming a size spectra exponent of $\beta = -1.05$, a typical steady state value taken from Kerr and Dickie (2001), Barnes et al. (2010) estimated TE values in the range of 5.8 to 13.4% using eq. 4.2, based on their PPMR estimates from a compilation of global stomach content data. Hunt et al. (2015) assumed the same size spectra exponent to directly estimate TEs of 6.3, 8.5 and 2.4% for pelagic mesozooplankton, macrozooplankton and nekton respectively using *in situ* community PPMRs estimated from δ^{15}N. For the North Sea, Jennings, Warr, and Mackinson (2002) combined *in situ*

PPMRs and biomass spectra to estimate a community TE ranging from 3.7 to 12.4%, with lower TE estimates when larger bodied fish were included, suggesting reduced TE at higher trophic levels. The time averaged TE estimated here, at 1.2%, is lower than these previously estimated values. However, seasonal estimates showed large variation encompassing previously recorded TEs, with winter values of up to 27.4% being higher than those recorded, to an autumn low of 3.6×10^{-5}%. Given the more narrow intervals around TE of approximately 2-20% estimated from mass balance models (Pauly & Christensen, 1995), it is unlikely that such large variation solely reflects actual variability in TE, as defined in section 4.2, in Southampton Water.

Conceptually, eq. 4.2 estimates the trophic transfer efficiency as the difference in biomasses between two trophic levels in a size structured system, where the distance between trophic levels on the size spectrum is determined by the PPMR. This approach matches the notion of TE as parameterised in mass-balanced food web models (Pauly & Christensen, 1995; Tanaka & Mano, 2012), under the assumption of a closed system in steady-state equilibrium. Empirical estimates of TE are taken from point samples of system biomasses in both time and space, and therefore reflects the differences in biomasses between trophic levels only at that point in time and space. The argument therefore is in whether the assumptions of a closed system and steady-state equilibrium hold for such point estimates.

With regard to the first assumption of a closed system, this is clearly violated in Southampton Water: seasonal fish movements known to occur within Southampton Water result in asymmetric movements of biomass in and out of the estuary over the seasonal cycle. In fact, it is likely violated in all but the most isolated of systems. For example, Hunt et al. (2015) estimated TEs for open ocean, surface waters. While lateral movements in biomass may be considered limited here, vertical diel migrations of mesopelagic nekton rapidly draw down surface production to deeper waters, referred to as the biological carbon pump (Trueman et al., 2014). The second assumption of steady-state equilibrium is also clearly violated in Southampton Water, where the size spectrum and PPMR are highly dynamic, varying widely over seasons (Fig. 4.4): the food web is not static within the estuary, and further, not wholly sampled using this

approach (only fish were used to parameterise the size spectrum and estimate PPMR). Therefore, the ecological interpretation of changes in this apparent TE seen here are more nuanced than simple changes in trophic transfer efficiencies.

If one assumes that actual TE is, as modelling studies suggest, convergent and relatively stable at around 10% per trophic level, then one could potentially interpret the results shown in Fig. 4.5 not as estimates of trophic transfer efficiency, but the relative energy fluxes into and out of the system given the size structure (the size spectrum) and the trophic behaviour of the food web (the PPMR). In other words, the overall changes in biomass at lower trophic levels, either through the direct movement of individuals or other forms of biomass change (e.g. somatic growth vs. respiratory losses) compared to those at higher trophic levels.

For example, if the estimated TE is higher than 10%, then this would imply that the higher trophic levels within the system would appear to be (or have recently been) "subsidised" energetically from outside of the *in situ* system, either spatially or temporally (or both). In other words, larger individuals are acquiring or have acquired resources to sustain them from outside of Southampton Water, and/or are using up energy stores acquired within Southampton Water but during an earlier period. Conversely, TEs lower than 10% would suggest that not all of the biomass available at lower trophic levels is being utilised *in situ* by higher trophic levels within the pelagic fish community, implying either an export of biomass and / or increased growth at lower trophic levels. These interpretations and the observed trend of high TEs in winter and low TEs during summer in Southampton Water thus matches well with known fish movement patterns as well as seasonal patterns of lipid storage and energy allocation in temperate fishes (J. R. Post & Parkinson, 2001; C. Jørgensen & Fiksen, 2006).

4.5.3 Implications

Recent efforts have focused on large scale modelling to estimate patterns in ecosystem services, such as fish biomass production, and predict their projections with expected scenarios of climate change (e.g. Blanchard et al., 2012; Merino et al., 2012; Jennings & Collingridge, 2015; van Denderen et al., 2018). These approaches rely on representative

but static estimates of, for example, PPMR. However data here suggest that estimates calculated from a single point maybe inappropriate in temperate coastal regions due to the strong seasonal dynamics observed. A further issue may arise due to under-estimation of production losses via averaging over dynamics. Here, the size spectra steepened considerably over the summer (see Figs. 4.4 and 3.3), implying that the total biomass consisted of a much greater proportion of small sized individuals during this period. This is also the period when *in situ* temperatures are much higher (see Fig. 3.8). Metabolic theory predicts a compounding effect of reduced body size and higher temperature on increasing mass-specific respiration rates (Brown et al., 2004), and therefore whole system, time integrated respiration rates likely will be higher than those estimated from temporal averages. The assumption of temporally static size spectra and PPMRs, and therefore TEs, used in large scale predictions should therefore be re-evaluated, especially in temperate and polar regions with strong seasonality, in order to improve models and forecasting (Reum & Hunsicker, 2012).

The data presented here start to address this issue, potentially allowing for absolute local fish production rates of Southampton Water to be more realistically modelled, as the dynamics in whole (or at least partial) ecosystem properties have been estimated (size spectrum and PPMR), and the environmental setting is well quantified (see Chapter 3). As a first order approximation, the low value of 1.2% for the temporally averaged TE is suggestive of a net efflux of fish biomass through time, either through movements out the estuary, or greater than average respiratory losses. Considering the estuary's role as a nursery ground (Chapter 5) and the coincident high biomass of small individuals in summer when temperatures are high, an efflux of fish biomass would be logically expected.

Due to the inefficient transfer of biomass through trophic interactions (i.e. TE is always < 1), Lindeman (1942) put forward the conjecture that all food webs must exhibit pyramids of biomass that are bottom heavy. Due to the very high rates of production to standing biomass, top-heavy pyramids have been observed in oligotrophic plankton communities (Gasol et al., 1997). However more recent observations have also noted top-heavy pyramids of biomass within some fish communities, notably reef habitats with

sharks as apex predators (Singh et al., 2012; Mourier et al., 2016; Trebilco et al., 2016). Obviously such observations have been met with skepticism due to energetic implications of such food web structures (Bradley et al., 2017). Potential suggested mechanisms for their occurrence include increased levels of generalism within apex predators and therefore higher PPMRs at the largest body sizes (Woodson et al., 2018). However, criticisms have also been made against methods used to estimate the biomass of larger, more motile and patchily distributed predators, which have been shown to vastly over estimate their abundances in reef systems (Nadon et al., 2012; Bradley et al., 2017).

Trebilco et al. (2013) emphasise the importance of the spatial extent over which food webs function, and that abundance estimates should encompass the whole area over which the top predators range. For example, apparent top-heavy pyramids found in kelp fish communities are likely sustained by energy subsidies from different habitats at higher trophic levels (Trebilco et al., 2016). However, results here also highlight the importance of temporal dynamics in food webs with regard to inversions of pyramids of biomass. The seasonal, size segregated movements of fish resulted in shallow size spectra during winter, and therefore a reduction in the bottom-heaviness of the *in situ* pyramid of biomass. In fact, some months exhibited top heavy structure as the size spectra exponents were greater than -0.75 (see Fig. 3.3, Trebilco et al., 2013). Therefore both spatial and temporal movements and energy subsidies are important to consider when determining biomass mass structure and hence estimating energy flows through food webs (Barneche & Allen, 2018). Nevertheless, the dynamics of the apparent TE, as estimated here, can provide valuable insight into such ecosystem processes.

5 Individual Specialisation in Juvenile Sea Bass: Implications for the Local Management of a Commercially Important Species

This chapter is a reproduction of text currently written for submission with the *ICES Journal of Marine Science*, and, as such, is written in the style of the journal.

Matthew R. D. Cobain, Will Steward, Clive N. Trueman and Antony Jensen

MRDC and AJ conceptualised the study, MRDC and WS collected and processed samples, MRDC conducted statistical analyses and wrote first manuscript draft, and all authors contributed equally to study development and manuscript review and editing.

5.1 Abstract

Stocks of the commercially important European sea bass, *Dicentrarchus labrax*, have declined in recent years, and national and international recovery efforts have focused on increasing the Minimum Conservation Reference Size and

restricting fishing effort. Additional management strategies at the local (and national) level, focused on maximising survival and growth of juvenile bass in inshore nursery grounds, will complement these efforts. Information regarding habitat and prey utilisation by individual juvenile bass is lacking, but such data can greatly increase the effectiveness of management policy. To address this knowledge gap, we explored individual dietary behaviours in juvenile sea bass from a common nursery area using stomach content and stable isotope analyses at monthly resolution over an annual cycle. We found strong evidence for individual specialisation in stomach contents after accounting for seasonal and age effects on diet. This was corroborated by stable isotope analyses, which showed significantly higher variance in sea bass compared to two other concurrently sampled, sympatric bentho-pelagic predators. Our findings suggest that juvenile sea bass represent trophically-generalist populations composed of specialised individuals. Therefore a variety of microhabitats in nursery areas should be preserved to best protect the vulnerable life stages of this commercially important species.

5.2 Introduction

European sea bass, *Dicentrachus labrax* (Linnaeus, 1758), have been, until recently, an important resource for inshore fisheries in the southern UK, both commercially and recreationally. DEFRA (2013) reports that, in 2012, 897t of sea bass were landed into the UK (mostly into England by the UK commercial fleet), with a first sale value of £5.6million (MMO, 2013) and it is estimated that an additional 230 - 440t of sea bass were kept by recreational sea anglers in England (DEFRA, 2013). A large drop in sea bass standing stock since ∼2010 (*circa* 18kt in 2010 to below 7kt in 2017) has resulted in the ICES advice on fishing opportunities, catch and effort identifying that sea bass stocks are now below Blim, the limit reference point for spawning stock biomass (ICES, 2017). For 2018, strict EU fishing regulations have come into force in an effort to improve sea bass stock levels (MMO, 2018). Coupled with these EU-wide regulations, localised management strategies within England are currently being reviewed, in conjunction with

MPA designation and the conservation of other species of interest, notably inshore netting regulations and fishing within sea bass nursery areas. However it has been highlighted that uncertainties in sea bass ecology are impeding policy development for the protection of this species (López et al., 2015).

Nursery areas are critical habitats for any efforts to conserve and re-build populations, and management efforts aiming to maximise the survival and recruitment of juvenile seabass should consider the variety of habitats utilised by juvenile sea bass. For predatory fish such as sea bass, the variety of habitats occupied typically coincides with the variety of prey consumed. Current knowledge on the diet of sea bass is biased towards young of the year (Aprahamian & Barr, 1985; Laffaille et al., 2001; Cabral & Costa, 2001; Martinho et al., 2008) or mature adults (Kelley, 1987; Spitz et al., 2013). However, the consensus is that sea bass are opportunistic, generalist predators, with diet reflecting the *in situ* seasonally abundant prey within the locality that are available to the given life history stage (Pickett & Pawson, 1994; Rogdakis et al., 2010; Pérez-Ruzafa & Marcos, 2014). This can lead to diverse estimates of diet compositions when assimilating data on sea bass from different regions and localities due to the spatial variability in potential prey (Kelley, 1987).

At a more local scale, a generalist diet in a population may reflect either cosmopolitan foraging within individuals, or the aggregation of individuals that specialise on differing prey. Increasing levels of individual specialisation is a potential mechanism through which levels of intra- and interspecific competition, as well as predation, can be modulated (Araújo et al., 2011), and therefore maximise population growth when fish densities are high, as is typical in nursery grounds. Individual specialisation may also arise due to variation in individual behavioural traits such as boldness (reviewed by Toscano et al., 2016), an evolutionary hedge betting strategy reflecting that differing ecological trade offs may impart the same long-term fitness (B. R. Smith & Blumstein, 2008).

Individual specialisation in diet can be quantified directly using either stomach content data (Bolnick et al., 2002; Araújo et al., 2008; Zaccarelli et al., 2013), stable isotopes (Layman et al., 2007; Dermond et al., 2018) or a combination of both (Araújo et al., 2009). Stomach content analyses offer high taxonomic resolution, however the

information it provides is limited to a narrow time window of up to several hours prior to capture, and therefore may not reflect the true, time averaged diet (Nielsen et al., 2018). Further, potential biases due to restricted sampling location(s) of motile individuals and patchily distributed prey items can falsely be interpretted as high levels of "apparent" individual specialisation. Conversely, stable isotopes contain information on the diet over a time frame of up to several weeks in the case of muscle, as they are incorporated into the body via tissue turnover and somatic growth (Vander Zanden, Casselman, & Rasmussen, 1999b; R. Ramos & González-Solís, 2012; Thomas & Crowther, 2015), at the cost of reduced dietary resolution. High levels of individual specialisation in diet causes individuals to equilibrate to (assumably) isotopically distinct food sources and therefore increases dispersion within the population in isotopic space, allowing relative levels of specialisation to be inferred (Layman et al., 2012).

Anecdotal evidence suggests that individual specialisation does occur in juvenile sea bass populations: local differences in habitat preferences have been noted, with individuals occupying tidal creeks, deep pools and faster flowing channels within estuaries (Kelley, 1986). Differential feeding patterns have also been reported within young of the year (Fonseca et al., 2011). However, despite its potential conservation importance, information on the dietary strategies at the individual level for sea bass, including measures levels of individual specialisation, are lacking.

In this study, we address this knowledge gap to better inform conservation efforts of this threatened species. We assess the dietary behaviour of juvenile sea bass, including young of the year, one year aged and two year aged cohorts, across a seasonal cycle within an estuarine nursery ground. We then test the hypothesis that the juvenile sea bass population consists of specialised individuals rather than individuals with cosmopolitan foraging behaviours using both stomach content and stable isotope data.

5.3 Materials and Methods

5.3.1 Study Area, Sample Collection and Processing

We utilised Southampton Water for this study, a partially mixed estuary located in southern England (50°52′N, 01°22′W) that is 1.96km wide at its mouth and approximately 10km in length. It has an artificially deepened channel for much of its length that is maintained by periodic dredging. It is fed by three rivers, the Test, Itchen and Hamble, which have a catchment area of around 1500km^2. The estuary itself is hypernutrified with relatively low turbidity: suspended particulates average 40mgl^{-1} at the mouth falling to 5-10mgl^{-1} at the head, making it a highly productive environment (Townend, 2008).

Individual fish were sampled opportunistically on a monthly basis from November 2015 through to January 2017 from a water intake pipe within Southampton Water using a collection net over a 24-hour period (one 18-hour overnight collection and six hourly collections). Catches were sorted, identified, counted and measured, and all available sea bass collected. Samples were supplemented with quarterly trawl surveys, all of which fell within 3km of the intake pipe and within the Southampton Water. A 10m-bottom otter trawl was used with a 10mm mesh cod end trawled for 10 minutes at a time with up to 10 trawls per quarter. With both modes of sampling, only fish deemed unable to survive being returned were taken. While survivability is likely to be influenced by body condition, which is dependent upon feeding behaviour and therefore may bias results, most individuals sampled came from the overnight net collection with limited returns from this method. Therefore the action of only collecting those deemed unsuitable to return is unlikely to have a major influence on results. All fish were collected under licence as part of on-going environmental monitoring of the estuary and were frozen post-collection until further analysis.

For dietary analyses, sea bass specimens were defrosted, standard length and wet-mass measured, and stomachs excised. Stomach contents were weighed separately, contents identified and sorted into 12 broad trophic categories under a binocular microscope (pelagic copepods, amphipods, isopods, mysids, shrimps, crabs, polychaetes, bivalves,

gastropods, fish, algae and detritus). For each category, numeric counts were taken and volume estimated.

Stable isotope analyses (SIA) were conducted on a subset of individuals, due to logistical constraints, representative of the size distribution and temporal variation in abundance. Small plugs of muscle (*circa* 0.5cm^3) were taken from below the second dorsal fin, with skin removed, and stored in eppendorf tubes and refrozen. For small individuals, whole fillets were taken with skin, bone and spines removed to avoid isotopic disparity between tissue types. Samples were freeze-dried at -55°c for 24 hours (Heto Power dry LL3000) then stored at room temperature in sealed containers. Dehydrated tissue samples were homogenised and weighed using a Sartorius microbalance with precision of 0.001mg. Samples of 1.9mg +/- 0.1mg were weighed out into tin capsules and were analysed at NERC Life Sciences Mass Spectrometry Facility, SUERC, using an Elementar vario Pyrocube (Hanau, Germany) coupled to an IsoPrime (now Elementar) VisION Mass Spectrometer (Cheadle, UK).

All isotopic values are reported relative to their respective international standards: Pee Dee Belemnite (PBD) for carbon, atmospheric air for nitrogen and Cañon Diablo Troilite (CDT) for sulfur. Isotopic compositions are expressed as delta (δ) per mille (‰) notation, given by:

$$\delta X = \left[\frac{R_{sample}}{R_{standard}} - 1 \right] \times 1000 \tag{5.1}$$

where X is either ^{13}C, ^{15}N or ^{34}S and R is the ratio of ^{13}C:^{12}C, ^{15}N:^{14}N or ^{34}S:^{32}S. Equipment calibration and compensation for drift over time was corrected for by internal standards run between every 10 samples, with analytical measurement errors of 0.1‰, 0.2‰ and 0.6‰ for δ^{13}C, δ^{15}N and δ^{34}S respectively.

5.3.2 Dietary Analyses

Sea bass were assigned an age class determined by their standard length and month of capture following data from Claridge and Potter (1983). Two dietary indices were employed to describe overall trophic behaviour for each seasonal age class following Rosecchi et al. (1988):

$$I_{RI} = p_F \times (p_N + p_V) \tag{5.2}$$

$$I_{MF} = \sqrt{\left\{ \frac{p_V \times (p_N + p_F)}{2} \right\}} \tag{5.3}$$

where p_F is the proportional frequency of occurrence of prey categories across stomachs, p_N is the proportional numerical abundance of prey categories and p_V is the proportional volume of each prey category. The index of relative importance, I_{RI}, was described by Pineas et al. (1971) and the main food item index, I_{MF}, was described by Zander (1982). While Zander (1982) originally used percentage dry weight, we used percentage volume (Rosecchi et al., 1988) and normalised each index to its total to allow comparisons between different age classes and seasons. In addition, the vacuity index, I_V, was calculated as the proportion of empty stomachs out the total examined for each group.

5.3.3 Statistical Analyses of Individual Specialisation

Since individual-level diet variation can be confounded with other sources of intra-population diet variation, we tested for differences in diet associated with ontogeny and seasonality. We utilised the proportional similarity index, PS, (Schoener, 1968):

$$PS_{ij} = 1 - \frac{1}{2} \sum_k |p_{ik} - p_{jk}| \tag{5.4}$$

such that p_{ik} and p_{jk} are the proportions of prey category k in the diets i and j respectively. PS_{ij} is a measure of the overlap in the diets i and j, ranging from 0 (no overlap) to 1 (complete overlap). We calculated the PS between each individual and the whole population average diet, the age class average diet, the seasonal average diet and seasonal age class average diet (average diets taken as the mean of individual proportional diets). Increasing mean PS values within group comparisons compared to the whole population suggests that the grouping explains some of the variation in individual diet. To test that this explained diet variation was not due to a random grouping effect, we used a Monte Carlo method to generate null groupings, where the age classes and seasons of individuals were randomly permutated. We compared the actual values to those from 10,000 permutations to obtain approximate p-values for the groupings. Results indicated that the increase in average proportional similarity from

0.287 for the whole population to 0.439 for seasonal age classes was not due to a random grouping effect ($p \approx 0.0049$). Sea bass were therefore grouped into seasonal age classes for subsequent analyses (average proportional similarity for age classes and seasons were 0.360 and 0.349 respectively).

To quantify the strength of individual specialisation based on stomach content data within each seasonal age class, we calculated two metrics. Firstly, we calculated the E index, which is based on pair-wise individual diet overlap (Araújo et al., 2008), given by:

$$E = 1 - \frac{2 \times \sum_{pairs} PS_{ij}}{n(n-1)} \tag{5.5}$$

such that the proportional similarity, PS, is calculated between two individuals, i and j, in the population of size n. The E index ranges from 0 (no individual specialisation) to 1 (maximum individual specialisation), however it can be biased towards specialisation when individuals consume low numbers of prey items. The observed index is therefore adjusted based on a null value calculated from Monte Carlo resampling methods (Zaccarelli et al., 2013):

$$E_{adj} = \frac{E_{obs} - E_{null}}{1 - E_{null}} \tag{5.6}$$

The second metric we calculated was the ratio of the Within Individual Component (WIC) of diet variation to the Total Niche Width (TNW):

$$\begin{aligned} TNW &= Var(x_{ij}) = WIC + BIC \\ WIC &= E[Var(x_j|i)] \\ BIC &= Var[E(x_j|i)] \end{aligned} \tag{5.7}$$

where x_{ij} is the frequency of prey item j in individual i's diet. This follows Roughgarden's (1972) conjecture that the total niche width of a population, TNW, can be broken down into the variation in resource use within individuals, WIC, and the variation in resource use between individuals, BIC. The relative degree of individual specialisation is then given by the ratio of variation within individuals compared to the total, WIC:TNW, with low ratios indicating high levels of individual specialisation (see Zaccarelli et al., 2013 for details on calculation of different components). Individuals with empty stomachs

were excluded from these analyses.

The statistical significance of the two metrics was tested using Monte Carlo resampling methods to derive null diet distributions, based on individuals stochastically sampling from a shared distribution (the average population diet), with the number of prey items for each individual held constant to maintain data structure. This null diet is based on the assumption that individual items within the stomachs of individuals constitute independent feeding events. Across all statistical analyses, we used the frequency of diet items within individual stomachs rather than volume, as this is required for the generation of null models. Mean proportional diets were calculated as the average proportional diet of individuals (i.e. not the proportional diet of summed prey items across all individuals).

Individual specialisation can be inferred using stable isotopes by quantifying population structure in isotopic space, with greater variance typically associated with a higher degree of specialisation, given the same isotopic baseline (Layman et al., 2012). Quantifying the isotopic composition of the diverse suit of prey of sea bass represents a major logistical challange. Therefore, we inferred the relative individual specialisation in sea bass by comparing their dispersion in isotopic space against two sympatric, generalist bentho-pelagic predators collected concurrently along with sea bass: pout, *Trisopterus luscus* (Linnaeus, 1758), and whiting, *Meralngius merlangus* (Linnaeus, 1758). The juveniles of pout and whiting occur within estuarine habitats, exhibit limited movements and predate on a variety of invertebrate and fish prey (Heessen et al., 2015) making them suitable candidates for comparison. Variance in isotopic space was compared graphically by constructing standard ellipses, a two-dimensional equivalent of standard deviation and differences in dispersion were tested using the Euclidean distances of individuals from the population centroids based on methods described by M. J. Anderson (2006). Prior to analyses, isotope values were first normalised to their observed range across all species so that distances in each dimension were weighted equally. Post-hoc pair-wise comparisons using a Tukey test followed a significant difference in dispersion.

All statistical analyses were conducted in R 3.3.2 (R-Core-Team, 2016), with individual specialisation metric calculations conducted using the package 'RInSp' v1.2 (Zaccarelli

Table 5.1: Total number of sea bass sampled during the study separated into season and age group.

Season	Months	Age Class	N
Winter 2015	November 2015	0	7
	December 2015	1	7
	January 2016	2+	9
Spring 2016	February 2016	0	14
	March 2016	1	15
	April 2016	2+	5
Summer 2016	May 2016	0	0
	June 2016	1	1
	July 2016	2+	0
Autumn 2016	August 2016	0	17
	September 2016	1	0
	October 2016	2+	4
Winter 2016	November 2016	0	19
	December 2016	1	7
	January 2017	2+	10
Total		0	57
		1	30
		2+	28
		All	115

et al., 2013), dispersion tests using the package 'vegan' v2.4-5 (Oksanen et al., 2017) and standard ellipse construction and bayesian estimation using the package 'SIBER' v2.1.1 (A. L. Jackson et al., 2011). The priors used to calculate the posterior distributions of standard ellipse areas for each bi-plot were the inverse Wishart distribution with 2 degrees of freedom and a normal prior around the mean with a precision of 10^{-3}. Two chains were run of 10,000 iterations, with a burn in of 1000 and thinned by a factor of 10.

5.4 Results

5.4.1 Dietary Analyses

The number of individual sea bass collected are summarised in table 5.1, totalling 115 individuals over the whole period. The age class of 2+ includes all individuals estimated to be 2 years or older: only 2 individuals were estimated to be 3 years of age and 1 individual estimated at 4 years of age. As there was only one individual sampled during Summer 2016, this period was excluded from further analyses.

Although there were moderate levels of stomach vacuity, the I_{RI} and I_{MF} indices for dietary items across age classes and seasons generally showed broad agreement and are summarised in table 5.2. Briefly, polychaetes appear to be a highly important food source for sea bass across all age classes and seasons, particularly the year 1 age

class. Amphipods were a key resource for young of the year bass throughout the entire seasonal cycle, however they were only important for the year 1 sea bass in winter 2015 and were absent in all but one individual from the 2+ age class. Copepods were only present in the diet of the young of the year in the autumn, where they were the dominant food source, but absent in all other seasons and age classes. Prey fish showed a similar pattern, being the main food source in autumn for age class 2+ but only minor contributions during other seasons and practically absent in the other age classes. Shrimp and crabs contributed to the diet in all age classes, although more so to the 2+ bass, with contributions shifting over seasons. Over the winter period, bivalves were considerable components of the diets of the young of the year and the 2+ age class. Other prey categories made only minor contributions to sea bass diet.

5.4.2 Individual Specialisation

For the six seasonal age class groups where sufficient non-empty stomachs were available, levels of individual specialisation were typically high, table 5.3. The WIC:TNW metric was significant for all cohorts, although this measure can overestimate the degree of specialisation when there are high proportions of stomachs with only one food category present. However, the more conservative E_{adj} index also recorded significant levels of individual specialisation: only the young of the year and one year age classes of spring showed insignificant dietary specialisation for this metric.

A total of 53, 42 and 44 individuals of pout, bass and whiting respectively, distributed relatively evenly over the sampling period, were analysed for stable isotope composition. The individual size distributions for which isotopic signatures were measured are shown in Fig. 5.1, and are relatively similar across species, although whiting were slightly larger on average (mean body mass = 64.7g, 51.9g and 145g for bass, pout and whiting respectively). The three isotope bi-plots for carbon, nitrogen and sulphur are shown in Fig. 5.2. Sea bass appear to vary more greatly in isotopic space, indicated by the larger standard ellipses (which contain approximately 40% of the data) - the posterior distributions of the standard ellipse areas were greater for sea bass across all three stable isotope bi-plots, Fig. 5.2. This was confirmed by significance in the test of homogeneity

Table 5.2: Dietary indices based on stomach content analyses of sea bass grouped into seasonal age class cohorts, see Materials and Methods for description of indices. Values of 0.1 or greater (major components) highlighted in bold. N denotes the number of stomachs sampled.

	Age Class 0				**Age Class 1**				**Age Class 2+**			
	Winter 2015	Spring 2016	Autumn 2016	Winter 2016	Winter 2015	Spring 2016	Autumn 2016	Winter 2016	Winter 2015	Spring 2016	Autumn 2016	Winter 2016
N	7	14	17	19	7	15	0	7	9	5	4	10
I_V	0.57	0.29	0.29	0.42	0.43	0.13	-	0.86	0.44	0.4	0	0.3
Food Category	I_{RI} (I_{MF})											
Amphipods	**0.53 (0.38)**	**0.35 (0.26)**	**0.22 (0.22)**	**0.50 (0.27)**	**0.51 (0.54)**	0.01 (0.01)	-	0 (0)	0 (0)	0 (0)	0.01 (0.01)	0 (0)
Copepods	0 (0)	0 (0)	**0.68 (0.39)**	0 (0)	0 (0)	0 (0)	-	0 (0)	0 (0)	0 (0)	0 (0)	0 (0)
Isopods	0 (0)	0.04 **(0.12)**	0.01 (0.02)	0.03 (0.07)	0 (0)	0.02 (0.08)	-	0 (0)	0 (0)	0 (0)	0 (0)	0.01 (0.03)
Mysids	0 (0)	0 (0)	0 (0)	**0.11 (0.13)**	0 (0)	0 (0)	-	0 (0)	0 (0)	0 (0)	0 (0)	0 (0)
Decapod Crabs	0 (0)	0 (0)	0.03 **(0.10)**	0.03 **(0.10)**	0.04 (0.09)	0.01 (0.04)	-	0 (0)	**0.47 (0.46)**	0.01 (0.03)	0.05 **(0.10)**	**0.55 (0.40)**
Decapod Shrimp	**0.20 (0.24)**	0.01 (0.05)	0.02 (0.08)	0.05 **(0.11)**	0 (0)	0.02 (0.07)	-	0 (0)	0.03 (0.07)	0.04 (0.09)	**0.20 (0.22)**	**0.26 (0.17)**
Polychaetes	**0.15 (0.20)**	**0.60 (0.51)**	0.04 **(0.11)**	**0.28 (0.30)**	**0.44 (0.33)**	**0.93 (0.70)**	-	**1.00 (1.00)**	**0.40 (0.28)**	**0.94 (0.82)**	**0.16 (0.14)**	0.04 (0.08)
Fish	0 (0)	0 (0)	0 (0)	0 (0)	0 (0)	0.02 (0.08)	-	0 (0)	0.07 **(0.15)**	0 (0)	**0.53 (0.43)**	0.07 **(0.14)**
Bivalve	**0.12 (0.17)**	0 (0)	0.01 (0.04)	0 (0)	0 (0)	0 (0)	-	0 (0)	0.03 (0.05)	0.02 (0.06)	0.05 **(0.11)**	0.06 **(0.14)**
Gastropod	0 (0)	0.01 (0.04)	0.01 (0.04)	0 (0)	0 (0)	0 (0)	-	0 (0)	0 (0)	0 (0)	0 (0)	0 (0)
Algae	0 (0)	0 (0)	0 (0)	0.01 (0.03)	0.01 (0.05)	0.01 (0.02)	-	0 (0)	0 (0)	0 (0)	0 (0)	0 (0)
Detritus	0 (0)	0.01 (0.02)	0 (0)	0 (0)	0 (0)	0.01 (0.01)	-	0 (0)	0 (0)	0 (0)	0 (0)	0.02 (0.06)

Table 5.3: Metrics of individual specialisation for groups with 5 or more individuals with non-empty stomachs, see Materials and Methods for description of indices. Significance of each index denoted by the number of asterisks (* = $p < 0.05$, ** = $p < 0.01$, *** = $p < 0.001$). Number of stomachs containing only one food category are also reported as they can cause the WIC:TNW metric to overestimate the degree of individual specialisation. Further, we additionally analysed the pooled two winters for the 2+ age class to increase the number of stomachs to make it comparable to those of the other groups.

Age Class	**Season**	**Non-Empty Stomachs**	E_{adj}	WIC: TNW	**Stomachs with only one food category**
0	Spring 2016	10	0.245	0.304***	7
0	Autumn 2016	12	0.324**	0.305***	6
0	Winter 2016	11	0.334*	0.357***	5
1	Spring 2016	13	0.123	0.487***	4
2+	Winter 2015	5	0.505*	0.267*	2
2+	Winter 2016	7	0.664***	0.111***	4
2+	Winter 2015/16	12	0.446***	0.136***	6

in dispersion distances ($F_{2,135} = 14.538$, $p < 0.001$), with post-hoc testing indicating that bass were over-dispersed compared to pout (difference in mean distance from centroid of 0.929, $p < 0.001$) and whiting (difference of 1.091, $p < 0.001$). Pout and whiting showed no significant difference in dispersion (difference of 0.161, $p = 0.719$).

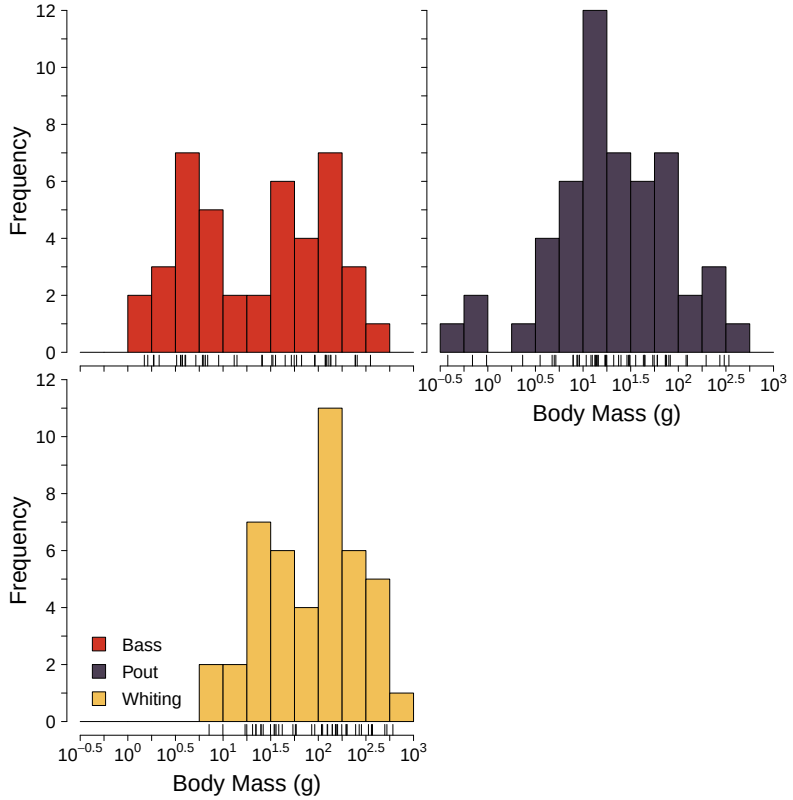

Figure 5.1: Size-frequency distributions of the individuals of the three species, sea bass (top left, n = 42), pout (top right, n = 53), and whiting (bottom left, n = 44), for which stable isotopic signatures were measured. Vertical lines beneath the histograms mark the values of individuals. Axes are the same across three graphs. Note that the body mass axes are on a logarithmic scale.

5.5 Discussion

The research presented here, to the best of our knowledge, is the first quantitative study on the extent of individual diet specialisation in juvenile sea bass. We hypothesised that juvenile sea bass within Southampton Water, an important nursery ground for this species, exhibit individual specialisation in diet. This hypothesis was confirmed utilising two distinct but complementary sources of evidence: stomach content data and stable

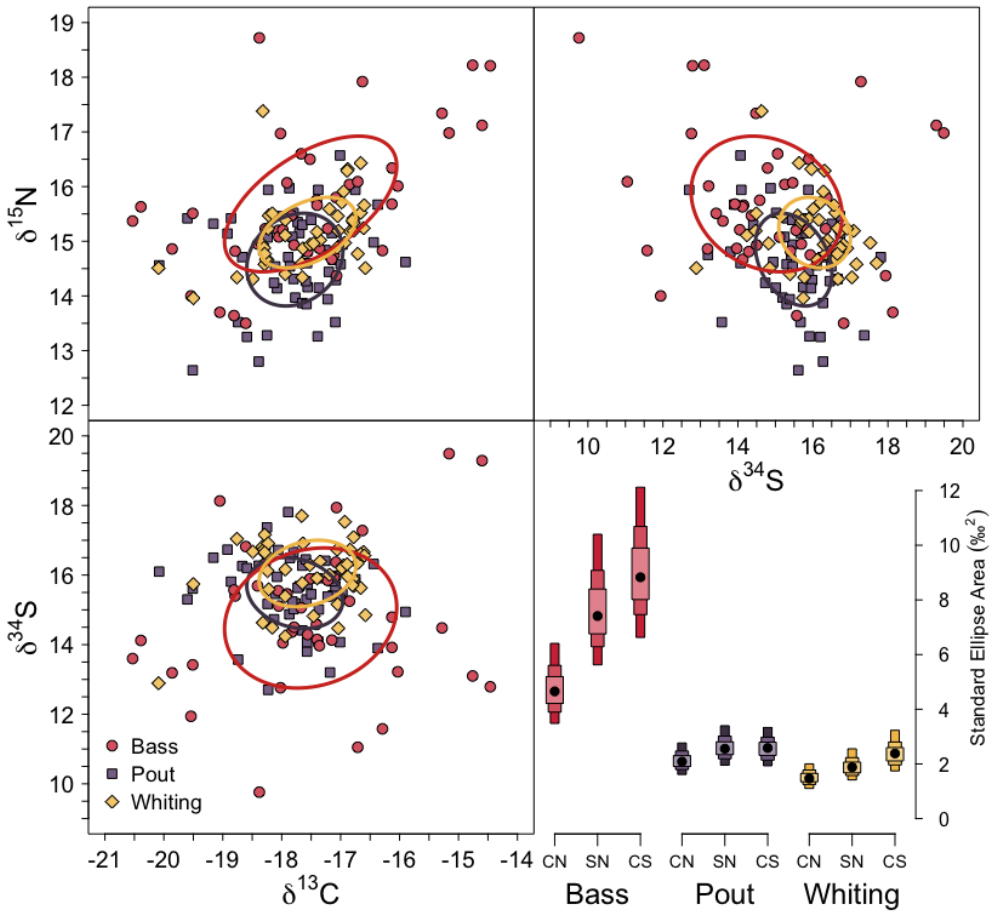

Figure 5.2: Stable isotope bi-plots of individual pout, bass and whiting, with standard ellipses plotted for each species. Bottom-right panel shows the bayesian posterior distribution of the standard ellipse area for each species for each bi-plot, where CN is carbon-nitrogen (top-left), SN is sulfur-nitrogen (top-right) and CS is carbon-sulfur (bottom-left). Credible intervals are 50, 75 and 95% with the mode of each distribution indicated by a black circle.

isotope analyses. The two metrics of individual specialisation from stomach content data yielded significant results for a majority of groupings after accounting for seasonal and ontogenetic influences on diet. Similarly, stable isotopes revealed that sea bass were over-dispersed in isotopic space compared to two sympatric predatory species, suggestive of comparatively higher levels of specialisation within sea bass.

These findings appear to contradict the previous assumption of generalist feeding behaviour in sea bass populations (Pickett & Pawson, 1994; Pérez-Ruzafa & Marcos, 2014). This inference is based on to observation of sea bass utilising different prey that are patchily distributed in space at the regional scale, e.g. Nereis spp., amphipods and

Carcinus maenas in salt marshes in south east England (Fonseca et al., 2011), similar to the results in this study, versus the brown shrimp, *Crangon crangon*, which dominate the prey base in the Wadden Sea (Cardoso et al., 2015). However no previous dietary study has tested whether the population-level generalist feeding behaviour in sea bass was due to generalism at the individual level or varying specialisations in diet. Here, we explicitly tested for the presence of individual specialisation within a single locality, Southampton Water, within which juvenile sea bass are assumably exposed to the same potential prey base, and found that the population consists of specialised individuals.

Individual specialisation has been well documented in various other fish species however, due to limited research, the extent to which it is found across species is currently unknown (Araújo et al., 2011). Studies have shown strong correlations between population density (a proxy for intraspecific competition) and the degree of individual specialisation in fishes (Svanbäck & Persson, 2009), suggestive of density dependence in the expression of individual specialisation. Frédérich et al. (2010) found that group density partially explained variation in specialisation in a site-attached damselfish. In experimental manipulation studies, larger young of the year eurasian perch (*Perca fluviatilis*) switched from consuming predominantly zooplankton to benthic macroinvertebrates when densities became high (Huss et al., 2008). Similar behaviour has also been noted in 0-class sea bass, with smaller conspecifics feeding mainly on pelagic copepods and larger individuals on epibenthic invertebrates (Fonseca et al., 2011).

Changes in *in situ* environment have also been suggested as mechanisms driving variation in the degree of individual specialisation, such as environmental stability, an increase in which has been shown to cause higher levels of specialisation in brown trout, *Salmo trutta* (Dermond et al., 2018). However, here data comparisons with sympatric predators exposed to the same environmental dynamics are suggestive of behavioural traits rather than extrinsic drivers. Phenotypic differences in foraging behaviours have been recorded in juvenile sea bass in terms of risk aversion (Millot et al., 2009; Killen et al., 2011), and shoaling (Boulineau-Coatanea, 1969). Juveniles also potentially segregate along temperature and salinity gradients within estuaries (López et al., 2015), and variation in habitat occupancy has been noted (Kelley, 1986). These variations in

behavioural traits and microhabitat occupancy, can also impart individual specialisation in diet as they result in individuals being exposed to different potential prey within a locality (Toscano et al., 2016).

It is important to note that compared to other dietary studies on sea bass, we acknowledge the total number of sea bass sampled here, 115 total, is relatively low (e.g. 404 in Spitz et al., 2013 and 570 in Rogdakis et al., 2010), and that suitable sample sizes were not available to test across all combinations of age class and season. However, this study was undertaken during a period when destructive sampling of juveniles is counter to efforts to rebuild sea bass stocks. To minimise this impact at a time of conservation concern, fish showing vigorous life signs and little to no damage by the sampling screens or trawling were immediately released, reducing sample sizes. For statistical analyses, we used null models based on random permutations, which maintain data structure and therefore incorporate small sample sizes when testing for significance (Zaccarelli et al., 2013). For stable isotope analyses, we included as balanced a design as feasible, given the sampling available. Given the agreement between stomach content data and stable isotope analyses, we therefore have confidence, despite the more limited sampling, in the results presented herein and the conclusions that are drawn.

While the concept of individual specialisation within populations is now well established (Araújo et al., 2011; Layman et al., 2015; Toscano et al., 2016), its ecological consequences have rarely been considered in terms of management strategies. We have shown high levels of individual specialisation in juvenile sea bass, which are typically a response to intraspecific competition and due to differences in behavioural traits. It likely follows therefore that individuals also specialise in their occupancy of the diverse microhabitats available within the estuary to limit competition between and within cohorts. High microhabitat dispersal within estuaries may also serve to reduce cannibalism, which is known to occur in sea bass (Henderson & Corps, 1997). Facilitating these specialisation behaviours, will therefore promote increased survival and population growth in juvenile sea bass during these early, vulnerable life stages of sea bass. Southampton Water already has special protection area (SPA) status with a variety of intertidal areas designated as Sites of Special Scientific Interest, predominantly due to the community of seabirds that

they support (Natural England, 2018). These encompass a variety of habitats such as salt water marshes, seagrass beds, mud, sand and coarse sediment flats. By extending the variety of microhabitats protected to also include subtidal areas, sea bass may also further benefit from this protection status. However, if protected areas are designed such that they only encompass a limited diversity in microhabitats, then intraspecific competition may reduce overall population condition, making juvenile sea bass more susceptible to climatic fluctuations (Henderson & Corps, 1997; Bento et al., 2016). This would reduce nursery ground contributions to standing stocks at a time when efforts are required at multiple levels to aid the recovery of this commercially important species (ICES, 2017; MMO, 2018).

5.6 Acknowledgements

The work presented here was funded by a NERC SPITFIRE PhD studentship (award number 1498909); a University of Southampton masters project; and a NERC LSMSF grant-in-kind, number EK272-08/16.

6 General Discussion

6.1 Summary of Findings

The inherent complexity of ecosystems makes them difficult to mechanistically study, yet capturing the ecological processes and interactions that determine ecosystem structure and function, in a quantitative manner, is crucial in order to test and develop ecological theory, to create realistic models and for the implementation of effective management and conservation strategies. Recent advances in the metabolic theory of ecology, MTE, have shown that power law relationships effectively capture much of the variation in biological processes, rates, times etc. across the huge diversity of life, condensing information along the single dimension of individual body size (Brown et al., 2004; Sibly et al., 2012). As such, power law based approaches are now commonly used for ecosystem modelling (Blanchard et al., 2017), and as metrics of ecosystem behaviour (Petchey & Belgrano, 2010), however this typically occurs over large spatial and temporal scales with a coarse resolution (globally or regionally, e.g. Jennings & Collingridge, 2015). The work presented in this thesis explored the dynamics of some of these ecological power law relationships at smaller scales compared to previous work. Their variability at smaller spatial and temporal scales was determined to assess whether this matched with expected ecological behaviour and therefore their viability as ecosystem metrics at these smaller scales.

6.1.1 Chapter 1

In Chapter 1, I introduced the functional form of the power law relationship and the prevalence at which it occurs in ecology. Their mathematical simplicity makes them a

computationally effective tool for modelling complex ecosystem processes (Guiet et al., 2016; Blanchard et al., 2017) and recent statistical developments have also improved their empirical parameterisation (Clauset et al., 2009; Edwards et al., 2017). While their pervasiveness has led to some scepticism (Stumpf & Porter, 2012), the allometric foundation of many power laws in biology provides a robust mechanistic underpinning (Thompson, 1942). This was further developed by West et al. (1997), who constructed a mechanistic model of individuals that, when scaled up to higher levels of biological organisation, predicted many of the ecological scaling relationships empirically derived during the 20^{th} century (Peters, 1983), and has since become the foundation of the metabolic theory of ecology.

6.1.2 Chapter 2

The relationship between the mean and variance has been of scientific interest since the introduction of ANOVA and the key requirement of equal variances between samples (Fisher, 1919, 1921). It was not until 1961 that Taylor showed empirically across many different populations of taxa that the variance in abundance was well described as a power law of the mean, and suggested the exponent as a metric of aggregation in the data. This proposal has since been questioned due to the ubiquity of TPL in complex systems and apparent lack of ecological inference (Downing, 1986; Kalyuzhny et al., 2014), yet studies have shown that TPL does appear to capture ecological information (Lagrue et al., 2015; Kuo et al., 2016).

I showed that in the size structured fish community of the North Sea, systematic differences in TPL, when populations were considered by individual size, were linked to the abiotic environment, namely hydrographic boundaries for temporal variability and basin type for spatial aggregation. This work suggests that TPL exponents capture community spatio-temporal dynamics as influenced by abiotic drivers. While links have been made between TPL and body size, either as trait effects (Kuo et al., 2016) or via mean abundance and size scaling (J. E. Cohen et al., 2016), this work is the first to consider individual body size explicitly, despite the importance of body size at the individual level (Brown et al., 2004).

6.1.3 Chapter 3

The size distribution of individual body sizes within a community follows a power law distribution, the exponent of which has been suggested as an ecological indicator of ecosystem health (Petchey & Belgrano, 2010). While fishing pressures are known steepen the size spectrum (e.g. Robinson et al., 2017), seasonal dynamics are less well studied, with limited research suggesting nuanced but limited influences on the exponent in fish communities (McGarvey & Kirk, 2018). I showed that the size spectrum in an estuarine fish community exhibits large seasonal periodicity, that corresponds to the known movements of different sized fish in response to temperature changes. This suggests that, if steady-state temporal average measures of the size spectrum are required, single point estimates may not be suitable even if data are collected across a relatively large spatial area.

In Chapter 3, I also explored trends in the stable isotope composition of the fish community. Stable isotopes can be used as natural geochemical tracers to elucidate information on trophic interactions (R. Ramos & González-Solís, 2012; Nielsen et al., 2018), and since size-based predator-prey dynamics strongly affect the size spectrum (Kerr & Dickie, 2001), SIA provide complementary information to size spectra. Results showed that, while some benthic bacterially derived sources are expressed in the food web, the majority of basal production is from pelagic phytoplankton as new production inputs during the spring bloom that is then remineralised over the winter. A key aspect of SIA is the rate at which assimilated material is incorporated into body tissues. I showed that during the summer when growth rates are high, stable isotopes are rapidly incorporated into fish biomass, faster than expected given published estimates of turnover rates (Thomas & Crowther, 2015; Vander Zanden et al., 2015).

6.1.4 Chapter 4

Due to the size-based constraints of predator-prey interactions, they are well described by the ratio between the body size of the predator and the body size of prey. Community based average PPMRs can be estimated using SIA and appear to exhibit high spatial variability (Jennings, Warr, & Mackinson, 2002; Reum et al., 2015; Ohshimo et al., 2016),

however the temporal variability, which is important for *in situ* energy flux dynamics, is poorly resolved. I showed that, over a seasonal cycle, PPMR varied over several orders of magnitude, similar to the variability recorded across space.

Under the assumption of energetic equivalence and steady state, the slope of the individual size spectrum within a community is (Trebilco et al., 2013):

$$M^{\beta} \propto M^{-\frac{3}{4}} \times M^{\frac{\log(\mathrm{TE})}{\log(\mathrm{PPMR})}} \tag{6.1}$$

which highlights how predator-prey interactions influence the size spectrum (Kerr & Dickie, 2001), and shows how the trophic transfer efficiency can be derived *in situ*. Similarly to the PPMR, TE also exhibited temporal variation of several orders of magnitude. However, the ecological inference of this *in situ* TE likely not a simple assimilation biomass ratio, due to assumption violation. I suggest that this may instead provide information of the flux of energy into or out of the system if one assumes the "true" efficiency is relatively constant.

6.1.5 Chapter 5

In Chapter 5, although not strictly utilising a power law relationship, I explored the level of individual specialisation within the diet of a commercially important but overexploited species, *Dicentrachus labrax* or the European sea bass. Previous diet studies have found generalist feeding behaviour within sea bass populations, inferred as opportunistic predation strategies (Pickett & Pawson, 1994). However, population level generalism can manifest itself either as a population of individual generalists or as a population of varied individual specialists (Araújo et al., 2011). This distinction had not, until this research, been resolved for sea bass, but is important as dietary specialisation can modulate intraspecific competition (Svanbäck & Persson, 2009), which will affect the recovery of this species. Both stomach content analysis and SIA suggested that the juvenile sea bass population within Southampton Water consists of individual specialists. Therefore the effective conservation of key nursery grounds should incorporate a diversity of microhabitats, and therefore prey, to facilitate this dietary behaviour.

6.2 A Brief Synthesis: Pattern and Scale

Pattern implies repetition, and the existence of repetition implies that some form of prediction is possible (MacArthur, 1972), and so in lies the aim of macroecology - to discern broad patterns within and across whole ecosystems to better understand and predict ecological processes. The question is then in defining "broad", or over what scale in which pattern should be quantified. This obviously depends upon the process of interest, however Levin (1992) highlighted that scientists, as observers, impose bias in how a system is viewed, to match a scale that suits us, rather than the scales over which patterns are expected based on theory and the often different scale of the mechanism(s) that give rise to them. Pattern is an emergent property in these complex systems. Some 25 years later, this ecological mismatch is still apparent (Chave, 2013; Estes et al., 2018), with scales often being selected for logistical convenience rather than biological reasoning (H. B. Jackson & Fahrig, 2015). In this thesis, care has been taken, within the limit of sampling constraints, to use data that has been collected at assumably ecologically relevant scales - aggregative behaviour across the North Sea but determined across swept area (on the order of $1km^2$) and the size distribution and trophic interactions based at the individual level measured at monthly intervals within a seasonally dynamic estuary.

It is not only scale that is important but, coupled with this, the dimension over which patterns are observed, namely time and space. Many studies focus on just one of these dimensions, yet it is nigh on impossible to sample and therefore explore patterns in one dimension at a fixed point in the other - coordinating the simultaneous sampling across the North Sea at the same point in time for example. Metrics are then typically estimated by averaging over the sampling regime with variation due to the other dimension implicitly dismissed as noise, with the researcher assuming dynamics are predominately expressed in the dimension of interest, either space or time. In reality, spatiotemporal dynamics exist across many scales (Levin, 1992) and should be accounted for. An exaggerated example would be the diel migration of mesopelagic food webs that could result in erroneous spatial distributions in surface pelagic biomass estimates if sampling varied over the course of a few hours at different sites. Of course, when scales

of measure become arbitrarily small, it can be argued that observed variation is merely stochastic noise. Such and argument should be used with caution however during the up-scaling of measure in macroecology, as it belies the inherent complexity of ecosystems. The results in this thesis highlight the importance of both dimension and scale when using common ecological metrics and tools.

In Chapter 2, I showed that at the regional scale (across the North Sea and at a time scale of several decades) patterns in the aggregative behaviour of the size structured fish community emerge both across space and through time, with trends exhibiting similar orders of magnitude, that relate to *in situ* hydrography. This implies that at these dimensional scales for this system, both spatial and temporal effects on community structure are important. Interestingly, Taylor's Power Law (TPL) that was used as a metric of aggregation does not depend on the scale of measure, and therefore can be quantified across a multitude of spatial and temporal scales. Such an approach could be used to derive the temporal and spatial scales over which aggregative behaviour is most prominent in fish and other communities. While the idea of scale and its importance has been highlighted for TPL in terms of generality and therefore usefulness (Xu, 2015), the converse argument is that it a lack of evidence for TPL for a particular species / community at a particular scale is evidence for its interpretation being ecologically redundant at that scale.

The size spectrum quantifies the size structure within the community as a power law distribution (Kerr & Dickie, 2001) and is now being used as a relatively simple ecological metric indicative of perturbations, notably fishing pressures (Sprules & Barth, 2016). In Chapter 3, I showed that the size spectrum of an estuarine fish community exhibited stark but consistent fluctuations across a seasonal cycle. The implication is that if spatial patterns in size structure are required, small differences in the time of sampling (on the order of only a few weeks) could impart large variation within the data, that, if the sampling regime is conducted systematically in space, could be falsely interpreted as a spatial trend. Similarly, I demonstrated that seasonal dynamics are rapidly incorporated into the stable isotope composition of the fish community during the summer period. Stable isotopes analyses are now a common ecological tool used to

elucidate information on the trophic niche structure and spatial patterns of individuals, populations and communities (R. Ramos & González-Solís, 2012), often blindly without regard to the multiple sources of variation, most notably temporal effects. For example, raw stable isotope values are now being used as a direct ecological "trait" in some studies (e.g. Wood et al., 2017). Results here suggest that temporal patterns can impart strong variation in isotopes over smaller scales than have been previously assumed and therefore should be considered in sampling designs. The size spectrum and stable isotope approaches were then naïvely but purposefully combined in Chapter 4 to demonstrate high temporal variability in predator-prey mass ratios and apparent trophic transfer efficiencies and to show that temporal dynamics need to be considered to better interpret results when applying metrics derived from theory.

Data here indicates that temporal dynamics in ecology can be strong at smaller scales. However with the advent of remote sensing with global coverage and ever more computing power, it is not surprising that macroecology is turning towards ever larger spatial scales. Coupled with this is the focus of climatic effects on ecosystems across large temporal scales. At these most certainly broad scales, dynamic ecosystem models can be constructed to predict and forecast large scale processes such as global fish production in a warming world (Blanchard et al., 2012; Jennings & Collingridge, 2015), in order to better inform management and policy. However, if smaller scale dynamics are large then empirical verification of such predictions becomes challenging, and their usefulness at local and regional levels is reduced. That is not to say that these large scale studies should be abandoned, but that an understanding and appreciation of ecological processes at smaller scales improves the context in which macroecological theory and forecasts can be placed. In fact, many statistical approaches that are employed to account for temporal effects when exploring spatial data or vice versa could be used to facilitate multi-dimensional exploration of dynamics given suitable data.

A final note is given to the concept of body size and its apparent ubiquity in explaining ecological variation (Peters, 1983). Indeed, individual body size is the cornerstone of MTE (Brown et al., 2004) and has featured strongly in this thesis. Much of this inference has been made by compiling data across large scales and it is important to

clarify however that, as demonstrated here, as scales are reduced then the import of size also appears to reduce. In Chapter 2, considering individuals by size revealed strong aggregative patterns compared to a species approach at a regional scale. In Chapter 3, while seasonal variations in size distributions were apparent at the local scale, linear mixed effects models identified influences of functional group and individual species in stable isotope data. Distinctions in size based trophic interactions between functional groups were also apparent in Chapter 4 with the local benthic food web seeming to lack size structure as inferred by stable isotopes. Finally, at the local species level within Southampton Water, differences in trophic behaviours were found between sea bass and two sympatric gadoid species. Other studies have made similar conclusions, with the predictive power of body size waning as food web complexity increases (Jonsson et al., 2018) or argue for a combined size-species approach for forecasting the population and community responses to, for example, changes in temperature (Lindmark et al., 2018). An integration and appreciation of both size and species (or functional group) would therefore improve macroecological theory and prediction, potentially explaining much of the residual variation in metabolic theory and other power law relationships.

6.3 Considerations and Future Directions

The results presented herein have focused on two locations: the North Sea for TPL and Southampton Water for size spectra. While the results are promising, showing strong temporal variability (and spatial for TPL) in these two areas for the associated metrics, location effects cannot be excluded, since the effective replication is one. In fact, Southampton Water was chosen as the ecological dynamics are especially stark in estuarine environments, and therefore more likely to show seasonality. Since both TPL and size spectra can be readily calculated from size and species abundance data, this allows for the testing of such dynamics in other locations. For example, while the North Sea IBTS was utilised here, similar surveys are conducted in other European shelf seas with appropriate data also readily accessible through the DATRAS data portal. Likewise there exists impingement data similar to that used for calculating the size spectrum of Southampton Water for many locations where cooling water is extracted for industrial

use and regulations require the monitoring of environmental impacts. Ecological datasets in general are becoming more openly available with the advent of data repositories, such as the global biodiversity information facility (www.gbif.org), which would allow for testing among differing taxa as well as locations.

A key aspect for any metric is its accurate parameterisation, particularly if the expected ranges over which they vary are relatively small. Whilst significant development has been made for more accurate parameterisation of power law distributions, i.e. size spectra, using maximum likelihood approaches (Clauset et al., 2009; Edwards et al., 2017), as of yet, no such methods exist for power law relationships. Researchers are thus limited to applying linear based regression approaches on logarithmically transform data (Sibly et al., 2012). Given the variety of regression methods available, e.g. ordinary vs. orthogonal least squares, Bayesian and median based, it is surprising that, currently, no quantitative comparison has been made in relation to power law parameterisation. In Chapter 2, I utilised two regression methods that qualitatively reproduced the same results, improving confidence in the conclusions drawn and something not conducted in other studies. However a full cross-comparison on simulated data would be useful to test for potential biases in regression methods applied to power law relationships. Similarly, there exists two separate methods for estimating PPMR, stomach content analysis and SIA, with no study conducting a direct comparison between the two. Given the importance of PPMR in modelling ecosystem processes, and the fact that physical samples are required for both approaches, this should also be addressed.

Sources of variability in stable isotopes can be categorised broadly into trophic (including physiological) processes, temporal variability and spatial variability (Boecklen et al., 2011; R. Ramos & González-Solís, 2012). In this thesis I have focused on the trophic and temporal sources of variability while quantifying system dynamics within Southampton Water. The assumption therefore is that spatial variability is negligible. Fish examined here are all relatively small, (on the order of 1kg or less) and therefore movements are relatively restricted even when individuals move out of the estuary. For example, tagging data on sea bass show that larger juveniles stay within a few kilometres of their estuarine nursery ground (Pawson et al., 1987). Studies on spatial variability of

isotopes typically show that variability occurs on the order of hundreds to thousands of kilometres and therefore should not influence results here, although spatial variability in inshore waters is poorly resolved but likely higher (Bowen, 2010).

Finally, the isotopic sampling, although spanning 15 months, only captured one full seasonal cycle. Confidence in the seasonal dynamics would therefore be improved if they were repeated over another or multiple cycles. Additionally, higher number of isotopic samples per month would also help reduce the uncertainty in regression estimates and therefore more tightly constrain, for example PPMR estimates, pertinent when errors are propagated. However, such an undertaking, although more ideal, would require logistical efforts that were beyond the scope of this research project.

7 | Appendices

7.1 Appendix: Taylor's Power Law in the North Sea Fish Community

Due to the large quantity of plots characterising individual TPL exponents, the supplementary material for this chapter is provided as a separate pdf document.

7.2 Appendix: Isotope Incorporation Model

This appendix corresponds to the incorporation of δ^{13}C into fish biomass in Southampton Water, as discussed in Chapter 3.

7.2.1 Model of Isotope Incorporation

Following Fry and Arnold (1982), a simple toy model was constructed to explore carbon isotope incorporation in pelagic fish within Southampton Water following the seasonal dynamics of the plankton. The model, defined by a difference equation, is based on two pathways in which isotopes are incorporated: catabolic turnover and somatic growth. Catabolic turnover follows first order kinetics (Fry & Arnold, 1982; Cerling et al., 2007), and here is modelled as a simple exponential decay toward equilibrium with a single source (a one compartment model). The isotopic composition of the consumer tissue due to turnover, $\delta^{13}\mathrm{C}_{cons}$, at time t is defined as:

$$\begin{aligned} \delta^{13}\mathrm{C}_{cons}(t) &= \lambda_t.\rho. + \big(1-\lambda_t\big).\delta^{13}\mathrm{C}_{cons}(t-1) \\ \rho &= \delta^{13}\mathrm{C}_{prey}(t) + \mathrm{TDF}_{cons} \end{aligned} \tag{7.1}$$

where each time step is considered one day. The first part of the equation gives the isotopic composition of the turned over tissue, ρ, defined as the temporally varying isotopic composition of the prey / diet ($\delta^{13}C_{prey}$) plus the consumer trophic discrimination factor (TDF_{cons}). The second part gives the isotopic composition of the tissue that is not turned over, which is equivalent to $\delta^{13}C_{cons}$ from the previous time step. The turnover rate, λ_t, defines the proportion of tissue mass that is replaced each time step.

By assuming that growth is not limited, i.e. exponential, then the dilution effect of newly formed somatic tissue can be included by a mass-specific growth term, λ_g such that:

$$\delta^{13}C_{cons}(t) = \frac{\lambda_t.\rho + \big(1-\lambda_t\big).\delta^{13}C_{cons}(t-1) + \lambda_g.\rho}{\big(1+\lambda_g\big)} \tag{7.2}$$

Using eq. 7.2, a two step food chain was constructed with the basal prey being phytoplankton, which were fed upon by zooplankton, which were likewise fed upon by fish.

7.2.2 Parameterisation of Model

Phytoplankton carbon isotopic composition, $\delta^{13}C_p$, is dependent upon the concentration of DIC which affects fractionation during fixation (Laws et al., 1995; Riebesell et al., 2000). Here, I assume that the concentration of DIC is a linear function of logarithmically transformed chlorophyll concentration, a proxy for phytoplankton density. The relationship is rescaled to approximately match measured values of phytoplankton from Goering et al. (1990), such that:

$$\delta^{13}C_p = \frac{\ln\left[Chl_a\right]}{2} - 20 \tag{7.3}$$

where Chl_a is the chlorophyll-a concentration (Fig. 3.9).

Zooplankton often have very high turnover rates, with a value of $\lambda_{t(zoo)} = 0.15$ assumed here, taken as the typical value from the literature review in Jardine et al. (2014). Zooplankton turnover rates are typically measured *in situ* as the rate of isotope incorporation, and therefore include both catabolic turnover and somatic growth. Therefore

zooplankton isotopic composition was modelled via eq. 7.1 with $\delta^{13}C_{prey}(t)$ given by eq. 7.3.

For fish, turnover rates were determined by using the equations described in Thomas and Crowther (2015) and Vander Zanden et al. (2015). Body mass was taken as the average of those sampled in May 2016 (0.61g) and temperate as the *in situ* measured over that period (11°c), as this is the period of interest. This gave $\lambda_{t(fish)} = 0.024$ and 0.043 respectively. Growth rates in fish are variable but can be as high as $0.16d^{-1}$ in fast growing post larval juveniles (Munk, 1991). Here, two growth rates were utilised, $\lambda_{g(fish)} = 0$ for no growth (which makes eq. 7.2 equivalent to eq. 7.1) and $\lambda_{g(fish)} = 0.05$ for high growth. For simplicity, $\lambda_{g(fish)}$ is assumed not to vary with time. Finally, for both zooplankton and fish, a TDF_{cons} of 1‰ was assumed.

7.3 Appendix: Stable Isotope Data

This appendix includes tables of species and stable isotope data used in Chapters 3, 4 and 5.

Table 7.1: List of fish species sampled from Southampton Water for which SIA were conducted (N = number of samples).

Common Name	**Species Name**	**N**
5-BeardedRockling	*Ciliata mustela*	4
BaillonsWrasse	*Symphodus bailloni*	2
BallanWrasse	*Labrus bergylta*	1
Bass	*Dicentrachus labrax*	42
BlackGoby	*Gobius niger*	7
CommonGoby	*Pomatoschistus microps*	2
CorkwingWrasse	*Symphodus melops*	3
Dogfish	*Scyliorhinus canicula*	2
Eel	*Anuilla anguilla*	2
Flounder	*Platichthys flesus*	10
GreaterPipefish	*Syngnathus acus*	2
GreyGurnard	*Eutrigla gurnardus*	4
GreyMullet	*Liza ramada*	4
GiltheadBream	*Sparus aurata*	5
Herring	*Clupe harengus*	26
LongSpineSeaScorpion	*Taurulus bubalis*	1
PaintedGoby	*Pomatoschistus pictus*	3
Plaice	*Pleuronectes platessa*	2
Pollock	*Pollachius pollachius*	1
Pout	*Trisopterus luscus*	53
ReticulatedDragonette	*Callionymus reticulatus*	6
RockGoby	*Gobius paganellus*	18
SandGoby	*Pomatoschistus minutus*	40
SandSmelt	*Atherina spp.*	40
Scad	*Trachurus trachurus*	3
Sole	*Solea solea*	11
Sprat	*Sprattus sprattus*	52
StarrySmoothHound	*Mustelus asterias*	5
ThornbackRay	*Raja clavata*	9
TransparentGoby	*Aphia minuta*	42
TubGurnard	*Chelidonichthys lucerna*	7
Whiting	*Merlangius merlangus*	44

Table 7.2: Raw stable isotope values of muscle from individual fish sampled from Southampton Water.

Month	Date	Species	SL (mm)	Weight (g)	Sample (mg)	δ^{15}N	δ^{13}C	δ^{34}S	N%	C%	S%	C/N	C/S
Oct-15	03/11/15	5-BeardedRockling	108	11.94	1.997	14.75	-17.2	17.07	14.50	45.54	1.42	3.14	32.04
Oct-15	03/11/15	Bass	65	3.7	1.994	16.97	-18.02	12.76	13.35	44.23	1.48	3.31	29.84
Oct-15	03/11/15	Bass	126	33.37	1.998	14.82	-18.79	15.4	13.97	46.85	1.38	3.35	33.94
Oct-15	03/11/15	Herring	71	3.57	1.869	13.86	-18.35	15.13	12.71	41.16	1.31	3.24	31.41
Oct-15	03/11/15	Herring	71	3.17	1.822	14.14	-17.85	15.7	12.90	41.58	1.26	3.22	33.1
Oct-15	03/11/15	Pout	100	13.82	1.949	15.15	-17.7	15.68	13.82	43.89	1.47	3.18	29.93
Oct-15	03/11/15	Pout	96	13.48	1.865	14.71	-18.67	16.26	14.40	45.66	1.50	3.17	30.46
Oct-15	03/11/15	RockGoby	34	0.65	1.839	13.33	-18.5	17.09	13.04	43.69	1.52	3.35	28.81
Oct-15	03/11/15	RockGoby	39	0.87	1.815	13.07	-18.69	16.88	12.66	43.10	1.51	3.4	28.5
Oct-15	03/11/15	RockGoby	53	2.06	1.878	12.28	-19.11	16.67	13.79	45.84	1.62	3.32	28.3
Oct-15	03/11/15	SandGoby	41	0.74	1.833	13.83	-18.62	15.48	13.13	43.03	1.48	3.28	29.09
Oct-15	03/11/15	SandGoby	48	1.18	1.84	13.54	-20.02	13.55	13.44	43.86	1.55	3.26	28.31
Oct-15	03/11/15	SandGoby	53	1.53	1.934	14.07	-18.34	14.26	13.47	44.04	1.45	3.27	30.37
Oct-15	03/11/15	SandGoby	61	2.92	1.898	13.69	-19.12	12.54	13.43	44.11	1.46	3.28	30.17
Oct-15	03/11/15	SandSmelt	96	9.7	1.997	14.39	-19.69	14.74	13.90	46.23	1.41	3.32	32.8
Oct-15	03/11/15	SandSmelt	102	12.36	1.961	14.31	-18.03	13.67	14.53	46.72	1.41	3.22	33.24
Oct-15	03/11/15	Sole	176	72.6	1.914	14.37	-16.26	16.19	13.07	43.30	1.27	3.31	34.13
Oct-15	03/11/15	Sole	162	48.23	1.973	12.47	-19.1	14.14	14.58	46.27	1.47	3.17	31.53
Oct-15	03/11/15	Sole	106	11.54	1.851	13.11	-14.36	12.12	14.49	45.81	1.60	3.16	28.67
Oct-15	03/11/15	Sprat	42	0.69	1.858	12.52	-19.82	15.69	13.00	42.10	1.25	3.24	33.72
Oct-15	03/11/15	Sprat	43	0.84	1.92	12.54	-19.6	16.41	13.85	43.55	1.25	3.14	34.91
Oct-15	03/11/15	TransparentGoby	33	0.28	1.911	13.95	-19.11	17.77	11.46	40.65	1.28	3.55	31.86
Oct-15	03/11/15	TransparentGoby	39	0.56	1.798	14.07	-18.96	16.85	11.83	41.79	1.30	3.53	32.18
Oct-15	03/11/15	Whiting	248	107.97	1.826	14.87	-17.64	16.91	14.24	44.39	1.29	3.12	34.28
Oct-15	03/11/15	Whiting	180	54.14	1.903	14.66	-18.24	16.12	14.88	46.55	1.28	3.13	36.29
Nov-15	01/12/15	Bass	131	32.48	1.919	15.75	-17.41	14.58	13.96	45.40	1.43	3.25	31.69
Nov-15	01/12/15	Herring	67	0.59	1.926	13.55	-18.25	15.96	12.78	41.25	1.33	3.23	31.1
Nov-15	01/12/15	Herring	88	5.53	1.86	13.76	-18.34	15.75	13.64	43.03	1.27	3.15	33.99
Nov-15	01/12/15	Herring	101	9.07	1.851	13.89	-18.28	15.67	13.67	42.68	1.32	3.12	32.38
Nov-15	01/12/15	Pout	123	29.95	1.928	15.35	-17.73	15.63	14.52	45.77	1.52	3.15	30.16
Nov-15	01/12/15	Pout	150	42.96	1.948	14.71	-17.89	17.81	14.76	45.65	1.48	3.09	30.94
Nov-15	01/12/15	Pout	156	53.96	1.87	15.94	-16.75	15.88	14.56	45.35	1.43	3.11	31.64
Nov-15	01/12/15	RockGoby	35	0.62	1.971	12.98	-19.17	17.35	12.60	42.35	1.49	3.36	28.34
Nov-15	01/12/15	RockGoby	59	3.38	1.968	13.91	-16.39	17.1	13.88	44.81	1.64	3.23	27.3
Nov-15	01/12/15	SandGoby	41	0.68	1.848	14.03	-20.27	12.06	12.92	43.48	1.40	3.37	31.14
Nov-15	01/12/15	SandGoby	46	0.99	1.946	13.92	-19.34	11.73	14.26	46.18	1.49	3.24	30.93
Nov-15	01/12/15	SandGoby	52	1.62	1.905	14.94	-17.8	13.57	14.36	46.16	1.61	3.21	28.63
Nov-15	01/12/15	SandGoby	54	1.62	1.871	14.71	-17.21	15.17	14.10	45.21	1.55	3.21	29.15
Nov-15	01/12/15	SandGoby	64	3.47	1.909	14.49	-17.2	12.36	13.81	44.57	1.55	3.23	28.8
Nov-15	01/12/15	SandSmelt	47	0.9	1.949	14.26	-17.72	16.29	12.38	42.23	1.29	3.41	32.65
Nov-15	01/12/15	SandSmelt	100	11.25	1.892	14.79	-17.57	15.85	13.71	45.30	1.33	3.31	34.11
Nov-15	01/12/15	SandSmelt	115	17.95	1.855	14.57	-18.23	14.74	14.26	46.54	1.45	3.26	32.18
Nov-15	01/12/15	SandSmelt	102	13.58	1.92	13.92	-20.43	14.3	13.34	44.68	1.38	3.35	32.35
Nov-15	01/12/15	Sprat	41	0.51	1.839	12.63	-19.4	16.92	11.68	39.69	1.10	3.4	36.16
Nov-15	01/12/15	Sprat	120	21.54	1.843	11.8	-19.7	17.03	11.10	50.13	0.93	4.52	53.96
Nov-15	01/12/15	TransparentGoby	32	0.19	1.963	13.2	-19.29	17.11	11.38	40.31	1.21	3.54	33.25
Nov-15	01/12/15	TransparentGoby	36	0.33	1.972	13.87	-19.32	15.69	12.27	42.59	1.34	3.47	31.83
Nov-15	01/12/15	Whiting	239	125.31	1.879	14.77	-16.71	16.34	14.73	45.38	1.11	3.08	40.96
Nov-15	01/12/15	Whiting	250	159.42	1.833	15.91	-16.95	16.28	14.52	45.28	1.12	3.12	40.27
Nov-15	01/12/15	Whiting	284	246.51	1.873	15.24	-16.61	16.66	14.55	45.52	1.08	3.13	42.23
Dec-15	17/12/15	Bass	149	52.16	1.831	15.08	-18.05	15.11	13.95	45.79	1.39	3.28	32.95
Dec-15	17/12/15	Herring	78	5.19	1.981	14.45	-18.32	16.58	13.02	42.23	1.26	3.24	33.54
Dec-15	17/12/15	Herring	90	6.41	1.878	14.82	-17.94	16.97	13.43	43.13	1.32	3.21	32.65
Dec-15	17/12/15	SandSmelt	63	2.27	1.874	13.86	-19.34	14.39	13.63	45.03	1.45	3.3	31.13
Dec-15	17/12/15	SandSmelt	71	2.81	1.86	14.14	-18.73	14.31	13.61	44.74	1.37	3.29	32.7
Dec-15	17/12/15	SandSmelt	109	16.02	1.902	14.41	-18.18	14.66	14.28	46.51	1.43	3.26	32.55
Dec-15	17/12/15	SandSmelt	52	1.33	1.859	13.37	-19.51	14.86	11.78	40.44	1.25	3.43	32.37
Dec-15	17/12/15	SandSmelt	52	1.25	1.861	12.54	-20	15.88	12.71	42.02	1.38	3.31	30.37
Dec-15	17/12/15	Sprat	54	1.15	1.838	12.6	-19.32	16.01	13.04	41.30	1.16	3.17	35.51
Dec-15	17/12/15	Sprat	94	10.92	1.969	13.29	-18.44	17.22	11.93	47.12	0.95	3.95	49.54
Dec-15	17/12/15	Sprat	118	18.47	1.918	12.52	-18.78	16.74	11.81	48.82	0.93	4.13	52.51
Dec-15	17/12/15	Sprat	43	0.76	1.883	12.54	-19.86	16.6	12.66	41.40	1.20	3.27	34.43
Dec-15	17/12/15	Sprat	49	1.1	1.981	11.95	-19.15	16.35	13.43	41.14	1.11	3.06	37.21
Dec-15	17/12/15	Sprat	51	1.31	1.824	12.7	-19.56	16.5	12.10	39.86	1.21	3.3	33.04
Dec-15	17/12/15	TransparentGoby	35	0.25	1.906	13.51	-19.23	16.58	12.01	42.10	1.29	3.51	32.76
Dec-15	17/12/15	TransparentGoby	38	0.45	1.814	13.73	-18.66	17.5	12.01	42.40	1.30	3.53	32.53
Dec-15	17/12/15	TransparentGoby	40	0.5	1.996	13.66	-19.56	16.2	12.07	42.52	1.31	3.52	32.42
Dec-15	17/12/15	TransparentGoby	37	0.36	1.927	13.28	-19.91	16.19	11.96	43.02	1.33	3.6	32.29
Dec-15	17/12/15	Whiting	131	22.16	1.962	14.94	-18.33	16.81	14.16	44.51	1.29	3.14	34.61
Dec-15	17/12/15	Whiting	146	34.36	1.963	15.47	-18.22	15.59	14.83	46.42	1.34	3.13	34.7
Dec-15	17/12/15	Whiting	234	200.86	1.983	15.51	-18.16	14.49	14.82	46.77	1.11	3.16	42.32
Dec-15	17/12/15	Whiting	265	268.77	1.995	15.52	-16.66	16.6	14.40	45.39	1.07	3.15	42.45
Dec-15	10/12/15	Bass	210	152.66	1.939	14.75	-17.11	15.93	14.49	46.62	1.35	3.22	34.44
Dec-15	10/12/15	Bass	198	133.27	1.959	15.2	-18.06	15.55	13.98	45.63	1.38	3.26	33.08
Dec-15	10/12/15	Bass	196	135.58	1.913	15.66	-17.4	14.15	14.73	47.99	1.35	3.26	35.63
Dec-15	10/12/15	Herring	163	58.12	1.86	14.17	-18.53	14.93	13.67	46.82	1.09	3.42	43.03
Dec-15	10/12/15	Herring	156	49.77	1.874	14.22	-18.79	15.39	12.90	47.40	1.18	3.67	40.13
Dec-15	10/12/15	Herring	148	41.96	1.863	14.65	-18.64	15.85	14.03	47.52	1.37	3.39	34.73
Dec-15	10/12/15	Whiting	350	607.07	1.843	15.18	-16.84	16.73	15.27	47.77	1.10	3.13	43.4
Dec-15	10/12/15	Whiting	335	525.18	1.8	15.19	-16.78	17.09	14.88	47.06	1.13	3.16	41.49
Dec-15	10/12/15	Whiting	305	370.61	1.862	15.34	-16.78	15.68	14.81	45.88	1.15	3.1	39.93
Dec-15	10/12/15	Whiting	285	336.1	1.89	15.41	-16.79	15.89	14.24	44.84	1.06	3.15	42.43

Table 7.2 continued.

Month	Date	Species	SL (mm)	Weight (g)	Sample (mg)	δ^{15}N	δ^{13}C	δ^{34}S	N%	C%	S%	C/N	C/S
Jan-16	21/01/16	Bass	134	35.56	1.841	15.63	-20.39	14.12	14.17	45.44	1.41	3.21	32.23
Jan-16	21/01/16	Bass	47	1.49	1.854	16.6	-17.67	15.06	13.06	44.73	1.38	3.42	32.32
Jan-16	21/01/16	Bass	162	66.75	1.991	16.5	-17.52	15.89	14.20	45.75	1.39	3.22	32.91
Jan-16	21/01/16	Herring	128	14.93	1.837	14.17	-17.93	18	12.69	40.70	1.23	3.21	32.97
Jan-16	21/01/16	Herring	85	5.03	1.934	14.41	-17.82	16.63	12.71	40.56	1.24	3.19	32.69
Jan-16	21/01/16	Pout	104	17.76	1.856	15.42	-18.86	15.81	14.13	44.82	1.51	3.17	29.7
Jan-16	21/01/16	Pout	115	25.02	1.945	15.97	-17.87	14.87	13.62	43.71	1.41	3.21	30.93
Jan-16	21/01/16	SandGoby	54	1.92	1.964	15.26	-18.25	12.7	13.11	43.37	1.34	3.31	32.26
Jan-16	21/01/16	SandGoby	44	0.95	1.933	14.15	-19.19	12.35	13.84	44.87	1.54	3.24	29.18
Jan-16	21/01/16	SandGoby	53	2.17	1.82	15.88	-19.47	14.62	13.76	44.86	1.40	3.26	32.11
Jan-16	21/01/16	SandSmelt	65	2.35	1.973	14.29	-19.53	15.35	12.98	45.82	1.39	3.53	32.88
Jan-16	21/01/16	SandSmelt	95	10.16	1.93	14.57	-18.76	13.66	13.75	45.99	1.48	3.35	31.04
Jan-16	21/01/16	Sprat	52	1.3	1.875	13.65	-19.19	16.28	13.22	44.17	1.24	3.34	35.54
Jan-16	21/01/16	Sprat	42	0.65	1.88	12.54	-19.5	16.27	13.86	43.19	1.22	3.12	35.5
Jan-16	21/01/16	Sprat	89	6.4	1.983	13.33	-17.8	17.74	13.10	42.69	1.16	3.26	36.74
Jan-16	21/01/16	Sprat	103	11.92	1.836	13.26	-17.06	16.38	13.78	44.83	1.12	3.25	40.03
Jan-16	21/01/16	Sprat	81	6.04	1.888	13.55	-18.68	15.53	13.35	43.68	1.22	3.27	35.84
Jan-16	21/01/16	TransparentGoby	33	0.23	1.906	14.13	-19.09	15.92	13.40	46.26	1.30	3.45	35.49
Jan-16	21/01/16	TransparentGoby	39	0.5	1.944	14.09	-18.98	16.49	11.85	41.73	1.29	3.52	32.33
Jan-16	21/01/16	TransparentGoby	37	0.38	1.87	13.94	-19.5	16.3	11.27	40.19	1.29	3.57	31.26
Jan-16	21/01/16	TubGurnard	171	78.15	1.893	15.2	-17.23	11.21	14.13	45.72	1.30	3.24	35.05
Jan-16	21/01/16	TubGurnard	232	189.23	1.938	16.19	-15.8	14.33	14.46	45.92	1.30	3.18	35.45
Jan-16	21/01/16	Whiting	125	17.02	1.804	14.34	-18.76	17.04	13.54	42.50	1.22	3.14	34.91
Jan-16	21/01/16	Whiting	187	58.6	1.958	15.02	-17.35	16.39	14.55	45.26	1.22	3.11	37.05
Jan-16	21/01/16	Whiting	225	176.33	1.89	15.59	-17.19	16.01	14.10	44.38	1.07	3.15	41.37
Jan-16	21/01/16	Whiting	252	196.09	1.969	15.17	-17.4	15.91	14.48	45.29	1.12	3.13	40.52
Feb-16	25/02/16	Bass	76	6.07	1.885	13.7	-19.05	18.13	11.31	39.68	1.26	3.51	31.6
Feb-16	25/02/16	Bass	123	25.51	1.995	18.72	-18.38	9.76	14.00	45.04	1.26	3.22	35.72
Feb-16	25/02/16	Bass	118	25.85	1.931	14	-19.54	11.94	13.67	44.78	1.31	3.28	34.08
Feb-16	25/02/16	Bass	62	3.26	1.834	16.98	-15.16	19.49	13.68	44.92	1.40	3.28	31.99
Feb-16	25/02/16	Bass	68	3.74	1.806	17.12	-14.6	19.29	14.17	46.48	1.47	3.28	31.71
Feb-16	25/02/16	Herring	97	9.24	1.942	16.46	-20.56	15.43	13.69	42.95	1.23	3.14	34.8
Feb-16	25/02/16	Herring	106	9.1	1.881	13.75	-17.98	17.06	12.98	39.75	1.14	3.06	34.89
Feb-16	25/02/16	Pout	117	30.97	1.864	15.46	-18.06	16.72	13.99	44.78	1.37	3.2	32.73
Feb-16	25/02/16	Pout	133	44.52	1.952	16.57	-17.01	14.07	14.19	45.33	1.41	3.2	32.06
Feb-16	25/02/16	Pout	146	60.38	1.948	14.94	-16.97	15.45	14.09	44.84	1.32	3.18	34.09
Feb-16	25/02/16	SandGoby	43	1.02	1.925	14.01	-20.6	10.95	12.93	44.00	1.49	3.4	29.48
Feb-16	25/02/16	SandGoby	55	2.3	1.844	15.58	-18.31	15.38	12.72	42.60	1.41	3.35	30.17
Feb-16	25/02/16	SandSmelt	51	0.87	1.824	13.26	-19.02	15.95	12.42	41.38	1.43	3.33	29.02
Feb-16	25/02/16	SandSmelt	92	8.27	1.956	14.64	-19.02	15.22	13.45	44.61	1.41	3.32	31.75
Feb-16	25/02/16	Sprat	44	0.85	1.82	12.79	-19.65	15.54	13.20	41.51	1.19	3.15	35.03
Feb-16	25/02/16	Sprat	52	1.45	1.94	13.21	-19.66	15.28	13.45	42.36	1.12	3.15	37.93
Feb-16	25/02/16	Sprat	57	1.95	1.933	14.03	-18.83	16.13	12.42	40.93	1.21	3.3	33.85
Feb-16	25/02/16	Sprat	63	3	1.894	13.44	-18.71	16.18	13.89	44.60	1.14	3.21	38.97
Feb-16	25/02/16	Sprat	102	9.8	1.886	11.49	-18.02	18.58	13.28	42.54	1.11	3.2	38.43
Feb-16	25/02/16	ThornbackRay	248	64.25	1.962	13.8	-17.51	16.26	15.90	44.22	1.00	2.78	44.36
Feb-16	25/02/16	ThornbackRay	307	145.98	1.808	14.77	-17.16	13.92	15.64	43.78	1.10	2.8	39.94
Feb-16	25/02/16	TransparentGoby	35	0.26	1.876	12.31	-17.27	17.87	12.97	46.26	1.15	3.57	40.09
Feb-16	25/02/16	TransparentGoby	40	0.46	1.989	13.88	-19.09	17.64	11.61	41.34	1.24	3.56	33.4
Feb-16	25/02/16	TransparentGoby	40	0.5	1.886	14.56	-19.49	16.13	11.50	40.43	1.30	3.52	31.05
Feb-16	25/02/16	Whiting	212	57.43	1.835	14.94	-17.52	16.29	13.93	43.80	1.07	3.14	41.06
Mar-16	23/03/16	Bass	80	6.52	1.863	17.92	-16.63	17.28	14.05	45.71	1.41	3.25	32.53
Mar-16	23/03/16	Bass	81	6.27	1.888	18.22	-14.76	13.1	13.55	45.21	1.41	3.34	32.15
Mar-16	23/03/16	BlackGoby	72	6.1	1.869	13.55	-18.43	14.99	13.99	46.63	1.36	3.33	34.31
Mar-16	23/03/16	Dogfish	541	619	1.926	14.2	-16.34	16.75	14.87	44.31	0.93	2.98	47.64
Mar-16	23/03/16	Dogfish	515	627	1.98	15.26	-16.45	15.92	15.62	44.41	0.97	2.84	45.64
Mar-16	23/03/16	Flounder	40	1.26	1.972	15.82	-26.12	3.5	12.56	41.74	1.21	3.32	34.49
Mar-16	23/03/16	Flounder	43	1.32	1.845	13.1	-29.46	5.35	12.38	41.79	1.25	3.37	33.4
Mar-16	23/03/16	Flounder	71	6.3	1.831	15.1	-25.13	11.06	11.87	39.55	1.28	3.33	30.91
Mar-16	23/03/16	Flounder	60	3.49	1.847	16.03	-28.04	-0.45	12.60	41.29	1.34	3.28	30.79
Mar-16	23/03/16	Flounder	63	4.26	1.828	12.65	-27.39	7.05	13.57	44.47	1.32	3.28	33.68
Mar-16	23/03/16	GuiltheadBream	126	60.96	1.873	15.42	-17.12	13.49	13.84	46.50	1.26	3.36	36.91
Mar-16	23/03/16	GuiltheadBream	121	50.29	1.843	14.47	-14.46	12.29	13.67	45.18	1.28	3.3	35.32
Mar-16	23/03/16	GuiltheadBream	114	45.14	1.893	16.6	-16.48	15.38	14.57	47.57	1.48	3.26	32.09
Mar-16	23/03/16	GuiltheadBream	103	30.59	1.876	16.5	-15.44	14.69	14.21	46.59	1.35	3.28	34.61
Mar-16	23/03/16	Herring	120	15.22	1.862	14.93	-18.24	17.6	13.64	43.45	1.25	3.19	34.73
Mar-16	23/03/16	Pout	95	13.29	1.968	15.32	-19.16	16.5	13.64	43.88	1.46	3.22	29.96
Mar-16	23/03/16	Pout	125	35.68	1.955	15.52	-17.8	15.02	13.34	43.28	1.35	3.25	32.13
Mar-16	23/03/16	Pout	161	73.76	1.885	15.94	-18.23	12.7	14.00	45.14	1.38	3.22	32.78
Mar-16	23/03/16	RockGoby	70	6.24	1.983	12.76	-18.75	17.58	12.84	42.68	1.57	3.32	27.26
Mar-16	23/03/16	SandGoby	35	0.36	1.862	13.76	-18.47	16.39	12.68	42.45	1.37	3.35	31.05
Mar-16	23/03/16	SandGoby	47	0.92	1.897	15.93	-16.74	11.43	11.89	40.42	1.39	3.4	29.08
Mar-16	23/03/16	SandGoby	43	0.81	1.861	14.29	-19.4	14.72	11.78	40.28	1.29	3.42	31.2
Mar-16	23/03/16	SandSmelt	69	3.1	1.929	14.21	-18.73	17.02	12.90	43.00	1.53	3.33	28.07
Mar-16	23/03/16	SandSmelt	71	3.18	1.879	14.02	-19.25	15.15	12.96	43.56	1.52	3.36	28.69
Mar-16	23/03/16	Sole	126	18.51	1.888	12.41	-19.29	11.58	13.62	43.48	1.47	3.19	29.68
Mar-16	23/03/16	Sprat	51	0.77	1.946	14.15	-20.04	16.32	12.64	43.88	1.10	3.47	39.93
Mar-16	23/03/16	Sprat	56	1.44	1.967	14.18	-20.07	15.5	12.32	42.14	1.15	3.42	36.7
Mar-16	23/03/16	TransparentGoby	40	0.46	1.987	14.16	-18.82	18.3	11.81	41.99	1.26	3.56	33.36
Mar-16	23/03/16	TransparentGoby	41	0.48	1.915	12.75	-18.29	18.2	12.13	42.16	1.26	3.48	33.47
Mar-16	23/03/16	TransparentGoby	42	0.66	1.938	14.58	-19	16.93	11.31	39.87	1.25	3.52	31.98
Mar-16	23/03/16	TubGurnard	124	28.78	1.968	14.42	-17.8	17.98	13.98	44.95	1.46	3.22	30.78
Mar-16	23/03/16	Whiting	248	124	1.892	14.97	-16.93	17.53	14.52	45.43	1.08	3.13	41.88
Mar-16	23/03/16	Whiting	103	7.13	1.829	13.96	-19.5	15.74	13.33	42.65	1.24	3.2	34.51

Table 7.2 continued.

Month	Date	Species	SL (mm)	Weight (g)	Sample (mg)	δ^{15}N	δ^{13}C	δ^{34}S	N%	C%	S%	C/N	C/S
Mar-16	29/03/16	Bass	246	243.99	1.925	16.01	-16.03	13.22	14.35	45.91	1.15	3.2	39.8
Mar-16	29/03/16	Bass	189	119.3	1.829	15.37	-20.53	13.6	13.34	44.33	1.22	3.32	36.29
Mar-16	29/03/16	Bass	182	91.5	1.85	15.23	-18.28	16.34	13.88	45.53	1.27	3.28	35.91
Mar-16	29/03/16	Herring	172	65	1.963	14.2	-18.08	15.31	13.57	43.85	1.04	3.23	42.04
Mar-16	29/03/16	Herring	179	67.19	1.897	14.14	-17.84	15.3	13.92	44.80	1.05	3.22	42.77
Mar-16	29/03/16	Herring	174	56.63	1.806	11.66	-17.36	18.77	14.18	43.23	1.11	3.05	38.82
Mar-16	29/03/16	Pout	236	272.97	1.97	15.94	-17.38	14.09	14.06	45.22	1.34	3.22	33.67
Mar-16	29/03/16	Pout	196	195.95	1.828	14.66	-17.13	15.42	14.77	46.12	1.18	3.12	38.96
Mar-16	29/03/16	Pout	239	339.81	1.905	15.3	-17.65	14.41	13.18	42.40	1.28	3.22	33.05
Mar-16	29/03/16	Whiting	307	499.49	1.851	17.38	-18.32	14.63	14.52	46.76	1.44	3.22	32.48
Mar-16	29/03/16	Whiting	272	361.47	1.816	15.71	-16.98	16.2	13.92	44.79	1.03	3.22	43.69
Apr-16	21/04/16	5-BeardedRockling	177	55.21	1.843	14.96	-19.84	15.18	13.92	44.93	1.43	3.23	31.32
Apr-16	21/04/16	BaillonsWrasse	62	4.63	1.892	11.4	-18.59	15.99	13.40	44.54	1.53	3.33	29.14
Apr-16	21/04/16	Bass	66	3.99	1.915	17.34	-15.28	14.48	13.09	45.44	1.48	3.47	30.66
Apr-16	21/04/16	Bass	102	13.09	1.801	15.68	-16.13	13.92	13.98	45.28	1.52	3.24	29.74
Apr-16	21/04/16	BlackGoby	66	5.81	1.878	13.63	-18.59	13.26	13.92	45.27	1.57	3.25	28.88
Apr-16	21/04/16	BlackGoby	94	19.6	1.989	13.7	-19.27	10.45	13.32	44.46	1.45	3.34	30.66
Apr-16	21/04/16	CorkwingWrasse	73	7.45	1.98	14.05	-18.83	16.07	13.92	46.29	1.38	3.32	33.51
Apr-16	21/04/16	Flounder	54	2.52	1.806	13.37	-27.41	6.29	13.34	44.34	1.31	3.32	33.8
Apr-16	21/04/16	Flounder	77	8.78	1.861	13.24	-29.37	7.58	12.48	45.48	1.16	3.64	39.34
Apr-16	21/04/16	PaintedGoby	41	0.79	1.828	14.18	-17.68	16.97	13.05	42.80	1.47	3.28	29.08
Apr-16	21/04/16	PaintedGoby	42	0.8	1.89	14.1	-20.2	14.21	13.07	44.07	1.53	3.37	28.83
Apr-16	21/04/16	Pollock	208	83.29	1.844	15.03	-18.48	16.51	14.47	45.56	1.28	3.15	35.47
Apr-16	21/04/16	Pout	170	82.35	1.943	15.42	-19.6	15.3	14.34	46.47	1.35	3.24	34.39
Apr-16	21/04/16	ReticulatedDragonette	108	12.96	1.968	12.52	-17.97	14.17	14.76	46.25	1.33	3.13	34.78
Apr-16	21/04/16	ReticulatedDragonette	78	5.65	1.972	13.33	-20.74	14.85	14.17	45.90	1.36	3.24	33.76
Apr-16	21/04/16	ReticulatedDragonette	46	1.24	1.981	12.77	-21.91	13.41	13.74	44.72	1.38	3.26	32.48
Apr-16	21/04/16	ReticulatedDragonette	39	0.38	1.84	13.46	-18.05	16.2	10.90	35.81	1.19	3.29	30.1
Apr-16	21/04/16	RockGoby	40	0.93	1.859	13.16	-20.91	15.73	11.35	47.62	1.18	4.2	40.47
Apr-16	21/04/16	RockGoby	61	3.49	1.83	11.84	-19.14	14.96	13.24	44.22	1.67	3.34	26.44
Apr-16	21/04/16	SandGoby	35	0.37	1.915	13.87	-19.32	15.92	12.60	43.53	1.27	3.46	34.36
Apr-16	21/04/16	SandGoby	45	0.76	1.875	13.59	-20.42	15.43	11.51	42.21	1.31	3.67	32.18
Apr-16	21/04/16	SandGoby	52	1.18	1.887	12.98	-21.9	12.96	12.41	40.94	1.46	3.3	27.98
Apr-16	21/04/16	SandSmelt	51	1.17	1.888	14.48	-17.74	16.13	11.35	39.81	1.38	3.51	28.85
Apr-16	21/04/16	SandSmelt	60	1.89	1.828	13.99	-18.82	15.65	12.38	41.22	1.41	3.33	29.3
Apr-16	21/04/16	SandSmelt	101	11.4	1.89	16.31	-18.08	14.18	13.53	44.62	1.47	3.3	30.3
Apr-16	21/04/16	SandSmelt	103	12.5	1.814	14.29	-19.03	15.65	14.12	46.14	1.40	3.27	32.91
Apr-16	21/04/16	SandSmelt	117	15.45	1.899	14.39	-18.29	17.25	14.33	45.52	1.37	3.18	33.11
Apr-16	21/04/16	Scad	222	131.65	1.868	14.32	-18.54	17.23	14.17	47.35	1.04	3.34	45.59
Apr-16	21/04/16	TransparentGoby	34	0.27	1.89	12.7	-18.89	17.29	10.94	39.40	1.24	3.6	31.91
Apr-16	21/04/16	TransparentGoby	37	0.35	1.914	12.02	-18.7	18.23	11.59	41.58	1.24	3.59	33.53
Apr-16	21/04/16	TransparentGoby	36	0.29	1.98	11.97	-18.76	17.81	10.48	37.86	1.20	3.61	31.51
Apr-16	21/04/16	TransparentGoby	46	0.9	1.849	13.42	-19.28	16.87	11.55	42.07	1.27	3.64	33.07
Apr-16	21/04/16	TubGurnard	132	39.08	1.811	15.24	-19.07	12.22	13.49	43.63	1.40	3.24	31.19
Apr-16	21/04/16	TubGurnard	121	22.06	1.87	15.4	-17.62	15.24	13.46	43.59	1.58	3.24	27.58
Apr-16	21/04/16	Whiting	148	31.48	1.989	14.51	-20.09	12.89	13.54	43.51	1.18	3.21	36.87
Apr-16	21/04/16	Whiting	245	156.82	1.879	15.66	-16.6	16.56	14.03	44.81	1.02	3.19	43.94
May-16	16/05/16	Flounder	182	109.95	1.89	14.48	-16.92	8.52	14.64	46.62	1.49	3.18	31.21
May-16	16/05/16	Sprat	32	0.29	1.935	11.15	-16.84	16.9	12.47	41.36	1.13	3.32	36.52
May-16	16/05/16	Sprat	34	0.35	1.832	10.88	-17.01	16.85	12.41	41.29	1.18	3.33	34.99
May-16	16/05/16	Sprat	38	0.48	1.987	11.23	-16.79	17.44	11.74	40.65	1.13	3.46	35.95
May-16	16/05/16	TransparentGoby	34	0.25	1.843	11.96	-17.51	17.21	11.59	42.94	1.22	3.71	35.07
May-16	16/05/16	TransparentGoby	44	0.68	1.888	12.27	-16.92	17.24	11.53	41.47	1.17	3.6	35.3
May-16	16/05/16	TransparentGoby	43	0.85	1.958	12.29	-16.9	16.69	12.31	42.68	1.24	3.47	34.4
May-16	16/05/16	TransparentGoby	44	0.68	1.828	12.69	-17.4	17.17	12.13	42.48	1.21	3.5	35.18
May-16	16/05/16	TransparentGoby	49	1.27	1.938	16.88	-15.29	14.56	13.48	43.05	1.24	3.19	34.65
Jun-16	23/06/16	Bass	116	245.3	1.836	15.23	-17.22	15.85	14.15	45.03	0.99	3.18	45.48
Jun-16	23/06/16	CommonGoby	34	0.41	1.977	14.4	-18.73	9.83	12.73	41.53	1.36	3.26	30.62
Jun-16	23/06/16	CommonGoby	38	0.87	1.912	14.94	-23.46	12.9	13.18	43.24	1.46	3.28	29.54
Jun-16	23/06/16	Pout	64	4.98	1.911	13.52	-17.09	15.67	12.67	41.95	1.25	3.31	33.68
Jun-16	23/06/16	Pout	75	7.89	1.89	13.26	-17.39	15.91	13.70	44.29	1.44	3.23	30.86
Jun-16	23/06/16	Pout	35	0.38	1.931	13.25	-18.59	16.2	13.04	43.97	1.34	3.37	32.74
Jun-16	23/06/16	Pout	37	0.69	1.915	12.8	-18.39	16.27	10.39	35.40	1.24	3.41	28.63
Jun-16	23/06/16	SandSmelt	103	13	1.936	13.9	-18.27	14.93	13.35	44.87	1.30	3.36	34.64
Jun-16	23/06/16	Sole	186	88.39	1.835	12.55	-19.97	13.08	13.41	47.06	1.26	3.51	37.3
Jun-16	23/06/16	Sole	189	84.76	1.931	12.57	-19.07	11.24	13.81	44.50	1.21	3.22	36.79
Jun-16	23/06/16	Sprat	30	0.18	1.856	11.07	-19.62	16.98	11.58	39.41	1.24	3.4	31.91
Jun-16	23/06/16	Sprat	31	0.21	1.966	10.66	-19.58	16.98	11.85	39.41	1.16	3.32	34.06
Jun-16	23/06/16	Sprat	33	0.28	1.973	10.88	-19.7	17.01	12.22	39.82	1.18	3.26	33.73
Jun-16	23/06/16	Sprat	34	0.37	1.835	10.82	-19.56	16.36	12.04	39.76	1.14	3.3	34.84
Jun-16	23/06/16	Sprat	35	0.31	1.846	10.49	-19.01	17.82	12.21	39.92	1.16	3.27	34.29
Jun-16	23/06/16	TransparentGoby	40	0.56	1.821	12.46	-18.09	17.03	12.09	42.55	1.22	3.52	35.02
Jun-16	23/06/16	TransparentGoby	45	0.81	1.998	12.72	-17.74	17.16	11.30	40.49	1.14	3.58	35.42
Jun-16	23/06/16	TransparentGoby	43	0.66	1.869	12.62	-17.99	16.83	12.23	43.54	1.10	3.56	39.75
Jun-16	23/06/16	TransparentGoby	45	0.91	1.903	13.09	-18.16	17.29	11.61	42.49	1.25	3.66	33.92
Jun-16	29/06/16	Pout	192	175.07	1.852	15.16		14.44	13.80		1.15		
Jun-16	29/06/16	Pout	175	124.42	1.836	14.15	-17.37	15.01	14.48	45.93	1.29	3.17	35.56
Jun-16	29/06/16	Whiting	232	152.72	1.962	15.11	-17.94	14.24	14.34	45.35	0.99	3.16	45.71
Jun-16	29/06/16	Whiting	219	140.2	1.911	14.51	-16.58	14.85	14.41	45.84	1.06	3.18	43.06
Jul-16	28/07/16	GreaterPipefish	296	10.96	2	12.89	-17.23	15.81	13.42	44.47	1.08	3.31	41.17
Jul-16	28/07/16	Pout	74	4.73	1.985	13.97	-17.77	15.19	13.23	42.92	1.25	3.24	34.33
Jul-16	28/07/16	Pout	87	8.67	1.953	14.16	-17.56	15.74	13.47	43.24	1.29	3.21	33.4
Jul-16	28/07/16	Pout	45	0.97	1.811	13.28	-18.25	17.37	11.91	40.58	1.21	3.41	33.43
Jul-16	28/07/16	RockGoby	66	5.71	1.856	11.81	-19.42	16.46	14.41	46.50	1.58	3.23	29.43
Jul-16	28/07/16	SandGoby	36	0.42	1.91	12.35	-18.17	15.98	12.21	40.83	1.31	3.34	31.09

Table 7.2 continued.

Month	Date	Species	SL (mm)	Weight (g)	Sample (mg)	δ^{15}N	δ^{13}C	δ^{34}S	N%	C%	S%	C/N	C/S
Jul-16	28/07/16	SandGoby	40	0.7	1.918	11.48	-18.91	13.89	12.74	42.46	1.30	3.33	32.74
Jul-16	28/07/16	SandGoby	29	0.21	1.876	13.16	-18.27	14.32	11.88	39.77	1.32	3.35	30.2
Jul-16	28/07/16	SandGoby	31	0.22	1.908	12.8	-17.73	13.37	11.78	40.18	1.31	3.41	30.61
Jul-16	28/07/16	SandGoby	45	0.95	1.867	12.04	-18.73	16.32	11.65	38.85	1.21	3.33	32.18
Jul-16	28/07/16	SandSmelt	40	0.53	1.893	11.68	-20.45	16.09	11.06	41.35	1.14	3.74	36.25
Jul-16	28/07/16	SandSmelt	82	5.55	1.879	12.72	-18.29	14.5	13.28	44.29	1.24	3.34	35.66
Jul-16	28/07/16	Sprat	32	0.27	1.995	12.29	-19.36	16.66	11.93	40.66	1.13	3.41	35.88
Jul-16	28/07/16	Sprat	32	0.22	1.847	12.05	-19.91	16.98	11.90	40.76	1.08	3.42	37.59
Jul-16	28/07/16	Sprat	39	0.43	1.837	12.09	-19.59	17.51	11.48	39.51	1.16	3.44	33.95
Jul-16	28/07/16	Sprat	41	0.51	1.988	10.44	-20.39	16.75	12.58	41.21	1.10	3.28	37.53
Jul-16	28/07/16	Sprat	49	0.95	1.95	11.44	-19.98	16.52	11.96	41.86	1.18	3.5	35.45
Jul-16	28/07/16	StarrySmoothHound	449	215.3	1.906	15.54	-14.1	13.99	14.97	42.49	0.92	2.84	46.1
Jul-16	28/07/16	TransparentGoby	40	0.56	1.8	12.72	-18.3	16.67	11.74	41.47	1.27	3.53	32.57
Jul-16	28/07/16	TransparentGoby	41	0.72	1.915	13.68	-17.52	17.44	11.02	40.26	1.19	3.65	33.72
Jul-16	28/07/16	TransparentGoby	45	0.64	1.872	13.18	-18.88	17.22	10.81	44.79	1.08	4.14	41.59
Aug-16	23/08/16	Bass	49	1.62	1.948	14.37	-17.07	17.94	12.78	42.76	1.27	3.35	33.75
Aug-16	23/08/16	Bass	53	1.86	1.892	13.5	-18.61	16.82	12.45	41.31	1.41	3.32	29.24
Aug-16	23/08/16	Eel	197	8.99	1.93	12.87	-22.3	9.77	12.52	49.89	0.87	3.99	57.31
Aug-16	23/08/16	GreaterPipefish	354	26.99	1.905	13.03	-17.39	15.48	14.29	44.14	1.07	3.09	41.28
Aug-16	23/08/16	Pout	56	2.32	1.846	14.31	-17.8	16.66	13.13	42.26	1.27	3.22	33.18
Aug-16	23/08/16	Pout	67	3.54	1.921	14.44	-17.2	15.89	13.70	44.35	1.46	3.24	30.48
Aug-16	23/08/16	Pout	83	7.85	1.959	14.29	-17.08	15.98	12.99	42.44	1.39	3.27	30.44
Aug-16	23/08/16	Pout	85	8.66	1.932	14.62	-15.9	14.94	12.90	41.18	1.33	3.19	30.89
Aug-16	23/08/16	Pout	87	9.14	1.921	14.98	-16.44	16.32	13.46	43.06	1.42	3.2	30.27
Aug-16	23/08/16	Pout	98	12.49	1.959	13.87	-17.65	16.27	14.11	44.95	1.44	3.19	31.18
Aug-16	23/08/16	Pout	104	14.46	1.908	13.85	-17.58	15.3	14.10	44.13	1.43	3.13	30.92
Aug-16	23/08/16	RockGoby	57	3.41	1.948	11.99	-20.26	16.86	12.67	45.77	1.56	3.61	29.37
Aug-16	23/08/16	RockGoby	61	4.34	1.86	12.88	-19.6	16.66	12.58	43.82	1.30	3.48	33.73
Aug-16	23/08/16	SandGoby	37	0.5	1.82	11.95	-18.59	13.27	12.91	41.97	1.24	3.25	33.99
Aug-16	23/08/16	SandGoby	39	0.62	1.897	13.41	-17.01	12.95	11.71	40.15	1.32	3.43	30.43
Aug-16	23/08/16	SandSmelt	86	7.03	1.9	14	-16.58	13.64	13.44	44.95	1.35	3.34	33.42
Aug-16	23/08/16	Sole	195	95.17	1.918	12.15	-19.62	12.47	13.64	43.40	1.26	3.18	34.35
Aug-16	23/08/16	Sprat	38	0.56	1.838	12.53	-19.86	16.11	12.39	41.19	1.41	3.32	29.13
Aug-16	23/08/16	Sprat	40	0.57	1.812	12.06	-19.82	17.02	12.30	42.01	1.13	3.42	37.11
Aug-16	23/08/16	Sprat	61	1.65	1.842	11.62	-19.35	17.8	13.01	42.50	1.24	3.27	34.33
Aug-16	23/08/16	StarrySmoothHound	331	130.7	1.806	13.08	-17.23	13.64	16.03	45.61	1.09	2.85	41.7
Aug-16	23/08/16	StarrySmoothHound	299	93.92	1.889	14.21	-16.84	17.08	15.68	45.59	1.10	2.91	41.27
Aug-16	23/08/16	ThornbackRay	452	294.82	1.916	13.28	-17.17	14.02	16.17	45.22	1.06	2.8	42.76
Aug-16	23/08/16	ThornbackRay	385	342.38	1.855	13.63	-16.91	16.04	15.14	44.49	1.11	2.94	40.22
Aug-16	23/08/16	ThornbackRay	306	155.95	1.874	13.52	-16.97	14.57	16.09	45.61	1.06	2.83	43.02
Aug-16	23/08/16	ThornbackRay	420	447.66	1.815	13.19	-17.04	13.55	16.11	45.29	1.01	2.81	44.91
Sep-16	28/09/16	5-BeardedRockling	87	5.2	1.995	13.57	-18.25	17.59	13.87	44.78	1.35	3.23	33.25
Sep-16	28/09/16	5-BeardedRockling	143	28.82	1.858	13.84	-17.41	17.84	14.32	45.44	1.41	3.17	32.29
Sep-16	28/09/16	BaillonsWrasse	37	0.84	1.843	14.71	-17.58	16.22	12.34	41.11	1.35	3.33	30.48
Sep-16	28/09/16	Bass	55	2.13	1.803	13.64	-18.81	15.57	13.00	43.27	1.47	3.33	29.41
Sep-16	28/09/16	Bass	72	5.18	1.944	14.67	-17.15	14.13	13.34	43.44	1.45	3.26	30.06
Sep-16	28/09/16	Bass	75	6.9	1.888	16.34	-16.13	14.79	13.58	44.56	1.37	3.28	32.53
Sep-16	28/09/16	BlackGoby	46	1.76	1.867	12.42	-19.48	16.53	12.97	44.17	1.43	3.41	30.79
Sep-16	28/09/16	Flounder	183	111.02	1.836	12.28	-19.51	12.44	13.87	44.67	1.30	3.22	34.46
Sep-16	28/09/16	LongSpineSeaScorpion	47	2.23	1.895	12.13	-20.24	17.38	13.49	44.60	1.59	3.31	27.96
Sep-16	28/09/16	Plaice	146	5.8	1.92	11.77	-20.42	11.58	13.91	46.18	1.37	3.32	33.64
Sep-16	28/09/16	Pout	86	9.11	1.888	14.14	-18.08	15.95	13.89	44.76	1.49	3.22	30.13
Sep-16	28/09/16	ReticulatedDragonette	60	2.47	1.849	13.12	-17.93	16.69	13.74	43.92	1.55	3.2	28.32
Sep-16	28/09/16	RockGoby	67	6.48	1.99	11.63	-20.42	17.32	13.38	46.13	1.51	3.45	30.49
Sep-16	28/09/16	SandGoby	39	0.55	1.854	13.9	-17.93	14.85	11.96	41.16	1.30	3.44	31.65
Sep-16	28/09/16	SandSmelt	61	2.11	1.935	13.11	-20.08	14.37	12.62	43.32	1.39	3.43	31.15
Sep-16	28/09/16	SandSmelt	61	1.91	1.863	13.16	-19.94	14.47	13.41	44.24	1.38	3.3	31.96
Sep-16	28/09/16	SandSmelt	65	2.71	1.956	12.86	-19.9	14.84	13.69	45.74	1.38	3.34	33.24
Sep-16	28/09/16	SandSmelt	111	16.05	1.801	14.3	-18.19	13.99	13.85	45.19	1.33	3.26	33.93
Sep-16	28/09/16	Scad	189	102.88	1.825	14.24	-17.48	17.38	14.22	47.66	1.23	3.35	38.89
Sep-16	28/09/16	Sole	58	1.93	1.969	12.09	-19.72	14.28	13.46	44.22	1.45	3.28	30.39
Sep-16	28/09/16	Sole	71	3.5	1.918	10.81	-21.03	13.49	13.97	45.76	1.47	3.27	31.21
Sep-16	28/09/16	Sprat	41	0.86	1.809	12.49	-19.54	16.43	13.51	42.77	1.23	3.17	34.73
Sep-16	28/09/16	Sprat	40	0.6	1.834	12.96	-18.99	16.84	12.87	41.65	1.18	3.24	35.24
Sep-16	28/09/16	Sprat	45	0.85	1.932	12.41	-19.98	17.47	13.50	43.52	1.18	3.22	37.03
Sep-16	28/09/16	Sprat	48	1.14	1.981	11.74	-19.84	17.56	13.95	42.78	1.12	3.07	38.04
Sep-16	28/09/16	StarrySmoothHound	301	87.04	1.835	13.89	-17.03	14.83	15.71	43.71	1.19	2.78	36.87
Sep-16	28/09/16	TransparentGoby	30	0.17	1.854	13.05	-20.08	17.06	10.83	38.48	1.25	3.55	30.83
Sep-16	28/09/16	TubGurnard	100	15.38	1.973	12.73	-19.33	15.19	12.89	42.00	1.47	3.26	28.48
Sep-16	28/09/16	Whiting	124	22.1	1.846	14.58	-18.29	17.16	13.90	44.88	1.28	3.23	35.03
Sep-16	28/09/16	Whiting	134	24.98	1.85	14.88	-18.3	16.74	13.67	43.93	1.44	3.21	30.61
Oct-16	27/10/16	Herring	76	4.35	1.874	12.9	-18.99	14.44	13.53	43.44	1.27	3.21	34.27
Oct-16	27/10/16	Herring	83	5.03	1.876	14.02	-17.54	15.37	13.73	43.44	1.24	3.16	35.01
Oct-16	27/10/16	Pout	107	17.51	1.913	13.52	-18.74	13.57	14.45	45.86	1.55	3.17	29.64
Oct-16	27/10/16	Pout	115	20.98	1.985	13.94	-17.22	15.38	14.03	45.33	1.36	3.23	33.23
Oct-16	27/10/16	Pout	115	23.62	1.875	14.75	-17.18	13.2	14.43	46.05	1.52	3.19	30.36
Oct-16	27/10/16	Pout	155	60.09	1.842	14.58	-17	15.3	14.14	45.84	1.38	3.24	33.2
Oct-16	27/10/16	RockGoby	41	1.19	1.954	12.59	-21.24	16.41	13.36	45.37	1.44	3.4	31.54
Oct-16	27/10/16	SandGoby	45	1.07	1.878	13.42	-17.95	14.14	12.87	42.85	1.24	3.33	34.58
Oct-16	27/10/16	SandGoby	49	1.39	1.932	12.81	-18.85	12.7	12.53	42.47	1.28	3.39	33.16
Oct-16	27/10/16	SandGoby	49	1.34	1.962	13.86	-17.71	15.42	12.90	43.67	1.26	3.38	34.64
Oct-16	27/10/16	SandGoby	53	1.65	1.909	14.19	-17.39	14.64	13.11	44.28	1.31	3.38	33.92
Oct-16	27/10/16	SandGoby	57	1.94	1.842	13.96	-17.18	14.73	12.86	43.49	1.35	3.38	32.31
Oct-16	27/10/16	Sprat	37	0.47	1.874	11.14	-19.87	16.51	13.18	41.59	1.11	3.15	37.33
Oct-16	27/10/16	Sprat	40	0.68	1.827	11.95	-19.7	16.22	13.35	42.74	1.11	3.2	38.47
Oct-16	27/10/16	Sprat	40	0.69	1.969	12.34	-19.64	16.81	13.35	42.81	1.12	3.21	38.08
Oct-16	27/10/16	Sprat	43	0.81	1.981	11.81	-19.83	16.8	13.10	41.49	1.10	3.17	37.79

Table 7.2 continued.

Month	Date	Species	SL (mm)	Weight (g)	Sample (mg)	δ^{15}N	δ^{13}C	δ^{34}S	N%	C%	S%	C/N	C/S
Oct-16	27/10/16	ThornbackRay	392	324.12	1.839	13.17	-16.67	15.22	16.61	44.15	0.85	2.66	52.03
Oct-16	27/10/16	TransparentGoby	31	0.21	1.813	13.15	-19.44	16.28	11.36	40.13	1.21	3.53	33.21
Oct-16	27/10/16	TransparentGoby	32	0.33	1.893	12.74	-20.08	16.83	11.04	39.90	1.29	3.61	31.05
Oct-16	27/10/16	TransparentGoby	31	0.31	1.976	12.89	-19.26	16.44	11.29	40.09	1.20	3.55	33.46
Oct-16	27/10/16	Whiting	159	35.99	1.914	14.31	-18.49	16.67	14.22	45.23	1.15	3.18	39.26
Oct-16	05/10/16	Bass	270	352.7	1.8888	14.81	-17.56	14.29	13.95	45.18	1.21	3.24	37.37
Oct-16	05/10/16	Bass	182	121.49	1.972	14.87	-17.36	13.97	14.76	47.18	1.34	3.2	35.19
Oct-16	05/10/16	Bass	175	92.41	1.83	14.83	-16.29	11.58	14.15	46.74	1.35	3.3	34.59
Oct-16	05/10/16	Pout	224	303.53	1.907	14.81	-17.57	13.8	14.76	47.09	1.34	3.19	35.27
Oct-16	05/10/16	Pout	143	55.79	1.903	14.84	-17.26	16.41	14.57	46.26	1.38	3.18	33.64
Oct-16	05/10/16	SandSmelt	121	21.96	1.837	14.41	-18.83	13.45	14.33	46.87	1.42	3.27	32.9
Oct-16	05/10/16	SandSmelt	124	22.07	1.804	14.28	-17.7	14.11	14.82	47.51	1.42	3.21	33.43
Oct-16	05/10/16	SandSmelt	114	17.24	1.934	14.52	-17.45	14.44	14.35	46.78	1.40	3.26	33.5
Oct-16	05/10/16	Whiting	295	283.65	1.821	15.19	-17.04	14.47	14.15	45.06	1.08	3.18	41.61
Oct-16	05/10/16	Whiting	268	196.31	1.934	14.96	-17.46	14.82	14.48	45.69	1.08	3.16	42.27
Nov-16	24/11/16	Bass	97	14	1.926	18.21	-14.46	12.79	13.56	44.43	1.36	3.28	32.58
Nov-16	24/11/16	BlackGoby	65	4.95	1.92	13.16	-18.81	14.63	13.43	45.03	1.42	3.35	31.71
Nov-16	24/11/16	BlackGoby	47	1.88	1.848	12.77	-19.39	12.88	12.68	43.11	1.30	3.4	33.2
Nov-16	24/11/16	CorkwingWrasse	110	33.17	1.936	15.06	-17.75	15.22	14.48	45.93	1.46	3.17	31.37
Nov-16	24/11/16	CorkwingWrasse	118	46.56	1.98	13.08	-20.38	15.71	13.57	44.62	1.34	3.29	33.37
Nov-16	24/11/16	Eel	776	1188.47	1.81	11	-28.05	4.15	6.98	57.13	0.47	8.19	121.03
Nov-16	24/11/16	PaintedGoby	31	0.24	1.97	14.03	-18.47	16.78	9.44	33.27	1.11	3.52	29.97
Nov-16	24/11/16	Plaice	86	9.33	1.817	13.1	-16.67	11.68	13.78	44.08	1.47	3.2	30.08
Nov-16	24/11/16	Pout	80	5.18	1.885	15.14	-18.92	16.73	13.59	44.11	1.35	3.25	32.6
Nov-16	24/11/16	Pout	92	10.79	1.898	14.54	-18.11	15.46	13.58	43.92	1.47	3.23	29.84
Nov-16	24/11/16	Pout	101	12.1	1.955	14.56	-20.08	16.1	14.01	45.26	1.40	3.23	32.24
Nov-16	24/11/16	Pout	114	16.96	1.92	14.27	-17.59	16.45	13.88	44.86	1.38	3.23	32.51
Nov-16	24/11/16	Pout	146	44.5	1.936	15.07	-18.24	15.17	13.85	43.86	1.35	3.17	32.44
Nov-16	24/11/16	RockGoby	61	4.26	1.847	12.54	-20.91	16.52	13.44	46.36	1.68	3.45	27.64
Nov-16	24/11/16	RockGoby	58	3.57	1.84	11.92	-19.53	16.09	12.76	47.05	1.41	3.69	33.4
Nov-16	24/11/16	SandGoby	39	0.53	1.967	13.74	-17.83	13.43	12.27	41.35	1.31	3.37	31.61
Nov-16	24/11/16	SandGoby	50	1.43	1.867	13.68	-18.26	13.97	12.70	42.78	1.40	3.37	30.63
Nov-16	24/11/16	SandGoby	59	3.15	1.955	13.31	-19.03		13.18	44.96		3.41	
Nov-16	24/11/16	SandGoby	60	3.04	1.894	13.44	-19.38	13.6	12.60	42.67	1.38	3.39	30.99
Nov-16	24/11/16	Sole	75	3.62	1.959	12.81	-19.58	15.28	13.33	43.48	1.61	3.26	27.06
Nov-16	24/11/16	Sprat	39	0.55	1.894	11.98	-19.73	16.21	12.99	41.40	1.11	3.19	37.3
Nov-16	24/11/16	Sprat	42	0.73	1.996	11.88	-19.9	15.56	13.09	41.51	1.11	3.17	37.31
Nov-16	24/11/16	TransparentGoby	33	0.31	1.884	12.16	-20.25	16.19	10.10	37.07	1.20	3.67	30.89
Nov-16	24/11/16	TransparentGoby	35	0.29	1.873	12.39	-20.23	16.98	11.13	39.02	1.23	3.5	31.68
Nov-16	24/11/16	Whiting	137	17.74	1.881	14.88	-17.06	16.73	13.53	42.88	1.09	3.17	39.43
Nov-16	24/11/16	Whiting	141	26.38	1.82	14.67	-18.27	16.6	13.34	42.44	1.12	3.18	37.76
Nov-16	24/11/16	Whiting	227	85.28	1.845	16.43	-16.66	15.63	13.23	41.69	1.03	3.15	40.44
Nov-16	24/11/16	Whiting	240	140.29	1.968	15.38	-16.8	15.71	13.65	42.57	0.93	3.12	46
Nov-16	24/11/16	Whiting	251	111.04	1.846	16.32	-16.88	15.96	13.64	42.52	1.09	3.12	38.91
Dec-16	16/12/16	BallanWrasse	116	36.22	1.848	13.03	-19.64	15.88	14.12	45.96	1.38	3.25	33.24
Dec-16	16/12/16	Bass	51	1.88	1.875	14.95	-18.41	15.69	13.11	43.40	1.41	3.31	30.71
Dec-16	16/12/16	Bass	64	3.57	1.892	14.86	-19.86	13.19	13.08	43.90	1.38	3.36	31.84
Dec-16	16/12/16	Bass	155	55.82	1.827	16.07	-17.91	15.46	13.35	43.89	1.23	3.29	35.66
Dec-16	16/12/16	GreyGurnard	128	22.86	1.897	13.99	-17.82	16.88	13.69	44.22	1.42	3.23	31.24
Dec-16	16/12/16	GreyMullet	83	8.72	1.976	8.3	-12.84	10.99	12.96	43.37	1.23	3.35	35.17
Dec-16	16/12/16	GreyMullet	151	50.18	1.843	13.23	-18.76	12.93	13.10	42.61	1.26	3.25	33.9
Dec-16	16/12/16	GuiltheadBream	140	77.91	1.851	14.02	-13.65	10.83	13.51	46.24	1.17	3.42	39.4
Dec-16	16/12/16	Herring	121	18.15	1.883	14.52	-17.1	16.51	12.56	41.10	1.13	3.27	36.25
Dec-16	16/12/16	Pout	104	14.25	1.923	14.54	-17.86	16.49	13.48	43.32	1.38	3.21	31.46
Dec-16	16/12/16	Pout	111	17.19	1.908	15.15	-17.15	15.82	13.74	43.51	1.53	3.17	28.37
Dec-16	16/12/16	Pout	130	30.94	1.919	15.08	-17.82	15.24	13.64	44.33	1.38	3.25	32.13
Dec-16	16/12/16	Pout	174	79.54	1.828	14.6	-17.57	14.07	13.41	43.21	1.33	3.22	32.45
Dec-16	16/12/16	ReticulatedDragonette	59	2.05	1.869	13.83	-17.87	15.66	13.50	44.11	1.39	3.27	31.83
Dec-16	16/12/16	RockGoby	56	3.76	1.916	12.14	-20.05	16.08	12.62	47.62	1.41	3.77	33.82
Dec-16	16/12/16	RockGoby	57	3.44	1.997	12.98	-19.72	16.17	12.50	46.99	1.40	3.76	33.58
Dec-16	16/12/16	SandGoby	37	0.54	1.87	13.36	-18.25	16.72	12.06	41.82	1.37	3.47	30.51
Dec-16	16/12/16	SandGoby	53	1.91	1.902	13.03	-19.67	13.23	12.62	43.59	1.39	3.45	31.42
Dec-16	16/12/16	SandSmelt	51	1.05	1.855	14.63	-17.86	15.11	11.70	39.25	1.18	3.36	33.28
Dec-16	16/12/16	SandSmelt	114	17.97	1.808	14.57	-18.91	14.61	12.78	42.88	1.27	3.36	33.75
Dec-16	16/12/16	Sole	235	157.39	1.862	12.81	-18.54	14.79	13.37	44.95	1.30	3.36	34.51
Dec-16	16/12/16	Sprat	63	2.94	1.856	12.94	-18.57	15.76	12.69	43.78	1.00	3.45	43.73
Dec-16	16/12/16	Sprat	135	24.05	1.865	13	-17.38	17.17	12.30	44.64	0.85	3.63	52.43
Dec-16	16/12/16	StarrySmoothHound	299	89.31	1.852	13.68	-16.63	14.51	15.30	44.67	1.08	2.92	41.26
Dec-16	16/12/16	ThornbackRay	348	201.82	1.927	13.31	-17.38	14.05	15.34	43.78	1.10	2.85	39.9
Dec-16	16/12/16	TransparentGoby	39	0.42	1.82	13.72	-18.44	16.86	11.17	40.34	1.22	3.61	33.11
Dec-16	16/12/16	TubGurnard	182	96.58	1.868	13.93	-15.72	12.13	13.36	43.87	1.29	3.28	34.13
Dec-16	16/12/16	Whiting	137	25.07	1.821	14.6	-17.66	17.7	13.53	42.64	1.16	3.15	36.61
Dec-16	16/12/16	Whiting	159	34.97	1.946	15.23	-18.23	16.91	13.34	42.63	1.16	3.2	36.76
Dec-16	16/12/16	Whiting	164	41.83	1.889	14.77	-18.29	16.65	13.94	44.29	1.16	3.18	38.29
Dec-16	16/12/16	Whiting	224	91.81	1.876	16.29	-16.89	16.31	14.17	43.72	0.93	3.09	46.83
Dec-16	14/12/16	Bass	239	256.44	1.962	16.04	-16.85	15.25	13.99	44.78	1.32	3.2	33.86
Dec-16	14/12/16	Bass	196	127	1.876	15.47	-17.83	14.36	14.08	46.33	1.28	3.29	36.32
Dec-16	14/12/16	Bass	190	117.92	1.963	14.93	-17.79	14.5	13.69	44.62	1.26	3.26	35.46
Dec-16	14/12/16	Herring	130	23.14	1.869	13.85	-18.12	17.26	13.30	46.16	1.03	3.47	44.68
Dec-16	14/12/16	Herring	124	19.05	1.999	14.14	-17.66	16.92	13.87	44.67	1.03	3.22	43.32
Dec-16	14/12/16	Pout	193	120.7	1.909	15.39	-17.5	15.45	14.16	45.11	1.19	3.19	37.97
Dec-16	14/12/16	Pout	165	73.05	1.955	15.67	-16.37	13.9	14.15	45.62	1.37	3.22	33.21
Dec-16	14/12/16	Pout	167	75.27	1.868	12.64	-19.51	15.61	14.39	48.25	1.51	3.35	32.06
Dec-16	14/12/16	SandSmelt	105	13.31	1.892	12.66	-20.53	12.97	13.24	43.77	1.46	3.31	29.99
Dec-16	14/12/16	SandSmelt	102	11.33	1.948	16.25	-16.02	16.01	12.97	43.25	1.38	3.34	31.33
Dec-16	14/12/16	SandSmelt	96	9.19	1.978	13.84	-18.21	12.76	13.95	46.03	1.53	3.3	30
Dec-16	14/12/16	Whiting	264	151.19	1.895	15.46	-17.05	15.16	13.69	42.82	1.06	3.13	40.41
Dec-16	14/12/16	Whiting	211	9.96	1.953	15.39	-17.94	16.16	13.82	43.85	1.05	3.17	41.83

Table 7.2 continued.

Month	Date	Species	SL (mm)	Weight (g)	Sample (mg)	δ^{15}N	δ^{13}C	δ^{34}S	N%	C%	S%	C/N	C/S
Jan-17	26/01/17	Bass	67	4.05	1.892	15.21	-17.98	14.05	13.18	43.10	1.47	3.27	29.34
Jan-17	26/01/17	Bass	87	9	1.898	15.51	-19.51	13.42	13.27	44.09	1.41	3.32	31.32
Jan-17	26/01/17	Bass	149	44.87	1.959	15.8	-17.08	16.37	13.49	44.35	1.23	3.29	36.08
Jan-17	26/01/17	Bass	164	59.15	1.862	16.09	-16.71	11.05	13.67	44.80	1.35	3.28	33.12
Jan-17	26/01/17	BlackGoby	29	0.31	1.974	12.18	-20.48	11.61	11.69	40.42	1.41	3.46	28.64
Jan-17	26/01/17	Flounder	187	93.54	1.803	13.47	-18.57	11.68	12.67	40.18	1.16	3.17	34.5
Jan-17	26/01/17	GreyGurnard	166	67.69	1.895	15.11	-15.51	10.28	13.73	45.06	1.28	3.28	35.23
Jan-17	26/01/17	GreyGurnard	161	60.64	1.862	15.81	-15.28	15.14	13.98	45.12	1.31	3.23	34.57
Jan-17	26/01/17	GreyGurnard	136	42.67	1.914	14.61	-16.5	14.6	13.86	45.06	1.44	3.25	31.33
Jan-17	26/01/17	GreyMullet	140	45.64	1.96	12.92	-13.3	15.76	14.13	45.93	1.25	3.25	36.77
Jan-17	26/01/17	GreyMullet	174	88.15	1.906	14.43	-13.73	14.11	14.14	45.79	1.17	3.24	39.18
Jan-17	26/01/17	Herring	90	5.5	1.84	13.53	-18.06	16.1	13.12	43.05	1.14	3.28	37.71
Jan-17	26/01/17	Herring	95	7.15	1.858	13.18	-18.15	14.81	13.11	41.80	1.20	3.19	34.92
Jan-17	26/01/17	Herring	194	54.59	1.942	11.83	-18.32	18.68	13.09	40.81	1.00	3.12	40.88
Jan-17	26/01/17	Pout	131	28.91	1.99	14.24	-18.13	14.73	14.04	44.30	1.31	3.16	33.8
Jan-17	26/01/17	RockGoby	53	2.46	1.852	12.73	-19.9	9.91	13.76	45.44	1.63	3.3	27.83
Jan-17	26/01/17	SandGoby	52	2.22	1.862	14.39	-18.96	10.55	12.87	43.46	1.42	3.38	30.61
Jan-17	26/01/17	SandSmelt	95	8.67	1.815	14.1	-19.26	13.73	13.24	42.85	1.29	3.24	33.24
Jan-17	26/01/17	SandSmelt	97	8.74	1.884	14.08	-17.8	14.52	14.17	46.10	1.37	3.25	33.61
Jan-17	26/01/17	Scad	208	117.21	1.848	13.54	-18.54	16.3	13.51	45.14	0.90	3.34	50.16
Jan-17	26/01/17	Sprat	51	1.16	1.815	12.96	-17.85	16.86	12.68	41.03	1.11	3.24	36.83
Jan-17	26/01/17	Sprat	52	1.4	1.877	12.96	-20.7	15.19	13.62	44.87	1.07	3.29	41.8
Jan-17	26/01/17	ThornbackRay	385	311.7	1.954	13.62	-16.45	13.15	16.37	44.30	0.78	2.71	56.82
Jan-17	26/01/17	TransparentGoby	40	0.48	1.934	13.36	-18.46	16.64	11.17	40.05	1.21	3.59	33.18
Jan-17	26/01/17	TransparentGoby	41	0.47	1.948	13.42		16.04	11.81		1.18		
Jan-17	26/01/17	Whiting	130	20.42	1.851	14.34	-17.65	15.77	13.36	43.32	1.05	3.24	41.39
Jan-17	26/01/17	Whiting	161	38.45	1.96	14.4	-17.94	15.39	13.61	43.42	1.02	3.19	42.52

Table 7.3: Raw stable isotope values of plankton filtrate (100μm mesh size).

Month	Date	Sample Type	Sample (mg)	δ^{15}N	δ^{13}C	δ^{34}S	N%	C%	S%	C/N	C/S
Oct-15	03/11/15	PlanktonFiltrate	5.524	8.07	-24.63	12.92	1.21	1.73	0.33	1.44	5.19
Oct-15	03/11/15	PlanktonFiltrate	5.976	8.07	-24.46	13.57	1.14	1.63	0.32	1.44	5.04
Oct-15	03/11/15	PlanktonFiltrate	5.695	7.99	-24.2	16.01	1.10	1.58	0.37	1.44	4.24
Nov-15	01/12/15	PlanktonFiltrate	7.61	8.17	-23.75	13.46	0.74	1.06	0.39	1.43	2.71
Nov-15	01/12/15	PlanktonFiltrate	6.649	8.15	-23.7	15.56	0.66	0.94	0.48	1.42	1.98
Nov-15	01/12/15	PlanktonFiltrate	6.033	8.34	-23.7	16.75	0.54	0.75	0.44	1.4	1.7
Dec-15	17/12/15	PlanktonFiltrate	7.439	9.51	-24.23	14.84	0.96	1.38	0.33	1.44	4.17
Dec-15	17/12/15	PlanktonFiltrate	7.182	9.82	-23.77	17.44	1.18	1.71	0.40	1.45	4.28
Dec-15	17/12/15	PlanktonFiltrate	6.985	9.73	-23.81	18.22	0.97	1.40	0.45	1.44	3.12
Jan-16	21/01/16	PlanktonFiltrate	7.734	7.24	-27.16	1.95	0.71	1.01	0.48	1.43	2.12
Jan-16	21/01/16	PlanktonFiltrate	7.853	7.28	-27.18	1.85	0.75	1.07	0.51	1.43	2.12
Jan-16	21/01/16	PlanktonFiltrate	6.966	7	-27.29	7.94	0.61	0.86	0.53	1.42	1.64
Feb-16	25/02/16	PlanktonFiltrate	6.272	10.32	-24.89	12.66	0.89	1.27	0.38	1.43	3.37
Feb-16	25/02/16	PlanktonFiltrate	6.429	10.52	-24.91	13.54	0.84	1.20	0.39	1.43	3.11
Feb-16	25/02/16	PlanktonFiltrate	7.253	10.29	-24.98	13.35	0.89	1.28	0.37	1.44	3.45
Mar-16	23/03/16	PlanktonFiltrate	6.319	9.21	-25.13	16.64	0.32	0.43	0.43	1.35	1
Mar-16	23/03/16	PlanktonFiltrate	6.015	9.06	-25.03	16.43	0.23	0.30	0.43	1.28	0.7
Mar-16	23/03/16	PlanktonFiltrate	6.181	8.85	-25.45	16.55	0.27	0.35	0.41	1.31	0.86
Apr-16	21/04/16	PlanktonFiltrate	6.518	9.52	-23.04	17.62	0.79	1.13	0.43	1.43	2.65
Apr-16	21/04/16	PlanktonFiltrate	7.192	9.77	-22.51	19.09	1.03	1.48	0.42	1.44	3.54
Apr-16	21/04/16	PlanktonFiltrate	6.578	9.64	-22.7	16.87	0.95	1.36	0.42	1.44	3.27
May-16	21/05/16	PlanktonFiltrate	7.854	7	-26.96	15.2	0.82	1.18	0.42	1.44	2.85
May-16	21/05/16	PlanktonFiltrate	9.882	7.26	-26.69	14.34	0.94	1.36	0.40	1.45	3.42
May-16	21/05/16	PlanktonFiltrate	11.35	7.18	-26.62	14.65	1.07	1.56	0.39	1.46	4.04
Jun-16	21/06/16	PlanktonFiltrate	11.822	7.71	-23.35	12.67	2.01	2.95	0.41	1.47	7.26
Jun-16	21/06/16	PlanktonFiltrate	9.975	7.65	-23.72	13.18	1.74	2.54	0.42	1.46	6.11
Jun-16	21/06/16	PlanktonFiltrate	8.575	7.66	-23.45	13.23	1.56	2.28	0.42	1.46	5.38
Jul-16	28/07/16	PlanktonFiltrate	7.287	8.89	-23.31	14.8	1.10	1.59	0.55	1.45	2.9
Jul-16	28/07/16	PlanktonFiltrate	7.475	8.86	-24.07	17.21	1.27	1.85	0.46	1.45	4.02
Jul-16	28/07/16	PlanktonFiltrate	7.475	8.83	-23.76	16.78	1.30	1.88	0.45	1.45	4.14
Aug-16	23/08/16	PlanktonFiltrate	8.032	9.33	-24.64	17.62	2.34	3.42	0.43	1.47	7.93
Aug-16	23/08/16	PlanktonFiltrate	7.906	9.4	-24.71	17.13	1.72	2.51	0.40	1.46	6.3
Aug-16	23/08/16	PlanktonFiltrate	7.491	9.46	-24.61	17.99	1.63	2.37	0.42	1.46	5.64
Sep-16	28/09/16	PlanktonFiltrate	7.86	7.51	-24.59	14.64	1.63	2.38	0.47	1.46	5.1
Sep-16	28/09/16	PlanktonFiltrate	9.84	7.74	-24.59	17.08	1.69	2.47	0.40	1.46	6.12
Sep-16	28/09/16	PlanktonFiltrate	11.136	7.92	-24.4	15.67	1.78	2.60	0.40	1.47	6.49
Oct-16	27/10/16	PlanktonFiltrate	7.695	6.98	-23.87	16.66	0.83	1.20	0.43	1.44	2.77
Oct-16	27/10/16	PlanktonFiltrate	10.291	7.36	-23.89	16.73	1.46	2.14	0.39	1.46	5.46
Oct-16	27/10/16	PlanktonFiltrate	8.333	6.99	-24.29	16.97	1.19	1.72	0.42	1.45	4.15
Nov-16	24/11/16	PlanktonFiltrate	7.033	7.17	-25.54	7.99	0.53	0.75	0.53	1.41	1.43
Nov-16	24/11/16	PlanktonFiltrate	10.196	7.38	-25.45	5.46	1.06	1.55	0.57	1.45	2.71
Nov-16	24/11/16	PlanktonFiltrate	9.247	7.34	-25.14	7.7	0.74	1.06	0.50	1.44	2.13
Dec-16	16/12/16	PlanktonFiltrate	8.111	8.6	-24.75	16.03	1.50	2.19	0.42	1.46	5.18
Dec-16	16/12/16	PlanktonFiltrate	7.391	9.22	-23.99	16.66	1.75	2.56	0.43	1.46	5.95
Dec-16	16/12/16	PlanktonFiltrate	7.231	8.58	-24.8	17.24	1.12	1.62	0.44	1.45	3.66

Table 7.4: Raw stable isotope values of production sources.

Month	Date	Species	Sample (mg)	d15N	d13C	d34S	N%	C%	S%	C/N	C/S
Jul-16	28/07/16	*Fucus serratus*	1.959	6.25	-18.88	20.25	2.54	35.68	1.08	14.04	33.16
Jul-16	28/07/16	*Fucus vesiculosus*	1.868	14.66	-18.87	15.95	12.26	46.53	1.63	3.79	28.49
Jul-16	28/07/16	*Laminaria sp.*	1.912	5.8	-19.68	20.39	3.30	37.02	0.86	11.23	42.99
Jul-16	28/07/16	*Tricellaria (inoptinata)*	1.952	6.1	-12.95	19.11	1.22	14.78	0.52	12.08	28.28
Jul-16	28/07/16	*Tricellaria (inoptinata)*	1.987	5.83	-11.89	19.55	1.38	14.53	0.54	10.5	26.74
Jul-16	28/07/16	*Tricellaria (inoptinata)*	1.82	5.71	-12.65	18.62	1.71	15.20	0.60	8.89	25.28
Jul-16	28/07/16	*Ulva lactusa*	1.847	9.57	-11.64	19.84	4.65	37.38	2.80	8.03	13.34
Jul-16	28/07/16	*Ulva lactusa*	1.868	9.78	-13.49	19.95	4.22	36.91	2.94	8.75	12.57
Jul-16	28/07/16	*Ulva lactusa*	1.893	8.56	-13.77	19.49	5.11	38.01	2.55	7.44	14.93
Jul-16	28/07/16	PlanktonFiltrate	7.287	8.89	-23.31	14.8	1.10	1.59	0.55	1.45	2.9
Jul-16	28/07/16	PlanktonFiltrate	7.475	8.86	-24.07	17.21	1.27	1.85	0.46	1.45	4.02
Jul-16	28/07/16	PlanktonFiltrate	7.475	8.83	-23.76	16.78	1.30	1.88	0.45	1.45	4.14
Jul-16	28/07/16	*Ceramium sp.*	1.871	9.2	-23.1	20.54	5.97	38.58	3.26	6.46	11.85
Jul-16	28/07/16	*Chondrus crispus*	1.841	7.5	-28.11	21.71	3.34	32.84	5.00	9.84	6.57
Jul-16	28/07/16	*Gracilaria sp.*	1.857	10.26	-19.54	21.63	3.24	29.60	5.11	9.14	5.8
Jul-16	28/07/16	*Halurus flosculosus*	1.844	6.96	-33.93	20.01	5.71	40.00	3.10	7.01	12.92
Jul-16	28/07/16	*Porphyra umbilicalis*	1.846	8.82	-21.1	20.73	3.99	38.36	2.26	9.61	16.99
Jul-16	28/07/16	Leaf litter	1.876	4.94	-27.79	11.32	1.16	45.44	0.31	39.25	146.35
Jul-16	28/07/16	Leaf litter	1.875	4.44	-27.5	15.33	0.73	44.95	0.28	61.18	158.34
Jul-16	28/07/16	Leaf litter	1.904	3.56	-28.11	12.51	0.62	41.32	0.52	66.3	79.15

References

Akimova, A., Núñez-Riboni, I., Kempf, A., & Taylor, M. H. (2016). Spatially-resolved influence of temperature and salinity on stock recruitment variability of commercially important fishes in the north sea. *PLoS ONE*, *11*, e0160917.

Amante, C., & Eakins, B. W. (2009). *Etopo1 1 arc-minute global relief model: procedures, data sources and analysis. noaa technical memorandum nesdis ngdc-24* (Tech. Rep.). National Geophysical Data Center, NOAA. (Doi:10.7289/V5C8276M [accessed 23/07/2015])

Andersen, K. H., Beyer, J., & Lundberg, P. (2009). Trophic and individual efficiencies of size-structured communities. *Proceedings of the Royal Society of London B: Biological Sciences*, *276*(1654), 109–114.

Anderson, M. J. (2006). Distance-based tests for homogeneity of multivariate dispersions. *Biometrics*, *62*(1), 245–253.

Anderson, R. M., & Gordon, D. M. (1982). Variability in the abundance of animal and plant species. *Nature*, *296*, 245–248.

Aprahamian, M. W., & Barr, C. D. (1985). The growth, abundance and diet of o-group sea bass, dicentrarchus labrax, from the severn estuary. *Journal of the Marine Biological Association of the United Kingdom*, *65*(1), 169–180.

Araújo, M., Bolnick, D., Martinelli, L., Giaretta, A., & Dos Reis, S. (2009). Individual-level diet variation in four species of brazilian frogs. *Journal of Animal Ecology*, *78*(4), 848–856.

Araújo, M., Bolnick, D. I., & Layman, C. A. (2011). The ecological causes of individual specialisation. *Ecology letters*, *14*(9), 948–958.

Araújo, M., Bolnick, D. I., Machado, G., Giaretta, A. A., & Dos Reis, S. F. (2007).

Using δ 13 c stable isotopes to quantify individual-level diet variation. *Oecologia*, *152*(4), 643–654.

Araújo, M., Guimarães, P. R., Svanbäck, R., Pinheiro, A., Guimarães, P., Reis, S. F. d., & Bolnick, D. I. (2008). Network analysis reveals contrasting effects of intraspecific competition on individual vs. population diets. *Ecology*, *89*(7), 1981–1993.

Arruda, L. M., Azevedo, J., & Neto, A. I. (1993). Abundance, age-structure and growth and reproduction of gobies (pisces, gobiidae) in the ria de aveiro lagoon (portugal).

Arruda-Neto, J. D. T., Righi, H., Cascino, M. A. G., Genofre, G. C., & Mesa, J. (2014). Variability in the abundance of animal and plant species. *Journal of Applied Mathematics and Physics*, *2*, 762–770.

Bacon, P., Gurney, W., Jones, W., McLaren, I., & Youngson, A. (2005). Seasonal growth patterns of wild juvenile fish: partitioning variation among explanatory variables, based on individual growth trajectories of atlantic salmon (salmo salar) parr. *Journal of Animal Ecology*, *74*(1), 1–11.

Bailey-Watts, A. (1986). Seasonal variation in size spectra of phytoplankton assemblages in loch leven, scotland. In *Seasonality of freshwater phytoplankton* (pp. 25–42). Springer.

Ballentyne IV, F., & Kerkhoff, A. J. (2007). The observed range for temporal mean-variance scaling exponents can be explained by reproductive correlation. *Oikos*, *116*, 174–180.

Barneche, D. R., & Allen, A. P. (2018). The energetics of fish growth and how it constrains food-web trophic structure. *Ecology letters*.

Barnes, C., Maxwell, D., Reuman, D. C., & Jennings, S. (2010). Global patterns in predator–prey size relationships reveal size dependency of trophic transfer efficiency. *Ecology*, *91*(1), 222–232.

Bastos, R. F., Corrêa, F., Winemiller, K. O., & Garcia, A. M. (2017). Are you what you eat? effects of trophic discrimination factors on estimates of food assimilation and trophic position with a new estimation method. *Ecological indicators*, *75*, 234–241.

Bates, D., Mächler, M., Bolker, B., & Walker, S. (2015). Fitting linear mixed-effects

models using lme4. *Journal of Statistical Software*, *67*(1), 1–48. doi: 10.18637/jss.v067.i01

Beck, M. W., Heck Jr, K. L., Able, K. W., Childers, D. L., Eggleston, D. B., Gillanders, B. M., ... others (2001). The identification, conservation, and management of estuarine and marine nurseries for fish and invertebrates: a better understanding of the habitats that serve as nurseries for marine species and the factors that create site-specific variability in nursery quality will improve conservation and management of these areas. *Bioscience*, *51*(8), 633–641.

Beggs, J. M., & Timme, N. (2012). Being critical of criticality in the brain. *Frontiers in physiology*, *3*, 163.

Bento, E. G., Grilo, T. F., Nyitrai, D., Dolbeth, M., Pardal, M. Â., & Martinho, F. (2016). Climate influence on juvenile european sea bass (dicentrarchus labrax, l.) populations in an estuarine nursery: A decadal overview. *Marine environmental research*, *122*, 93–104.

Bettencourt, L. M., Lobo, J., Helbing, D., Kühnert, C., & West, G. B. (2007). Growth, innovation, scaling, and the pace of life in cities. *Proceedings of the national academy of sciences*, *104*(17), 7301–7306.

Blanchard, J. L., Dulvy, N. K., Jennings, S., Ellis, J. R., Pinnegar, J. K., Tidd, A., & Kell, L. T. (2005). Do climate and fishing influence size-based indicators of celtic sea fish community structure? *ICES Journal of Marine Science*, *62*(3), 405–411.

Blanchard, J. L., Heneghan, R. F., Everett, J. D., Trebilco, R., & Richardson, A. J. (2017). From bacteria to whales: using functional size spectra to model marine ecosystems. *Trends in ecology & evolution*, *32*(3), 174–186.

Blanchard, J. L., Jennings, S., Holmes, R., Harle, J., Merino, G., Allen, J. I., ... Barange, M. (2012). Potential consequences of climate change for primary production and fish production in large marine ecosystems. *Phil. Trans. R. Soc. B*, *367*(1605), 2979–2989.

Blanchard, J. L., Jennings, S., Law, R., Castle, M. D., McCloghrie, P., Rochet, M.-J., & Benoît, E. (2009). How does abundance scale with body size in coupled size-structured food webs? *Journal of Animal Ecology*, *78*(1), 270–280.

Blanchard, J. L., Law, R., Castle, M. D., & Jennings, S. (2011). Coupled energy pathways and the resilience of size-structured food webs. *Theoretical Ecology*, *4*(3), 289–300.

Blanke, C. M., Chikaraishi, Y., Takizawa, Y., Steffan, S. A., Dharampal, P. S., & Vander Zanden, M. J. (2017). Comparing compound-specific and bulk stable nitrogen isotope trophic discrimination factors across multiple freshwater fish species and diets. *Canadian Journal of Fisheries and Aquatic Sciences*, *74*(8), 1291–1297.

Bodenheimer, F. S. (1938). *Problems of animal ecology.* Oxford University Press.

Boecklen, W. J., Yarnes, C. T., Cook, B. A., & James, A. C. (2011). On the use of stable isotopes in trophic ecology. *Annual Review of Ecology, Evolution, and Systematics*, *42*, 411–440.

Bolnick, D. I., Yang, L. H., Fordyce, J. A., Davis, J. M., & Svanbäck, R. (2002). Measuring individual-level resource specialization. *Ecology*, *83*(10), 2936–2941.

Boulineau-Coatanea, F. (1969). Régime alimentaire du bar dicentrarchus labrax (serranidae) sur la côte atlantique bretonne. *Bulletin du Muséum National d?Histoire Naturelle*, *41*, 1106–1122.

Bowen, G. J. (2010). Isoscapes: spatial pattern in isotopic biogeochemistry. *Annual Review of Earth and Planetary Sciences*, *38*, 161–187.

Bradley, D., Conklin, E., Papastamatiou, Y. P., McCauley, D. J., Pollock, K., Pollock, A., ... Caselle, J. E. (2017). Resetting predator baselines in coral reef ecosystems. *Scientific Reports*, *7*, 43131.

Britton, J. R., & Busst, G. M. (2018). Stable isotope discrimination factors of omnivorous fishes: influence of tissue type, temperature, diet composition and formulated feeds. *Hydrobiologia*, *808*(1), 219–234.

Brose, U. (2010). Body-mass constraints on foraging behaviour determine population and food-web dynamics. *Functional Ecology*, *24*(1), 28–34.

Brose, U., Cushing, L., Berlow, E. L., Jonsson, T., Banasek-Richter, C., Bersier, L.-F., ... others (2005). Body sizes of consumers and their resources. *Ecology*, *86*(9), 2545–2545.

Brose, U., Jonsson, T., Berlow, E. L., Warren, P., Banasek-Richter, C., Bersier, L.-F., ...

others (2006). Consumer–resource body-size relationships in natural food webs. *Ecology*, *87*(10), 2411–2417.

Brown, J. H., Gillooly, J. F., Allen, A. P., Savage, V. M., & West, G. B. (2004). Toward a metabolic theory of ecology. *Ecology*, *85*(7), 1771–1789.

Brownrigg, R., Minka, T. P., & Deckmyn, A. (2017). *maps: Draw geographical maps. r package version 3.2.0. original s code by richard a. becker, allan r. wilks.* (Tech. Rep.). (https://CRAN.R-project.org/package=maps)

Cabral, H., & Costa, M. J. (2001). Abundance, feeding ecology and growth of 0-group sea bass, dicentrarchus labrax, within the nursery areas of the tagus estuary. *Journal of the Marine Biological Association of the United Kingdom*, *81*(4), 679–682.

Calder, W. A. (1983). An allometric approach to population cycles of mammals. *Journal of Theoretical Biology*, *100*(2), 275–282.

Cardoso, J., Freitas, V., Quilez, I., Jouta, J., Witte, J. I., & Van Der Veer, H. (2015). The european sea bass dicentrarchus labrax in the dutch wadden sea: from visitor to resident species. *Journal of the Marine Biological Association of the United Kingdom*, *95*(4), 839–850.

Carleton, S. A., Kelly, L., Anderson-Sprecher, R., & Martínez del Rio, C. (2008). Should we use one-, or multi-compartment models to describe 13c incorporation into animal tissues? *Rapid Communications in Mass Spectrometry*, *22*(19), 3008–3014.

Carleton, S. A., & Martínez del Rio, C. (2005). The effect of cold-induced increased metabolic rate on the rate of 13 c and 15 n incorporation in house sparrows (passer domesticus). *Oecologia*, *144*(2), 226–232.

Caut, S., Angulo, E., & Courchamp, F. (2009). Variation in discrimination factors (δ15n and δ13c): the effect of diet isotopic values and applications for diet reconstruction. *Journal of Applied Ecology*, *46*(2), 443–453.

Cerling, T. E., Ayliffe, L. K., Dearing, M. D., Ehleringer, J. R., Passey, B. H., Podlesak, D. W., ... West, A. G. (2007). Determining biological tissue turnover using stable isotopes: the reaction progress variable. *Oecologia*, *151*(2), 175–189.

Certain, G., Bellier, E., Planque, B., & Bretagnolle, V. (2007). Characterising the temporal variability of the spatial distribution of animals: an application to

seabirds at sea. *Ecography*, *30*, 695–708.

Chave, J. (2013). The problem of pattern and scale in ecology: what have we learned in 20 years? *Ecology letters*, *16*(s1), 4–16.

Cherel, Y., Hobson, K., & Weimerskirch, H. (2005). Using stable isotopes to study resource acquisition and allocation in procellariiform seabirds. *Oecologia*, *145*(4), 533–540.

Claridge, P., & Potter, I. (1983). Movements, abundance, age composition and growth of bass, *Dicentrarchus labrax*, in the severn estuary and inner bristol channel. *Journal of the Marine Biological Association of the United Kingdom*, *63*(4), 871–879.

Claridge, P., Potter, I., & Hardisty, M. (1986). Seasonal changes in movements, abundance, size composition and diversity of the fish fauna of the severn estuary. *Journal of the Marine Biological Association of the United Kingdom*, *66*(1), 229–258.

Clauset, A., Shalizi, C. R., & Newman, M. E. (2009). Power-law distributions in empirical data. *SIAM review*, *51*(4), 661–703.

Cloern, J. E., & Nichols, F. H. (1978). A von bertalanffy growth model with a seasonally varying coefficient. *Journal of the Fisheries Board of Canada*, *35*(11), 1479–1482.

Cohen, J., Cohen, P., West, S. G., & Aiken, L. S. (2013). *Applied multiple regression/correlation analysis for the behavioral sciences*. Routledge.

Cohen, J. E. (2014). Taylor's law and abrupt biotic change in a smoothly changing environment. *Theoretical Ecology*, *7*(1), 77–86.

Cohen, J. E., Lai, J., Coomes, D. A., & Allen, R. B. (2016). Taylor's law and related allometric power laws in new zealand mountain beech forests: the roles of space, time and environment. *Oikos*, *125*(9), 1342–1357.

Cohen, J. E., Pimm, S. L., Yodzis, P., & Saldaña, J. (1993). Body sizes of animal predators and animal prey in food webs. *Journal of animal ecology*, 67–78.

Cohen, J. E., Xu, M., & Brunborg, H. (2012). Allometric scaling of population variance with mean body size is predicted from taylor's law and density-mass allometry. *PNAS*, *109*, 15829–15834.

Cohen, J. E., Xu, M., & Brunborg, H. (2013). Taylor's law applies to spatial variation

in a human population. *Genus*, *69*(1).

Cohen, J. E., Xu, M., & Schuster, W. S. (2013). Stochastic multiplicative population growth predicts and interprets taylor's power law of fluctuation scaling. *Proceedings of the Royal Society of London B: Biological Sciences*, *280*(1757), 20122955.

Connolly, R. M., Guest, M. A., Melville, A. J., & Oakes, J. M. (2004). Sulfur stable isotopes separate producers in marine food-web analysis. *Oecologia*, *138*(2), 161–167.

Connolly, S. R., Hughes, T. P., & Bellwood, D. R. (2017). A unified model explains commonness and rarity on coral reefs. *Ecology letters*, *20*(4), 477–486.

Crowley, B. E., Carter, M. L., Karpanty, S. M., Zihlman, A. L., Koch, P. L., & Dominy, N. J. (2010, Nov 01). Stable carbon and nitrogen isotope enrichment in primate tissues. *Oecologia*, *164*(3), 611–626. doi: 10.1007/s00442-010-1701-6

Daan, N., Gislason, H., G. Pope, J., & C. Rice, J. (2005). Changes in the north sea fish community: evidence of indirect effects of fishing? *ICES Journal of marine Science*, *62*(2), 177–188.

Damuth, J. (1981). Population density and body size in mammals. *Nature*, *290*(5808), 699.

Datta, S., & Blanchard, J. L. (2016). The effects of seasonal processes on size spectrum dynamics. *Canadian Journal of Fisheries and Aquatic Sciences*, *73*(4), 598–610.

Davis, M., & Pineda-Munoz, S. (2016). The temporal scale of diet and dietary proxies. *Ecology and evolution*, *6*(6), 1883–1897.

DEFRA. (2013). *Sea angling 2012 - a survey of recreational sea angling activity and economic value in england* (Tech. Rep.). (http:/www.marinemanagement.org.uk/seaangling 16)

DeNiro, M. J., & Epstein, S. (1976). You are what you eat (plus a few per mil): the carbon isotope cycle in food chains. *Geological Society of America*, *8*, 834–835. (Abstract)

DeNiro, M. J., & Epstein, S. (1978). Influence of diet on the distribution of carbon isotopes in animals. *Geochimica et cosmochimica acta*, *42*(5), 495–506.

DeNiro, M. J., & Epstein, S. (1981). Influence of diet on the distribution of nitrogen

isotopes in animals. *Geochimica et cosmochimica acta*, *45*(3), 341–351.

Dermond, P., Thomas, S. M., & Brodersen, J. (2018). Environmental stability increases relative individual specialisation across populations of an aquatic top predator. *Oikos*, *127*(2), 297–305.

Döring, T. F., Knapp, S., & Cohen, J. E. (2015). Taylor?s power law and the stability of crop yields. *Field Crops Research*, *183*, 294–302.

Dowle, M., & Srinivasan, A. (2017). *data.table: Extension of 'data.frame'. r package version 1.10.4-3.* (Tech. Rep.). (https://CRAN.R-project.org/package=data.table)

Downing, J. A. (1986). Spatial heterogeneity: evolved behaviour or mathematical artefact? *Nature*, *323*(6085), 255.

Dulvy, N., Polunin, N. V., Mill, A., & Graham, N. A. (2004). Size structural change in lightly exploited coral reef fish communities: evidence for weak indirect effects. *Canadian Journal of Fisheries and Aquatic Sciences*, *61*(3), 466–475.

Dunic, J. C., & Baum, J. K. (2017). Size structuring and allometric scaling relationships in coral reef fishes. *Journal of Animal Ecology*, *86*(3), 577–589.

Duplisea, D. E., & Kerr, S. R. (1995). Application of a biomass size spectrum model to demersal fish data from the scotian shelf. *Journal of Theoretical Biology*, *177*(3), 263–269.

Edwards, A. M., Robinson, J. P., Plank, M. J., Baum, J. K., & Blanchard, J. L. (2017). Testing and recommending methods for fitting size spectra to data. *Methods in Ecology and Evolution*, *8*(1), 57–67.

Eisler, Z., Bartos, I., & Kertész, J. (2008). Fluctuation scaling in complex systems: Taylor's law and beyond. *Advances in Physics*, *57*(1), 89–142.

Elsdon, T. S., Ayvazian, S., McMahon, K. W., & Thorrold, S. R. (2010). Experimental evaluation of stable isotope fractionation in fish muscle and otoliths. *Marine Ecology Progress Series*, *408*, 195–205.

Elton, C. S. (1927). *Animal ecology.* University of Chicago Press.

Ersoy, Z., Jeppesen, E., Sgarzi, S., Arranz, I., Cañedo-Argüelles, M., Quintana, X. D., ... Brucet, S. (2017). Size-based interactions and trophic transfer efficiency are

modified by fish predation and cyanobacteria blooms in lake mỳvatn, iceland. *Freshwater Biology*, *62*(11), 1942–1952.

Estes, L., Elsen, P. R., Treuer, T., Ahmed, L., Caylor, K., Chang, J., ... Ellis, E. C. (2018). The spatial and temporal domains of modern ecology. *Nature ecology & evolution*, 1.

Fenchel, T. (1974). Intrinsic rate of natural increase: the relationship with body size. *Oecologia*, *14*(4), 317–326.

Finlay, K., Beisner, B. E., Patoine, A., & Pinel-Alloul, B. (2007). Regional ecosystem variability drives the relative importance of bottom-up and top-down factors for zooplankton size spectra. *Canadian Journal of Fisheries and Aquatic Sciences*, *64*(3), 516–529.

Fisher, R. A. (1919). Xv.?the correlation between relatives on the supposition of mendelian inheritance. *Earth and Environmental Science Transactions of the Royal Society of Edinburgh*, *52*(2), 399–433.

Fisher, R. A. (1921). On the probable error of a coefficient of correlation deduced from a small sample. *Metron*, *1*, 3–32.

Florin, S. T., Felicetti, L. A., & Robbins, C. T. (2011). The biological basis for understanding and predicting dietary-induced variation in nitrogen and sulphur isotope ratio discrimination. *Functional Ecology*, *25*(3), 519–526.

Fogel, M. L., & Cifuentes, L. A. (1993). Isotope fractionation during primary production. In *Organic geochemistry* (pp. 73–98). Springer.

Fonseca, L., Colclough, S., & Hughes, R. G. (2011). Variations in the feeding of 0-group bass dicentrarchus labrax (l.) in managed realignment areas and saltmarshes in se england. *Hydrobiologia*, *672*(1), 15–31.

Frédérich, B., Lehanse, O., Vandewalle, P., & Lepoint, G. (2010). Trophic niche width, shift, and specialization of dascyllus aruanus in toliara lagoon, madagascar. *Copeia*, *2010*(2), 218–226.

Froese, R. (2006). Cube law, condition factor and weight–length relationships: history, meta-analysis and recommendations. *Journal of applied ichthyology*, *22*(4), 241–253.

Fronczak, A., & Fronczak, P. (2010). Origins of taylor's power law for fluctuation scaling in complex systems. *Physical Review E*, *81*(6), 066112.

Fry, B. (2002). Conservative mixing of stable isotopes across estuarine salinity gradients: a conceptual framework for monitoring watershed influences on downstream fisheries production. *Estuaries*, *25*(2), 264–271.

Fry, B., & Arnold, C. (1982). Rapid 13 c/12 c turnover during growth of brown shrimp (penaeus aztecus). *Oecologia*, *54*(2), 200–204.

Gaedke, U. (1992). The size distribution of plankton biomass in a large lake and its seasonal variability. *Limnology and Oceanography*, *37*(6), 1202–1220.

Gaeta, J. W., Ahrenstorff, T. D., Diana, J. S., Fetzer, W. W., Jones, T. S., Lawson, Z. J., ... Vander Zanden, M. J. (2018). Go big or... don't? a field-based diet evaluation of freshwater piscivore and prey fish size relationships. *PloS one*, *13*(3), e0194092.

Garcia, A. M., Claudino, M. C., Mont?Alverne, R., Pereyra, P. E. R., Copertino, M., & Vieira, J. P. (2017). Temporal variability in assimilation of basal food sources by an omnivorous fish at patos lagoon estuary revealed by stable isotopes (2010–2014). *Marine Biology Research*, *13*(1), 98–107.

García-Comas, C., Sastri, A. R., Ye, L., Chang, C.-Y., Lin, F.-S., Su, M.-S., ... Hsieh, C.-h. (2016). Prey size diversity hinders biomass trophic transfer and predator size diversity promotes it in planktonic communities. *Proc. R. Soc. B*, *283*(1824), 20152129.

Gasol, J. M., del Giorgio, P. A., & Duarte, C. M. (1997). Biomass distribution in marine planktonic communities. *Limnology and Oceanography*, *42*(6), 1353–1363.

Gillooly, J. F., Brown, J. H., West, G. B., Savage, V. M., & Charnov, E. L. (2001). Effects of size and temperature on metabolic rate. *science*, *293*(5538), 2248–2251.

Goering, J., Alexander, V., & Haubenstock, N. (1990). Seasonal variability of stable carbon and nitrogen isotope ratios of organisms in a north pacific bay. *Estuarine, Coastal and Shelf Science*, *30*(3), 239–260.

Goldstein, M. L., Morris, S. A., & Yen, G. G. (2004). Problems with fitting to the power-law distribution. *The European Physical Journal B-Condensed Matter and*

Complex Systems, *41*(2), 255–258.

Gómez-Canchong, P., Blanco, J. M., & Quiñones, R. A. (2013). On the use of biomass size spectra linear adjustments to design ecosystem indicators. *Scientia Marina*, *77*(2), 257–268.

Gorokhova, E. (2018). Individual growth as a non-dietary determinant of the isotopic niche metrics. *Methods in Ecology and Evolution*, *9*(2), 269–277.

Grey, J. (2016). The incredible lightness of being methane-fuelled: stable isotopes reveal alternative energy pathways in aquatic ecosystems and beyond. *Frontiers in Ecology and Evolution*, *4*, 8.

Griffiths, J. R., Kadin, M., Nascimento, F. J., Tamelander, T., Törnroos, A., Bonaglia, S., ... others (2017). The importance of benthic–pelagic coupling for marine ecosystem functioning in a changing world. *Global change biology*, *23*(6), 2179–2196.

Grman, E., Lau, J. A., Schoolmaster, D. R., & Gross, K. L. (2010). Mechanisms contributing to stability in ecosystem function depend on the environmental context. *Ecology Letters*, *13*(11), 1400–1410.

Guan, Q., Chen, J., Wei, Z., Wang, Y., Shiyomi, M., & Yang, Y. (2016). Analyzing the spatial heterogeneity of number of plant individuals in grassland community by using power law model. *Ecological modelling*, *320*, 316–321.

Guiet, J., Poggiale, J.-C., & Maury, O. (2016). Modelling the community size-spectrum: recent developments and new directions. *Ecological modelling*, *337*, 4–14.

Gutenberg, G., & Richter, C. (1950). Seismicity of the earth and associated phenomena, howard tatel. *Journal of Geophysical Research*, *55*, 97.

Heady, W. N., & Moore, J. W. (2013). Tissue turnover and stable isotope clocks to quantify resource shifts in anadromous rainbow trout. *Oecologia*, *172*(1), 21–34.

Healy, K., Guillerme, T., Kelly, S., Inger, R., Bearhop, S., & Jackson, A. L. (2017). Sider: an r package for predicting trophic discrimination factors of consumers based on their ecology and phylogenetic relatedness. *Ecography*.

Healy, K., Kelly, S. B., Guillerme, T., Inger, R., Bearhop, S., & Jackson, A. L. (2017). Predicting trophic discrimination factor using bayesian inference and phylogenetic,

ecological and physiological data. desir: Discrimination estimation in r. *PeerJ Preprints*.

Hecky, R., & Hesslein, R. (1995). Contributions of benthic algae to lake food webs as revealed by stable isotope analysis. *Journal of the North American Benthological Society*, *14*(4), 631–653.

Heessen, H. J., Daan, N., & Ellis, J. R. (2015). *Fish atlas of the celtic sea, north sea and baltic sea: Based on international research-vessel surveys*. Wageningen Academic Publishers.

Henderson, P. (2014). *Identification guide to the inshore fish of the british isles*. Pisces Conservation.

Henderson, P., & Corps, M. (1997). The role of temperature and cannibalism in interannual recruitment variation of bass in british waters. *Journal of Fish Biology*, *50*(2), 280–295.

Henderson, P., Turnpenny, A., & Bamber, R. (1984). Long-term stability of a sand smelt (atherina presbyter cuvier) population subject to power station cropping. *Journal of Applied Ecology*, 1–10.

Hinkley, D. V. (1969). On the ratio of two correlated normal random variables. *Biometrika*, *56*(3), 635–639.

Hobson, K. A., & Clark, R. G. (1992). Assessing avian diets using stable isotopes i: turnover of 13c in tissues. *Condor*, 181–188.

Hunt, B. P., Allain, V., Menkès, C., Lorrain, A., Graham, B., Rodier, M., ... Carlotti, F. (2015). A coupled stable isotope-size spectrum approach to understanding pelagic food-web dynamics: a case study from the southwest sub-tropical pacific. *Deep Sea Research Part II: Topical Studies in Oceanography*, *113*, 208–224.

Huss, M., Byström, P., & Persson, L. (2008). Resource heterogeneity, diet shifts and intra-cohort competition: effects on size divergence in yoy fish. *Oecologia*, *158*(2), 249–257.

Hussey, N., MacNeil, M., Olin, J., McMeans, B., Kinney, M., Chapman, D., & Fisk, A. (2012). Stable isotopes and elasmobranchs: tissue types, methods, applications and assumptions. *Journal of Fish Biology*, *80*(5), 1449–1484.

Hussey, N. E., MacNeil, M. A., McMeans, B. C., Olin, J. A., Dudley, S. F., Cliff, G., ... Fisk, A. T. (2014). Rescaling the trophic structure of marine food webs. *Ecology letters*, *17*(2), 239–250.

Huthnance, J., Weisse, R., Wahl, T., Thomas, H., Pietrzak, J., Souza, A. J., ... others (2016). Recent change?north sea. In *North sea region climate change assessment* (pp. 85–136). Springer.

ICES. (2012). *Manual for the international bottom trawl surveys. series of ices survey protocols* (Tech. Rep.). (SISP 1-IBTS, 7)

ICES. (2017). *Seabass (Dicentrarchus labrax) in divisions 4.b?c, 7.a, and 7.d?h (central and southern north sea, irish sea, english channel, bristol channel, and celtic sea)* (Tech. Rep.). (DOI: 10.17895/ices.pub.3334)

Irigoien, X., Klevjer, T. A., Røstad, A., Martinez, U., Boyra, G., Acuña, J., ... others (2014). Large mesopelagic fishes biomass and trophic efficiency in the open ocean. *Nature communications*, *5*, ncomms4271.

Isaac, N. J., & Carbone, C. (2010). Why are metabolic scaling exponents so controversial? quantifying variance and testing hypotheses. *Ecology letters*, *13*(6), 728–735.

Jackson, A. L., Inger, R., Parnell, A. C., & Bearhop, S. (2011). Comparing isotopic niche widths among and within communities: Siber–stable isotope bayesian ellipses in r. *Journal of Animal Ecology*, *80*(3), 595–602.

Jackson, H. B., & Fahrig, L. (2015). Are ecologists conducting research at the optimal scale? *Global Ecology and Biogeography*, *24*(1), 52–63.

Jardine, T. D., Hadwen, W. L., Hamilton, S. K., Hladyz, S., Mitrovic, S. M., Kidd, K. A., ... others (2014). Understanding and overcoming baseline isotopic variability in running waters. *River Research and Applications*, *30*(2), 155–165.

Jennings, S., & Blanchard, J. L. (2004). Fish abundance with no fishing: predictions based on macroecological theory. *Journal of Animal Ecology*, *73*(4), 632–642.

Jennings, S., & Collingridge, K. (2015). Predicting consumer biomass, size-structure, production, catch potential, responses to fishing and associated uncertainties in the world?s marine ecosystems. *PloS one*, *10*(7), e0133794.

Jennings, S., Greenstreet, S., Hill, L., Piet, G., Pinnegar, J., & Warr, K. (2002).

Long-term trends in the trophic structure of the north sea fish community: evidence from stable-isotope analysis, size-spectra and community metrics. *Marine Biology*, *141*(6), 1085–1097.

Jennings, S., Maxwell, T. A., Schratzberger, M., & Milligan, S. P. (2008). Body-size dependent temporal variations in nitrogen stable isotope ratios in food webs. *Marine Ecology Progress Series*, *370*, 199–206.

Jennings, S., Warr, K. J., & Mackinson, S. (2002). Use of size-based production and stable isotope analyses to predict trophic transfer efficiencies and predator-prey body mass ratios in food webs. *Marine Ecology Progress Series*, *240*, 11–20.

Jonsson, T., Kaartinen, R., Jonsson, M., & Bommarco, R. (2018). Predictive power of food web models based on body size decreases with trophic complexity. *Ecology letters*, *21*(5), 702–712.

Jørgensen, B., Demétrio, C. G., Kristensen, E., Banta, G. T., Petersen, H. C., & Delefosse, M. (2011). Bias-corrected pearson estimating functions for taylor?s power law applied to benthic macrofauna data. *Statistics & Probability Letters*, *81*(7), 749–758.

Jørgensen, C., & Fiksen, Ø. (2006). State-dependent energy allocation in cod (gadus morhua). *Canadian journal of fisheries and aquatic sciences*, *63*(1), 186–199.

Juanes, F., Buckel, J. A., & Scharf, F. S. (2001). Predatory behaviour and selectivity of a primary piscivore: comparison of fish and non-fish prey. *Marine Ecology Progress Series*, *217*, 157–165.

Kalyuzhny, M., Schreiber, Y., Chocron, R., Flather, C. H., Kadmon, R., Kessler, D. A., & Shnerb, N. M. (2014). Temporal fluctuation scaling in populations and communities. *Ecology*, *95*(6), 1701–1709.

Kearney, M. R., & White, C. R. (2012). Testing metabolic theories. *The American Naturalist*, *180*(5), 546–565.

Kelley, D. (1986). Bass nurseries on the west coast of the uk. *Journal of the Marine Biological Association of the United Kingdom*, *66*(2), 439–464.

Kelley, D. (1987). Food of bass in uk waters. *Journal of the Marine Biological Association of the United Kingdom*, *67*(2), 275–286.

Kerr, S. R., & Dickie, L. M. (2001). *The biomass spectrum: a predator-prey theory of aquatic production.* Columbia University Press.

Kerstan, M. (1991). The importance of rivers as nursery grounds for 0-and 1-group flounder (platichthys flesus l.) in comparison to the wadden sea. *Netherlands Journal of Sea Research*, *27*(3-4), 353–366.

Kiljunen, M., Grey, J., Sinisalo, T., Harrod, C., Immonen, H., & Jones, R. I. (2006). A revised model for lipid-normalizing δ13c values from aquatic organisms, with implications for isotope mixing models. *Journal of Applied Ecology*, *43*(6), 1213–1222.

Killen, S. S., Marras, S., & McKenzie, D. J. (2011). Fuel, fasting, fear: routine metabolic rate and food deprivation exert synergistic effects on risk-taking in individual juvenile european sea bass. *Journal of Animal Ecology*, *80*(5), 1024–1033.

Kilpatrick, A., & Ives, A. (2003). Species interactions can explain taylor's power law for ecological time series. *Nature*, *422*(6927), 65–68.

Kim, S. L., & Koch, P. L. (2012). Methods to collect, preserve, and prepare elasmobranch tissues for stable isotope analysis. *Environmental biology of fishes*, *95*(1), 53–63.

Kleiber, M. (1932). Body size and metabolism. *Hilgardia*, *6*(11), 315–353.

Kleiber, M. (1947). Body size and metabolic rate. *Physiological reviews*, *27*(4), 511–541.

Kleiber, M. (1961). *The fire of life: an introduction to animal energetics.* University of California; John Wiley. New York.

Komsta, L. (2013). *mblm: Median-based linear models. r package version 0.12.* (Tech. Rep.). (https://CRAN.R-project.org/package=mblm)

Kooijman, S. (1986). Energy budgets can explain body size relations. *Journal of Theoretical Biology*, *121*(3), 269–282.

Kuo, T.-C., Mandal, S., Yamauchi, A., & Hsieh, C.-H. (2016). Life history traits and exploitation affect the spatial mean-variance relationship in fish abundance. *Ecology*, *97*(5), 1251–1259.

Laffaille, P., Lefeuvre, J.-C., Schricke, M.-T., & Feunteun, E. (2001). Feeding ecology of o-group sea bass, dicentrarchus labrax, in salt marshes of mont saint michel bay (france). *Estuaries*, *24*(1), 116–125.

Lagrue, C., Poulin, R., & Cohen, J. E. (2015). Parasitism alters three power laws of scaling in a metazoan community: Taylor?s law, density-mass allometry, and variance-mass allometry. *Proceedings of the National Academy of Sciences*, *112*(6), 1791–1796.

Lam-Hoai, T., Guiral, D., & Rougier, C. (2006). Seasonal change of community structure and size spectra of zooplankton in the kaw river estuary (french guiana). *Estuarine, Coastal and Shelf Science*, *68*(1-2), 47–61.

Laws, E. A., Popp, B. N., Bidigare, R. R., Kennicutt, M. C., & Macko, S. A. (1995). Dependence of phytoplankton carbon isotopic composition on growth rate and [co2) aq: Theoretical considerations and experimental results. *Geochimica et cosmochimica acta*, *59*(6), 1131–1138.

Layman, C. A., Araújo, M. S., Boucek, R., Hammerschlag-Peyer, C. M., Harrison, E., Jud, Z. R., ... others (2012). Applying stable isotopes to examine food-web structure: an overview of analytical tools. *Biological Reviews*, *87*(3), 545–562.

Layman, C. A., Arrington, D. A., Montaña, C. G., & Post, D. M. (2007). Can stable isotope ratios provide for community-wide measures of trophic structure? *Ecology*, *88*(1), 42–48.

Layman, C. A., Newsome, S. D., & Crawford, T. G. (2015). Individual-level niche specialization within populations: emerging areas of study. *Oecologia*, *178*(1), 1–4.

Levin, S. A. (1992). The problem of pattern and scale in ecology: the robert h. macarthur award lecture. *Ecology*, *73*(6), 1943–1967.

Lindeman, R. L. (1942). The trophic-dynamic aspect of ecology. *Ecology*, *23*(4), 399–417.

Lindmark, M., Huss, M., Ohlberger, J., & Gårdmark, A. (2018). Temperature-dependent body size effects determine population responses to climate warming. *Ecology letters*, *21*(2), 181–189.

López, R., De Pontual, H., Bertignac, M., & Mahévas, S. (2015). What can exploratory modelling tell us about the ecobiology of european sea bass (dicentrarchus labrax): a comprehensive overview. *Aquatic Living Resources*, *28*(2-4), 61–79.

Lotka, A. J. (1926). The frequency distribution of scientific productivity. *Journal of the Washington academy of sciences*, *16*(12), 317–323.

Ma, Z. S. (2015). Power law analysis of the human microbiome. *Molecular ecology*, *24*(21), 5428–5445.

MacArthur, R. (1972). *Geographical ecology: patterns in the distribution of species harper and row*. New York, New York, USA.

Maino, J. L., Kearney, M. R., Nisbet, R. M., & Kooijman, S. A. (2014). Reconciling theories for metabolic scaling. *Journal of Animal Ecology*, *83*(1), 20–29.

Mann, R. (1971). The populations, growth and production of fish in four small streams in southern england. *The Journal of Animal Ecology*, 155–190.

Marquet, P. A., Quiñones, R. A., Abades, S., Labra, F., Tognelli, M., Arim, M., & Rivadeneira, M. (2005). Scaling and power-laws in ecological systems. *Journal of Experimental Biology*, *208*(9), 1749–1769.

Marsaglia, G. (1965). Ratios of normal variables and ratios of sums of uniform variables. *Journal of the American Statistical Association*, *60*(309), 193–204.

Martínez del Rio, C., & Carleton, S. A. (2012). How fast and how faithful: the dynamics of isotopic incorporation into animal tissues. *Journal of Mammalogy*, *93*(2), 353–359.

Martínez del Rio, C., Wolf, N., Carleton, S. A., & Gannes, L. Z. (2009). Isotopic ecology ten years after a call for more laboratory experiments. *Biological Reviews*, *84*(1), 91–111.

Martinho, F., Leitão, R., Neto, J. M., Cabral, H., Lagardère, F., & Pardal, M. (2008). Estuarine colonization, population structure and nursery functioning for 0-group sea bass (dicentrarchus labrax), flounder (platichthys flesus) and sole (solea solea) in a mesotidal temperate estuary. *Journal of Applied Ichthyology*, *24*(3), 229–237.

Matthews, B., & Mazumder, A. (2004). A critical evaluation of intrapopulation variation of δ 13 c and isotopic evidence of individual specialization. *Oecologia*, *140*(2), 361–371.

McCutchan, J. H., Lewis, W. M., Kendall, C., & McGrath, C. C. (2003). Variation in trophic shift for stable isotope ratios of carbon, nitrogen, and sulfur. *Oikos*,

102(2), 378–390.

McGarvey, D. J., & Kirk, A. J. (2018). Seasonal comparison of community-level size-spectra in southern coalfield streams of west virginia (usa). *Hydrobiologia*, *809*(1), 65–77.

McMahon, K. W., Fogel, M. L., Elsdon, T. S., & Thorrold, S. R. (2010). Carbon isotope fractionation of amino acids in fish muscle reflects biosynthesis and isotopic routing from dietary protein. *Journal of Animal Ecology*, *79*(5), 1132–1141.

McMahon, K. W., Thorrold, S. R., Elsdon, T. S., & McCarthy, M. D. (2015). Trophic discrimination of nitrogen stable isotopes in amino acids varies with diet quality in a marine fish. *Limnology and Oceanography*, *60*(3), 1076–1087.

McMahon, T. (1973). Size and shape in biology: elastic criteria impose limits on biological proportions, and consequently on metabolic rates. *Science*, *179*(4079), 1201–1204.

Medina, J. M., & Díaz, J. A. (2016). Fluctuation scaling in the visual cortex at threshold. *Physical Review E*, *93*(5), 052403.

Mellin, C., Huchery, C., Caley, M. J., Meekan, M. G., & Bradshaw, C. J. (2010). Reef size and isolation determine the temporal stability of coral reef fish populations. *Ecology*, *91*(11), 3138–3145.

Merino, G., Barange, M., Blanchard, J. L., Harle, J., Holmes, R., Allen, I., ... others (2012). Can marine fisheries and aquaculture meet fish demand from a growing human population in a changing climate? *Global Environmental Change*, *22*(4), 795–806.

Miller, P. (1975). Age-structure and life-span in the common goby, pomatoschistus microps. *Journal of Zoology*, *177*(3), 425–448.

Millot, S., Bégout, M.-L., & Chatain, B. (2009). Risk-taking behaviour variation over time in sea bass dicentrarchus labrax: effects of day–night alternation, fish phenotypic characteristics and selection for growth. *Journal of Fish Biology*, *75*(7), 1733–1749.

MMO. (2013). *Uk sea fisheries statistics 2012: Sections 1-3* (Tech. Rep.). (https://www.gov.uk/government/statistics/uk-sea-fisheries-annual-statistics-report-2012

98)

MMO. (2018). *Statutory guidance: bass industry guidance 2018* (Tech. Rep.). (https://www.gov.uk/government/publications/bass-industry-guidance-2018)

Monaghan, K. (2015). Taylor?s law improves the accuracy of bioassessment; an example for freshwater macroinvertebrates. *Hydrobiologia*, *760*(1), 91–103.

Mourier, J., Maynard, J., Parravicini, V., Ballesta, L., Clua, E., Domeier, M. L., & Planes, S. (2016). Extreme inverted trophic pyramid of reef sharks supported by spawning groupers. *Current Biology*, *26*(15), 2011–2016.

Munk, P. (1991). *Changes in mean size and distribution of juvenile north sea sprat (sprattus sprattus l.) in the period 1976-90.* Danmarks Fiskeri-og Havundersøgelser.

Nadon, M. O., Baum, J. K., Williams, I. D., Mcpherson, J. M., Zgliczynski, B. J., Richards, B. L., ... Brainard, R. E. (2012). Re-creating missing population baselines for pacific reef sharks. *Conservation Biology*, *26*(3), 493–503.

Naisbit, R. E., Kehrli, P., Rohr, R. P., & Bersier, L.-F. (2011). Phylogenetic signal in predator–prey body-size relationships. *Ecology*, *92*(12), 2183–2189.

Nakatsuka, T., Handa, N., Wada, E., & Wong, C. S. (1992). The dynamic changes of stable isotopic ratios of carbon and nitrogen in suspended and sedimented particulate organic matter during a phytoplankton bloom. *Journal of Marine Research*, *50*(2), 267–296.

Nakazawa, T. (2017). Individual interaction data are required in community ecology: a conceptual review of the predator–prey mass ratio and more. *Ecological Research*, *32*(1), 5–12.

Nakazawa, T., Ushio, M., & Kondoh, M. (2011). Scale dependence of predator–prey mass ratio: determinants and applications. In *Advances in ecological research* (Vol. 45, pp. 269–302). Elsevier.

Natural England. (2018). *Natural england conservation advice for marine protected areas solent and southampton water spa* (Tech. Rep.). (`https://designatedsites.naturalengland.org.uk/Marine/MarineSiteDetail.aspx?SiteCode=UK9011061&SiteName=solent%20&countyCode=&responsiblePerson=&SeaArea=&IFCAArea=` [Accessed: 19/06/2018])

Newman, M. E. (2005). Power laws, pareto distributions and zipf's law. *Contemporary physics*, *46*(5), 323–351.

Nicholson, M. D., & Jennings, S. (2004). Testing candidate indicators to support ecosystem-based management: the power of monitoring surveys to detect temporal trends in fish community metrics. *ICES Journal of marine Science*, *61*(1), 35–42.

Nielsen, J. M., Clare, E. L., Hayden, B., Brett, M. T., & Kratina, P. (2018). Diet tracing in ecology: method comparison and selection. *Methods in Ecology and Evolution*, *9*(2), 278–291.

Norin, T., & Gamperl, A. K. (2018). Metabolic scaling of individuals vs. populations: Evidence for variation in scaling exponents at different hierarchical levels. *Functional Ecology*, *32*(2), 379–388.

Núñez-Riboni, I., & Akimova, A. (2015). Monthly maps of optimally interpolated in situ hydrography in the north sea from 1948 to 2013. *Journal of Marine Systems*, *151*, 15–34.

Ohshimo, S., Tanaka, H., Nishiuchi, K., & Yasuda, T. (2016). Trophic positions and predator–prey mass ratio of the pelagic food web in the east china sea and sea of japan. *Marine and Freshwater Research*, *67*(11), 1692–1699.

Oksanen, J., Blanchet, F. G., Friendly, M., Kindt, R., Legendre, P., McGlinn, D., ... Wagner, H. (2017). *vegan: Community ecology package* (Tech. Rep.). (R package version 2.4-5. https://CRAN.R-project.org/package=vegan)

O'Reilly, C., Hecky, R., Cohen, A., & Plisnier, P.-D. (2002). Interpreting stable isotopes in food webs: recognizing the role of time averaging at different trophic levels. *Limnology and oceanography*, *47*(1), 306–309.

Pannella, G. (1971). Fish otoliths: daily growth layers and periodical patterns. *Science*, *173*(4002), 1124–1127.

Parnell, A. C., Inger, R., Bearhop, S., & Jackson, A. L. (2010). Source partitioning using stable isotopes: coping with too much variation. *PloS one*, *5*(3), e9672.

Parnell, A. C., Phillips, D. L., Bearhop, S., Semmens, B. X., Ward, E. J., Moore, J. W., ... Inger, R. (2013). Bayesian stable isotope mixing models. *Environmetrics*, *24*(6), 387–399.

Pauly, D., & Christensen, V. (1995). Primary production required to sustain global fisheries. *Nature*, *374*(6519), 255–257.

Pawson, M., Pickett, G., & Kelley, D. (1987). The distribution and migrations of bass, dicentrarchus labrax l., in waters around england and wales as shown by tagging. *Journal of the Marine Biological Association of the United Kingdom*, *67*(1), 183–217.

Pérez-Ruzafa, A., & Marcos, C. (2014). Ecology and distribution of dicentrarchus labrax (linnaeus 1758). *In: Biology of European Sea Bass*, 1.

Perry, J. N. (1981). Taylor's power law for dependence of variance on mean in animal populations. *Journal of Applied Statistics*, 254–263.

Perry, J. N. (1994). Chaotic dynamics can generate taylor?s power law. *Proceedings of the Royal Society of London B: Biological Sciences*, *257*(1350), 221–226.

Pertoldi, C., Bach, L. A., & Loeschcke, V. (2008). On the brink between extinction and persistence. *Biology direct*, *3*(1), 47.

Petchey, O. L., & Belgrano, A. (2010). *Body-size distributions and size-spectra: universal indicators of ecological status?* The Royal Society.

Peters, R. H. (1983). *The ecological implications of body size.* University Press, Cambridge, UK.

Peterson, B. J., & Fry, B. (1987). Stable isotopes in ecosystem studies. *Annual review of ecology and systematics*, *18*(1), 293–320.

Phillips, D. L., Inger, R., Bearhop, S., Jackson, A. L., Moore, J. W., Parnell, A. C., ... Ward, E. J. (2014). Best practices for use of stable isotope mixing models in food-web studies. *Canadian Journal of Zoology*, *92*(10), 823–835.

Pickett, G. D., & Pawson, M. G. (1994). *Sea bass: Biology* (Vol. 12). Springer Science & Business Media.

Pineas, L., Ouphant, M., & Iverson, I. (1971). Food habits of albacore, bluefin tuna, and bonito in california water. *California Department of Fish and Game: Fish Bulletin*, *152*, 1–105.

Pitcher, T., & MacDonald, P. (1973). Two models for seasonal growth in fishes. *Journal of applied ecology*, 599–606.

Platt, T., & Denman, K. (1977). Organisation in the pelagic ecosystem. *Helgoländer Wissenschaftliche Meeresuntersuchungen*, *30*(1), 575.

Podlesak, D. W., McWilliams, S. R., & Hatch, K. A. (2005). Stable isotopes in breath, blood, feces and feathers can indicate intra-individual changes in the diet of migratory songbirds. *Oecologia*, *142*(4), 501–510.

Post, D. M. (2002). Using stable isotopes to estimate trophic position: models, methods, and assumptions. *Ecology*, *83*(3), 703–718.

Post, J. R., & Parkinson, E. (2001). Energy allocation strategy in young fish: allometry and survival. *Ecology*, *82*(4), 1040–1051.

Potter, I., Claridge, P., & Warwick, R. (1986). Consistency of seasonal changes in an estuarine fish assemblage. *Marine Ecology Progress Series*, 217–228.

Price, C. A., Weitz, J. S., Savage, V. M., Stegen, J., Clarke, A., Coomes, D. A., ... others (2012). Testing the metabolic theory of ecology. *Ecology letters*, *15*(12), 1465–1474.

Rader, J. A., Newsome, S. D., Sabat, P., Chesser, R. T., Dillon, M. E., & Martínez del Rio, C. (2017). Isotopic niches support the resource breadth hypothesis. *Journal of Animal Ecology*, *86*(2), 405–413.

Ramos, C., Parrish, C., Quibuyen, T., & Abrajano, T. (2003). Molecular and carbon isotopic variations in lipids in rapidly settling particles during a spring phytoplankton bloom. *Organic geochemistry*, *34*(2), 195–207.

Ramos, R., & González-Solís, J. (2012). Trace me if you can: the use of intrinsic biogeochemical markers in marine top predators. *Frontiers in Ecology and the Environment*, *10*(5), 258–266.

Ramsayer, J., Fellous, S., Cohen, J. E., & Hochberg, M. E. (2012). Taylor's law holds in experimental bacterial populations but competition does not influence the slope. *Biology letters*, *8*(2), 316–319.

R-Core-Team. (2016). *R: A language and environment for statistical computing. r foundation for statistical computing* (Tech. Rep.). (Vienna, Austria. URL https://www.R-project.org/.)

Reed, D. H., & Hobbs, G. R. (2004). The relationship between population size and

temporal variability in population size. In *Animal conservation forum* (Vol. 7, pp. 1–8).

Rees, C., Jenkins, W., & Monster, J. (1978). The sulphur isotopic composition of ocean water sulphate. *Geochimica et Cosmochimica Acta*, *42*(4), 377–381.

Reum, J. C., & Hunsicker, M. E. (2012). Season and prey type influence size dependency of predator–prey body mass ratios in a marine fish assemblage. *Marine Ecology Progress Series*, *466*, 167–175.

Reum, J. C., Jennings, S., & Hunsicker, M. E. (2015). Implications of scaled δ15n fractionation for community predator–prey body mass ratio estimates in size-structured food webs. *Journal of Animal Ecology*, *84*(6), 1618–1627.

Reuman, D. C., Zhao, L., Sheppard, L. W., Reid, P. C., & Cohen, J. E. (2017). Synchrony affects taylor?s law in theory and data. *Proceedings of the National Academy of Sciences*, *114*(26), 6788–6793.

Rice, J., & Gislason, H. (1996). Patterns of change in the size spectra of numbers and diversity of the north sea fish assemblage, as reflected in surveys and models. *ICES Journal of Marine Science*, *53*(6), 1214–1225.

Riebesell, U., Revill, A. T., Holdsworth, D. G., & Volkman, J. K. (2000). The effects of varying co_2 concentration on lipid composition and carbon isotope fractionation in emiliania huxleyi. *Geochimica et Cosmochimica Acta*, *64*(24), 4179–4192.

Robinson, J. P., Williams, I. D., Edwards, A. M., McPherson, J., Yeager, L., Vigliola, L., ... Baum, J. K. (2017). Fishing degrades size structure of coral reef fish communities. *Global change biology*, *23*(3), 1009–1022.

Rochet, M.-J., & Benoît, E. (2011). Fishing destabilizes the biomass flow in the marine size spectrum. *Proceedings of the Royal Society of London B: Biological Sciences*, rspb20110893.

Rogdakis, Y., Ramfos, A., Koukou, K., Dimitriou, E., & Katselis, G. (2010). Feeding habits and trophic level of sea bass (dicentrarchus labrax) in the messolonghi-etoliko lagoons complex (western greece). *Journal of Biological Research*, *13*, 13–26.

Rosecchi, E., Tracey, D., & Webber, W. (1988). Diet of orange roughy, *Hoplostethus*

atlanticus (pisces: Trachichthyidae) on the challenger plateau, new zealand. *Marine Biology*, *99*(2), 293–306.

Roughgarden, J. (1972). Evolution of niche width. *The American Naturalist*, *106*(952), 683–718.

Rousseau, V., Becquevort, S., Parent, J.-Y., Gasparini, S., Daro, M.-H., Tackx, M., & Lancelot, C. (2000). Trophic efficiency of the planktonic food web in a coastal ecosystem dominated by phaeocystis colonies. *Journal of Sea Research*, *43*(3-4), 357–372.

Savage, V. M., Deeds, E. J., & Fontana, W. (2008). Sizing up allometric scaling theory. *PLoS computational biology*, *4*(9), e1000171.

Savoye, N., Aminot, A., Treguer, P., Fontugne, M., Naulet, N., & Kérouel, R. (2003). Dynamics of particulate organic matter δ15n and δ13c during spring phytoplankton blooms in a macrotidal ecosystem (bay of seine, france). *Marine ecology progress series*, *255*, 27–41.

Schlöke, B., Crowley, J., Cook, D., Briatte, F., Marbach, M., Thoen, E., ... Larmarange, J. (2017). *Ggally: Extension to 'ggplot2'. r package version 1.3.2.* (Tech. Rep.). (https://CRAN.R-project.org/package=GGally)

Schmidt-Nielsen, K. (1984). *Scaling: why is animal size so important?* University Press, Cambridge, UK.

Schoener, T. W. (1968). The anolis lizards of bimini: resource partitioning in a complex fauna. *Ecology*, *49*(4), 704–726.

Schramski, J. R., Dell, A. I., Grady, J. M., Sibly, R. M., & Brown, J. H. (2015). Metabolic theory predicts whole-ecosystem properties. *Proceedings of the National Academy of Sciences*, *112*(8), 2617–2622.

Schwinghamer, P. (1981). Characteristic size distributions of integral benthic communities. *Canadian Journal of Fisheries and Aquatic Sciences*, *38*(10), 1255–1263.

Sheldon, R., Prakash, A., & Sutcliffe, W. (1972). The size distribution of particles in the ocean. *Limnology and oceanography*, *17*(3), 327–340.

Shi, P.-J., Sandhu, H. S., & Reddy, G. V. (2016). Dispersal distance determines the

exponent of the spatial taylor?s power law. *Ecological modelling*, *335*, 48–53.

Sibly, R. M., Brown, J. H., & Kodric-Brown, A. (2012). *Metabolic ecology: a scaling approach*. John Wiley & Sons.

Siegel, A. F. (1982). Robust regression using repeated medians. *Biometrika*, *69*(1), 242–244.

Singh, A., Wang, H., Morrison, W., & Weiss, H. (2012). Modeling fish biomass structure at near pristine coral reefs and degradation by fishing. *Journal of Biological Systems*, *20*(01), 21–36.

Smith, B. N., & Epstein, S. (1971). Two categories of 13c/12c ratios for higher plants. *Plant physiology*, *47*(3), 380–384.

Smith, B. R., & Blumstein, D. T. (2008). Fitness consequences of personality: a meta-analysis. *Behavioral Ecology*, *19*(2), 448–455.

Spitz, J., Chouvelon, T., Cardinaud, M., Kostecki, C., & Lorance, P. (2013). Prey preferences of adult sea bass dicentrarchus labrax in the northeastern atlantic: implications for bycatch of common dolphin delphinus delphis. *ICES Journal of Marine Science*, *70*(2), 452–461.

Sprules, W. G., & Barth, L. E. (2016). Surfing the biomass size spectrum: some remarks on history, theory, and application. *Canadian Journal of Fisheries and Aquatic Sciences*, *73*(4), 477–495.

Sprules, W. G., Brandt, S., Stewart, D., Munawar, M., Jin, E., & Love, J. (1991). Biomass size spectrum of the lake michigan pelagic food web. *Canadian Journal of Fisheries and Aquatic Sciences*, *48*(1), 105–115.

Sprules, W. G., Casselman, J., & Shuter, B. (1983). Size distribution of pelagic particles in lakes. *Canadian Journal of Fisheries and Aquatic Sciences*, *40*(10), 1761–1769.

Sprules, W. G., & Munawar, M. (1986). Plankton size spectra in relation to ecosystem productivity, size, and perturbation. *Canadian Journal of Fisheries and Aquatic Sciences*, *43*(9), 1789–1794.

Stumpf, M. P., & Porter, M. A. (2012). Critical truths about power laws. *Science*, *335*(6069), 665–666.

Svanbäck, R., & Persson, L. (2009). Population density fluctuations change the selection

gradient in eurasian perch. *The American Naturalist*, *173*(4), 507–516.

Tanaka, Y., & Mano, H. (2012). Functional traits of herbivores and food chain efficiency in a simple aquatic community model. *Ecological modelling*, *237*, 88–100.

Taylor, L. R. (1961). Aggregation, variance and the mean. *Nature*, *189*, 732–735.

Taylor, L. R., Woiwod, I., & Perry, J. N. (1980). Variance and the large scale spatial stability of aphids, moths and birds. *The Journal of Animal Ecology*, 831–854.

Taylor, L. R., & Woiwod, I. P. (1982). Comparative synoptic dynamics. i. relationships between inter-and intra-specific spatial and temporal variance/mean population parameters. *The Journal of Animal Ecology*, 879–906.

Thomas, S. M., & Crowther, T. W. (2015). Predicting rates of isotopic turnover across the animal kingdom: a synthesis of existing data. *Journal of Animal Ecology*, *84*(3), 861–870.

Thompson, D. W. (1942). *On growth and form. 2nd edition.* University Press, Cambridge, UK.

Tippett, M. K., & Cohen, J. E. (2016). Tornado outbreak variability follows taylor?s power law of fluctuation scaling and increases dramatically with severity. *Nature communications*, *7*, 10668.

Tokeshi, M. (1995). On the mathematical basis of the variance-mean power relationship. *Researches on Population Ecology*, *37*(1), 43–48.

Toscano, B. J., Gownaris, N. J., Heerhartz, S. M., & Monaco, C. J. (2016). Personality, foraging behavior and specialization: integrating behavioral and food web ecology at the individual level. *Oecologia*, *182*(1), 55–69.

Townend, I. (2008). *A conceptual model of southampton water. vol 1.* (Tech. Rep.). ABPmer report. (21/05/2008)

Trebilco, R., Baum, J. K., Salomon, A. K., & Dulvy, N. K. (2013). Ecosystem ecology: size-based constraints on the pyramids of life. *Trends in ecology & evolution*, *28*(7), 423–431.

Trebilco, R., Dulvy, N. K., Anderson, S. C., & Salomon, A. K. (2016). The paradox of inverted biomass pyramids in kelp forest fish communities. *Proc. R. Soc. B*, *283*(1833), 20160816.

Trueman, C., Johnston, G., O'Hea, B., & MacKenzie, K. (2014). Trophic interactions of fish communities at midwater depths enhance long-term carbon storage and benthic production on continental slopes. *Proc. R. Soc. B*, *281*(1787), 20140669.

Tsai, C.-H., Hsieh, C.-h., & Nakazawa, T. (2016). Predator–prey mass ratio revisited: does preference of relative prey body size depend on individual predator size? *Functional ecology*, *30*(12), 1979–1987.

Tuszynski, J. (2014). *catools: Tools: moving window statistics, gif, base64, roc auc, etc.. r package version 1.17.1* (Tech. Rep.). (https://CRAN.R-project.org/package=caTools)

Ullah, M. I., & Aslam, M. (2014). *mctest: Multicollinearity diagnostic measures. r package version 1.1.1* (Tech. Rep.). (https://CRAN.R-project.org/package=mctest)

van Denderen, P. D., Lindegren, M., MacKenzie, B. R., Watson, R. A., & Andersen, K. H. (2018). Global patterns in marine predatory fish. *Nature ecology & evolution*, *2*(1), 65.

Vander Zanden, M. J., Casselman, J. M., & Rasmussen, J. B. (1999a). Stable isotope evidence for the food web consequences of species invasions in lakes. *Nature*, *401*(6752), 464.

Vander Zanden, M. J., Casselman, J. M., & Rasmussen, J. B. (1999b). Stable isotope evidence for the food web consequences of species invasions in lakes. *Nature*, *401*(6752), 464.

Vander Zanden, M. J., Clayton, M. K., Moody, E. K., Solomon, C. T., & Weidel, B. C. (2015). Stable isotope turnover and half-life in animal tissues: a literature synthesis. *PloS one*, *10*(1), e0116182.

Vander Zanden, M. J., Shuter, B. J., Lester, N., & Rasmussen, J. B. (1999). Patterns of food chain length in lakes: a stable isotope study. *The American Naturalist*, *154*(4), 406–416.

van Leeuwen, S., Tett, P., Mills, D., & van Der Molen, J. (2015). Stratified and nonstratified areas in the north sea: Long-term variability and biological and policy implications. *Journal of Geophysical Research: Oceans*, *120*(7), 4670–4686.

Villate, F. (1991). Annual cycle of zooplankton community in the abra harbour (bay of biscay): abundance, composition and size spectra. *Journal of Plankton Research*, *13*(4), 691–706.

Virkar, Y., & Clauset, A. (2014). Power-law distributions in binned empirical data. *The Annals of Applied Statistics*, 89–119.

Wang, S., & Brose, U. (2018). Biodiversity and ecosystem functioning in food webs: the vertical diversity hypothesis. *Ecology letters*, *21*(1), 9–20.

West, G. B., & Brown, J. H. (2005). The origin of allometric scaling laws in biology from genomes to ecosystems: towards a quantitative unifying theory of biological structure and organization. *Journal of experimental biology*, *208*(9), 1575–1592.

West, G. B., Brown, J. H., & Enquist, B. J. (1997). A general model for the origin of allometric scaling laws in biology. *Science*, *276*(5309), 122–126.

White, E. P., Enquist, B. J., & Green, J. L. (2008). On estimating the exponent of power-law frequency distributions. *Ecology*, *89*(4), 905–912.

White, E. P., Ernest, S. M., Kerkhoff, A. J., & Enquist, B. J. (2007). Relationships between body size and abundance in ecology. *Trends in ecology & evolution*, *22*(6), 323–330.

Wickham, H., et al. (2011). The split-apply-combine strategy for data analysis. *Journal of Statistical Software*, *40*(1), 1–29.

Wilson, S., Fisher, R., Pratchett, M., Graham, N., Dulvy, N., Turner, R., ... Polunin, N. (2010). Habitat degradation and fishing effects on the size structure of coral reef fish communities. *Ecological Applications*, *20*(2), 442–451.

Wood, C. M., McKinney, S. T., & Loftin, C. S. (2017). Intraspecific functional diversity of common species enhances community stability. *Ecology and evolution*, *7*(5), 1553–1560.

Woodson, C. B., Schramski, J. R., & Joye, S. B. (2018). A unifying theory for top-heavy ecosystem structure in the ocean. *Nature communications*, *9*(1), 23.

Woodward, G., & Warren, P. (2007). Body size and predatory interactions in freshwaters: scaling from individuals to communities. In *Body size: the structure and function of aquatic ecosystems* (pp. 98–117). Cambridge University Press Cambridge.

Woodworth-Jefcoats, P. A., Polovina, J. J., Dunne, J. P., & Blanchard, J. L. (2013). Ecosystem size structure response to 21st century climate projection: large fish abundance decreases in the central north pacific and increases in the california current. *Global change biology*, *19*(3), 724–733.

Xiao, X., Locey, K. J., & White, E. P. (2015). A process-independent explanation for the general form of taylor's law. *The American Naturalist*, *186*(2), E51–E60.

Xu, M. (2015). Taylor's power law: before and after 50 years of scientific scrutiny. *arXiv preprint arXiv:1505.02033*.

Xu, M., Kolding, J., & Cohen, J. E. (2016). Taylor's power law and fixed-precision sampling: application to abundance of fish sampled by gillnets in an african lake. *Canadian journal of fisheries and aquatic sciences*, *74*(1), 87–100.

Xu, M., Schuster, W. S., & Cohen, J. E. (2015). Robustness of taylor's law under spatial hierarchical groupings of forest tree samples. *Population Ecology*, *57*(1), 93–103.

Yemane, D., Field, J. G., & Leslie, R. W. (2008). Indicators of change in the size structure of fish communities: A case study from the south coast of south africa. *Fisheries Research*, *93*(1-2), 163–172.

York, J. K., Tomasky, G., Valiela, I., & Repeta, D. J. (2007). Stable isotopic detection of ammonium and nitrate assimilation by phytoplankton in the waquoit bay estuarine system. *Limnology and Oceanography*, *52*(1), 144–155.

Yvon-Durocher, G., & Allen, A. P. (2012). Linking community size structure and ecosystem functioning using metabolic theory. *Phil. Trans. R. Soc. B*, *367*(1605), 2998–3007.

Yvon-Durocher, G., Montoya, J. M., Trimmer, M., & Woodward, G. (2011). Warming alters the size spectrum and shifts the distribution of biomass in freshwater ecosystems. *Global change biology*, *17*(4), 1681–1694.

Zaccarelli, N., Bolnick, D. I., & Mancinelli, G. (2013). Rinsp: an r package for the analysis of individual specialization in resource use. *Methods in Ecology and Evolution*, *4*(11), 1018–1023.

Zander, C. (1982). Feeding ecology of littoral gobiid and blennioid fish of the banyuls area (mediterranean sea). i. main food and trophic dimension of niche and ecotope.

Vie et milieu. Paris, *32*(1), 1–10.

Zaoli, S., Giometto, A., Maritan, A., & Rinaldo, A. (2017). Covariations in ecological scaling laws fostered by community dynamics. *Proceedings of the National Academy of Sciences*, *114*(40), 10672–10677.

Zhou, M., Tande, K. S., Zhu, Y., & Basedow, S. (2009). Productivity, trophic levels and size spectra of zooplankton in northern norwegian shelf regions. *Deep Sea Research Part II: Topical Studies in Oceanography*, *56*(21-22), 1934–1944.

Zipf, G. K. (1949). Human behaviour and the principle of least-effort. cambridge ma edn. *Reading: Addison-Wesley*.